NTNU – Trondheim
Norwegian University of
Science and Technology

Iron Catalyzed Lipid Oxidation in Emulsions and the Influence of Antioxidants

Jorunn Aaneby

Chemical Engineering and Biotechnology
Submission date: June 2012
Supervisor: Turid Rustad, IBT
Co-supervisor: Vera Kristinova, Sintef Fiskeri og havbruk
Ivar Storrø, Sintef Fiskeri og havbruk
Revilija Mozuraityte, Sintef Fiskeri og havbruk

Norwegian University of Science and Technology
Department of Biotechnology

Preface

I declare that the work performed in this master thesis has been done independently and in accordance with the regulations at the Norwegian University of Science and Technology, NTNU. The laboratory work for the master thesis was conducted partly at the Department of Biotechnology at NTNU and partly at Sintef Sealab. The master thesis is connected to the project work “Phospholipids from Herring Roe – Suitability for Oxygen Uptake Measurements” carried out by the author autumn 2011.

For motivation and guidance throughout the work with the master thesis I want to thank my main supervisor Professor Turid Rustad at the Department of Biotechnology at NTNU and my co-supervisors PhD student Vera Kristinova, senior researcher Ivar Storrø and researcher Revilija Mozuraityte at Sintef Fisheries and Aquaculture. I would also like to thank PhD student Magnus Nergård Hattrem at the Department of Biotechnology at NTNU for help and advices regarding preparation and analyses of emulsions.

Finally, I want to thank my friends and fellow students for making the years as a student so memorable, and I would like to thank my mother for always supporting me.

Trondheim, 19.06.2012

Jorunn Aaneby

Abstract

Lipids from marine sources contain high amounts of omega-3 fatty acids which are known to have several beneficial effects on human health. Their use as food ingredients is however limited due to their high susceptibility to lipid oxidation resulting in development of rancidity. Liposomes prepared from marine phospholipids have previously been used as a model system to study lipid oxidation by measurement of oxygen consumption. It was of interest to study lipid oxidation by this method in oil-in-water emulsions which can be considered to be more similar to foods. Incorporation of antioxidants in foods is an approach to increase the stability of foods containing omega-3 fatty acids. Emulsions were used as a model system to study the influence of EDTA, citric acid, caffeic acid, propyl gallate, α-tocopherol, ascorbic acid, β-carotene and astaxanthin on iron catalyzed lipid oxidation.

Crude herring oil was washed with water to remove impurities. Analyses showed that impurities including carbonyl compounds and carotenoids were removed by the washing, while the oxidation level of the oil slightly increased. The herring oil was used for preparation of emulsions with herring phospholipids as emulsifier by the use of a dispersing tool where increased dispersing time resulted in larger oil droplets with a wider size distribution.

Iron catalyzed oxidation of lipids in the emulsions occurred at a lower rate than what has previously been measured in liposomes, but the initial reaction between lipid hydroperoxides and Fe^{2+} occurred at the same rate in the two systems. The use of soy lecithin as emulsifier inhibited oxidation of lipids in the emulsions.

Interactions between iron and antioxidants had a major impact on oxidation in the emulsions. EDTA and citric acid completely inhibited the oxidation when they were added in twice the ratio to iron. Citric acid was not able to inhibit the initial reaction between lipid hydroperoxides and Fe^{2+} which was thought to be due to its inability to bind Fe^{2+}. Caffeic acid and α-tocopherol enhanced the oxidation rates by reducing Fe^{3+} to the more catalytically active Fe^{2+}. The prooxidative activity of caffeic acid was significantly greater than that of α-tocopherol. Caffeic acid, α-tocopherol and propyl gallate inhibited the initial reaction between lipid hydroperoxides and Fe^{2+} to a similar degree which was thought to be related to their free radical scavenging and metal chelating activities. Propyl gallate was also able to reduce the oxidation rates. Ascorbic acid was itself oxidized by Fe^{2+} and Fe^{3+} which resulted in increased initial consumption of oxygen, but not increased oxidation of the lipids. Ascorbic acid was able to decrease the prooxidative activity of α-tocopherol by regeneration of α-tocopherol from the α-tocopheroxyl radical. β-Carotene and astaxanthin showed only minor influences on lipid oxidation in the emulsions.

Sammendrag

Lipider fra marine kilder inneholder store mengder omega-3 fettsyrer som er kjent for å ha flere gunstige effekter på menneskers helse. Bruk av omega-3 fettsyrer i mat er imidlertid begrenset på grunn av at disse fettsyrene lett oksideres og fører til til harskhet. Liposomer fremstilt fra marine fosfolipider har tidligere blitt brukt som et modellsystem for å studere lipidoksidasjon ved måling av oksygenopptak, og det var ønskelig å studere lipidoksidasjon ved å bruke denne metoden i olje-i-vann emulsjoner som kan anses å være et modellsystem mer likt mat. Tilsetning av antioksidanter til mat som inneholder omega-3 fettsyrer er en mulighet for å øke stabiliteten til disse matvarene. Emulsjoner ble brukt som et modellsystem for å studere påvirkningen av EDTA, sitronsyre, kaffesyre, propylgallat, α-tokoferol, askorbinsyre, β-karoten og astaxanthin på jernkatalysert lipidoksidasjon.

Råolje fra sild ble vasket med vann for å fjerne urenheter. Analyser viste at karbonylforbindelser og karotenoider ble fjernet i vaskeprosessen, samtidig som oksidasjonsnivået av oljen økte noe. Sildeoljen ble brukt til fremstilling av emulsjoner med fosfolipider fra sild som emulgator ved å benytte et dispergeringsverktøy der økt dispergingstid førte til større oljedråper med en bredere størrelsesdistribusjon.

Jernkatalysert oksidasjon av lipider i emulsjonene skjedde ved en lavere hastighet enn det som tidligere har blitt målt i liposomer, men den inititelle reaksjonenen mellom lipidhydroperoksider og Fe^{2+} skjedde ved samme hastighet i de to systemene. Bruke av soyalecitin som emulgator hemmet oksidasjon av lipider in emulsjonene.

Interaksjoner mellom jern og antioksidanter hadde en stor innvirkning på oksidasjon i emulsjonene. EDTA og sitronsyre hemmet oksidasjonen fullstending når de ble tilsatt i dobbel konsentrasjon i forhold til jern. Sitronsyre hemmet ikke den initielle reaksjonen mellom lipidhydroperoksider og Fe^{2+} som ble antatt å skyldes dens manglende evne til å binde Fe^{2+}. Kaffesyre og α-tokoferol økte oksidasjons-hastighetene ved å redusere Fe^{3+} til det mer katalytisk aktive Fe^{2+}. Den prooksidative aktiviteten til kaffesyre var betydelig større enn den til α-tokoferol. Kaffesyre, α-tokoferol og propylgallat hemmet den initielle reaksjonen mellom lipidhydroperoksider og Fe^{2+} i tilsvarende grad som ble antatt å være relatert til deres evne til å hemme frie radikaler og danne metall chelater. Propylgallat reduserte i tillegg oksidasjons-ratene. Askorbinsyre ble selv oksidert av Fe^{2+} og Fe^{3+} som resulterte i økt initielt opptak av oksygen, men ikke økt oksidasjon av lipidene. Askorbinsyre var i stand til å redusere den prooksidative aktiviteten til α-tokoferol ved å regenere α-tokoferol fra α-tokoferol radikalen. β-karoten og astaxanthin hadde kun små påvirkninger på lipidoksidasjon i emulsjonene.

Contents

Abbreviations

AH	Antioxidant
$A^{\bullet}$	Antioxidant radical
ALA	α-Linolenic acid
AV	Anisidine value
DHA	Docosahexaenoic acid
EDTA	Ethylenediaminetetraacetic acid
EPA	Eicosapentaenoic acid
$L^{\bullet}$	Lipid alkyl radical
LH	Unsaturated lipid
$LO^{\bullet}$	Lipid alkoxyl radical
$LOO^{\bullet}$	Lipid peroxyl radical
LOOH	Lipid hydroperoxide
OUR	Oxygen uptake rate
PV	Peroxide value
SD	Standard deviation
TBA	Thiobarbituric acid
TBARS	Thiobarbituric acid reactive substances

1 Introduction

1.1 Background and Motivation

Long chain omega-3 polyunsaturated fatty acids are known to have several beneficial effects on human health. An increase in the dietary intake of omega-3 fatty acids is recommended and several food products have been enriched with these fatty acids. However, the high degree of unsaturation makes omega-3 fatty acids very susceptible to lipid oxidation which causes development of off-flavours and off-odours and reduces the stability of products containing these fatty acids. Oxidation of lipids is accelerated in the presence of transition metals which are almost inevitably found in foods. It is desirable to develop methods to prevent the oxidation of lipids so oxidatively stable products with omega-3 fatty acids can be produced. Incorporation of antioxidants in the food products is one approach to achieve increased stability. Antioxidants work by several different mechanisms and it is important to understand the mechanisms and interactions involved in lipid oxidation, as well as the interactions of the antioxidants with the lipids and prooxidants in the foods to be able to counteract the process of lipid oxidation.

Lipid oxidation can be analyzed by measurement of oxidation products or by the loss of substrates in the oxidation reactions. Oxidation of lipids in pure oils has been thoroughly studied, but the application of this knowledge to real foods is often limited due to the complexity of foods. Oil-in-water emulsions have several similarities with real foods and can serve as a model system for investigating the effects of prooxidants, antioxidants and combinations of these to increase the knowledge of lipid oxidation and the factors involved. Oxidation of phospholipids in the form of liposomes has previously been studied by monitoring oxygen consumption in liposome dispersions in a closed system, and a similar approach can be used to study oxidation of lipids in emulsions. Phospholipids can be used as emulsifiers in oil-in-water emulsions which would give a model system more similar to foods than liposomes.

Herring (*Clupea harengus*) is a pelagic fish known for its high fat content. The Norwegian pelagic industry exports large quantities of herring each year and there is a potential for production of good quality oil from byproducts formed by the processing of herring into fillets, and herring roe is a good source of phospholipids with considerable amounts of omega-3 fatty acids (Aidos et al., 2002, Hyttan and Østvik, 2009). Oil and phospholipids from herring have potentials as supplements of omega-3 fatty acids, and they can be used to prepare oil-in-water emulsions where both the oil and the emulsifier come from marine sources.

1.2 Lipids

Lipids constitute a diverse group of various chemical compounds which are important structural and functional components of foods. The main constituents of lipids are fatty acids which consist of a hydrocarbon chain bound to a carboxylic group. The majority of naturally occurring fatty acids has an even number of carbon atoms and a chain length of 14 to 26 atoms, due to the biological process of fatty acid elongation where two carbons are added at a time (McClements and Decker, 2008). Saturated fatty acids contain solely single bonds between adjacent carbon atoms, whereas unsaturated fatty acids contain one or more double bonds in the hydrocarbon chain. Fatty acids found in plants and animals are normally esterified to glycerol, where esterification of three fatty acids to glycerol to yield triacylglycerols is most common (Frankel, 2005). Phospholipids have a phosphate group bound to the glycerol molecule, and esterification of various molecules to the phosphate group gives phospholipids with different chemical properties (McClements and Decker, 2008). General structures of a triacylglycerol and a phospholipid are shown in Figure 1.2.1. Phospholipids are the major constituents of all biological membranes where they occur as bilayer structures (Chen et al., 2011). The polar head group of phospholipids makes the compounds amphiphilic and surface active which make them useful as emulsifiers in foods (Walstra and Vliet, 2008).

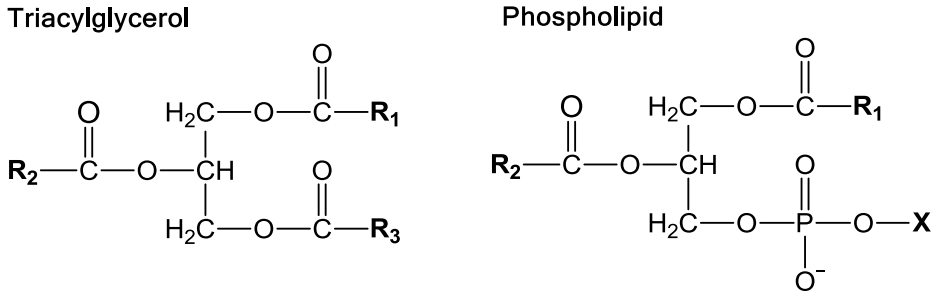

Figure 1.2.1: General structures of a triacylglycerol and a phospholipid. R_1, R_2 and R_3 are fatty acids esterified to the glycerol molecule. X can be a number of different compounds giving different types of phospholipids.

Polyunsaturated fatty acids contain at least two double bonds and are named according to the omega-system which indicates the position of the double bond with respect to the methyl end of the fatty acid (Ruxton et al., 2004). Lipids from marine sources contain high amounts of the long chain omega-3 fatty acids eicosapentaenoic acid (EPA; 20:5 n-3) and docosahexaenoic acid (DHA; 22:6 n-3)

(McClements and Decker, 2008). Structures of these fatty acids are shown in Figure 1.2.2.

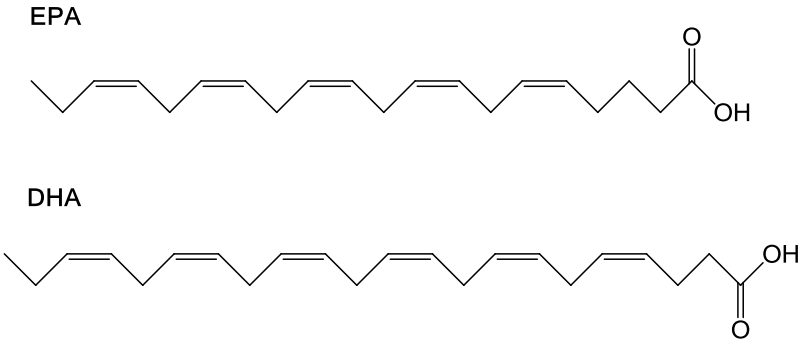

Figure 1.2.2: Structures of the omega-3 fatty acids eicosapentaenoic acid (EPA) and docosahexaenoic acid (DHA).

EPA and DHA have numerous documented beneficial effects on human health, which is thought to be related to their incorporation into the phospholipid membranes of the cells in the body (Riediger et al., 2009). They are known to reduce the risk of cardiovascular diseases and to have an immunomodulatory effect on conditions such as rheumatoid arthritis (Ruxton et al., 2004). They have also shown a positive effect regarding prevention of cancer, brain development and function, infant development, and various mental health illnesses including depression, attention-deficit hyperactivity disorder and dementia (Riediger et al., 2009).

Humans are able to synthesize EPA and DHA from the essential fatty acid α-linolenic acid (ALA; 18:3 n-3) but high levels of the precursor for omega-6 fatty acids can result in inhibition of the pathway that converts ALA to EPA and DHA since the biosynthetic pathways for formation of omega-3 and omega-6 fatty acids compete for the same enzyme. It is also suspected that the conversion of ALA to DHA is inefficient, resulting in inadequate amounts of this fatty acid (Ruxton et al., 2004). A number of authorities has recommended an increase in the intake of omega-3 fatty acids by the general population, but the fish intake is generally too low to meet the requirement. A variety of food products have therefore been enriched with omega-3 fatty acids to comply with the recommended intake level (Riediger et al., 2009). Examples of fortified food products are bread, spreadable fats, pasta and various dairy products. Modern food technology makes it possible to fortify food products without altering the quality of the food, but addition of fish oil may introduce stability problems due to oxidation of the unsaturated fatty acids (Kolanowski and Laufenberg, 2006).

1.3 Oxidation of Lipids

Polyunsaturated fatty acids are highly susceptible to lipid oxidation which is caused by the interaction between lipids and molecular oxygen. Lipid oxidation causes fatty acids to decompose into small, volatile molecules that are responsible for oxidative deterioration of foods (McClements and Decker, 2008). Quality attributes of the foods such as taste, smell, texture, shelf life, appearance and nutritional value are changed, and the oxidation can also cause development of reactive and toxic compounds which can be harmful for the consumer (McClements and Decker, 2000, Laguerre et al., 2007).

1.3.1 Autoxidation of Lipids

Autoxidation of unsaturated fatty acids occurs through a free radical chain mechanism which involves three general steps; initiation, propagation and termination (Frankel, 2005). The initiation step involves abstraction of hydrogen from an unsaturated fatty acid (LH) in the presence of an initiator resulting in the formation of a lipid alkyl radical ($L^{\bullet}$) as shown in equation (1). The initiator can be a physical agent such as heat or ionizing radiation, or a chemical agent such as transitions metals or free radicals (Laguerre et al., 2007).

$$LH \xrightarrow{Initiator} H^{+} + L^{\bullet} \quad (1)$$

The propagation step of lipid autoxidation involves reaction of the lipid alkyl radical with oxygen to form a lipid peroxyl radical ($LOO^{\bullet}$) as shown in equation (2). The peroxyl radical reacts further with another unsaturated fatty acid to form a new lipid alkyl radical as shown in equation (3). Reaction of this lipid radical with oxygen results in a self-catalyzing chain reaction.

$$L^{\bullet} + O_2 \rightarrow LOO^{\bullet} \quad (2)$$

$$LOO^{\bullet} + LH \rightarrow LOOH + L^{\bullet} \quad (3)$$

Termination of the oxidation process finds place when radical compounds accumulate and react with each other to form nonradical products (Frankel, 2005).

Lipid hydroperoxides formed during autoxidation of unsaturated fatty acids are not volatile and will not contribute to development of rancidity. They are however unstable and will decompose into radicals which can accelerate the propagation reactions or react further to produce volatile compounds. The β-scission reaction usually follows the decomposition of lipid hydroperoxides to lipid alkoxyl radicals ($LO^{\bullet}$), and involves breakage of the aliphatic chain to form an aldehyde and a lipid alkyl radical which can react with a hydrogen radical to form a hydrocarbon, a hydroxyl radical to form an alcohol, or oxygen to form a hydroperoxide (McClements and Decker, 2008). The volatile oxidation products formed can have an impact on flavour and odour of foods at extremely low concentrations (Frankel, 2005).

1.3.2 Iron Catalyzed Oxidation of Lipids

Prooxidants are compounds or factors that cause or accelerate lipid oxidation by direct interactions with unsaturated fatty acids, or by promoting formation of free radicals. Examples of prooxidants are transition metals, such as iron and copper, and transition metals associated with proteins, such as iron in haemoglobin (McClements and Decker, 2008). This is of great importance as these compounds can be found as endogenous compounds of foods where they contribute to oxidation of lipids (Hu et al., 2004).

Ferrous iron can promote decomposition of hydrogen peroxides by the Fenton reaction, shown in equation (4), in which highly reactive hydroxyl radicals capable of initiating lipid oxidation are formed (Miller, 2008).

$$Fe^{2+} + H_2O_2 \rightarrow Fe^{3+} + HO^{\bullet} + OH^{-} \quad (4)$$

Iron can also accelerate lipid oxidation by decomposition of lipid hydroperoxides into radicals through a redox cycling pathway as shown in equation (5) and (6) (McClements and Decker, 2008). The interaction between lipid hydroperoxides and trace metals is believed to be the most important promoter of oxidation of lipids in foods and biological systems (Frankel, 2005).

$$Fe^{2+} + LOOH \rightarrow Fe^{3+} + LO^{\bullet} + OH^{-} \quad (5)$$

$$Fe^{3+} + LOOH \rightarrow Fe^{2+} + LOO^{\bullet} + H^{+} \quad (6)$$

Ferrous iron is known to decompose lipid hydroperoxides by a rate an order of magnitude greater than that of ferric iron, and increased solubility of ferrous iron also makes them more available for promoting oxidation in aqueous systems (McClements and Decker, 2008, Miller, 2008). Transition metals are also capable of directly breaking down unsaturated lipids into lipid radicals, but this reaction occurs extremely slowly and is not believed to be important in promoting lipid oxidation (Reische et al., 2008).

1.4 Antioxidants

Antioxidants are compounds that are able to counteract the process of lipid oxidation, either by preventing the initiation reaction or by interfering with the chain propagation reactions (Frankel, 2005). Antioxidants have a potential as food additives to prevent development of undesirable odours and flavours caused by the oxidation of lipids. In recent years consumers have shown an increasing preference towards natural food additives, thus there is desirable to find antioxidants from natural sources to prevent lipid oxidation. There are a number of mechanisms by which antioxidants can inhibit lipid oxidation. They can function as metal chelators, as chain-breaking antioxidants by scavenging free radicals or they can quench singlet oxygen. Antioxidants can often exhibit antioxidant activity through several different mechanisms (Laguerre et al., 2007). The activity of an antioxidant will not only depend on its chemical properties but also on its physical location in the system, the presence of other components, such as transition metals, and on environmental conditions such as pH and oxygen concentration (McClements and Decker, 2000). It is thus important to select the right antioxidant for the right application.

1.4.1 Phenolic Compounds

Substituted phenolic compounds possess many of the properties of an efficient chain-breaking antioxidant. Chain-breaking antioxidants inhibit lipid oxidation by donation of hydrogen to peroxyl, alkoxyl and lipid alkyl radicals converting them to nonradical products, as shown in equation (7)-(9) (Reische et al., 2008). The resulting antioxidant radical ($A^{\bullet}$) is stabilized by delocalization of unpaired electrons which makes it relatively nonreactive and unlikely to promote further oxidation (Frankel, 2005).

$$AH + LOO^{\cdot} \rightarrow A^{\cdot} + LOOH \quad (7)$$

$$AH + LO^{\cdot} \rightarrow A^{\cdot} + LOH \quad (8)$$

$$AH + L^{\cdot} \rightarrow A^{\cdot} + LH \quad (9)$$

Synthetic phenolic antioxidants approved for use in foods include butylated hydroxyanisole (BHA), butylated hydroxytoluene (BHT), *tert*-butylhydroquinone (TBHQ) and propyl gallate (PG) (Frankel, 2005). A variety of phenolic compounds can also be found naturally in fruits, spices, tea, coffee, wine, seeds and grains, but the antioxidative activity of these compounds vary greatly, and some even exhibit prooxidant activity under certain conditions (Decker, 2008). Caffeic acid is a phenolic compound found widespread in nature which has received much attention due to its various activities including both antioxidative and prooxidative properties (Medina et al., 2011). The catechol group of caffeic acid allows for delocalization of electrons and the carboxylic acid substituent confers polarity to the compound. Propyl gallate differs from caffeic acid by bearing a galloyl group and an ester moiety, and the compound is only slightly water soluble (Reische et al., 2008). Chemical structures of caffeic acid and propyl gallate are shown in Figure 1.4.1.

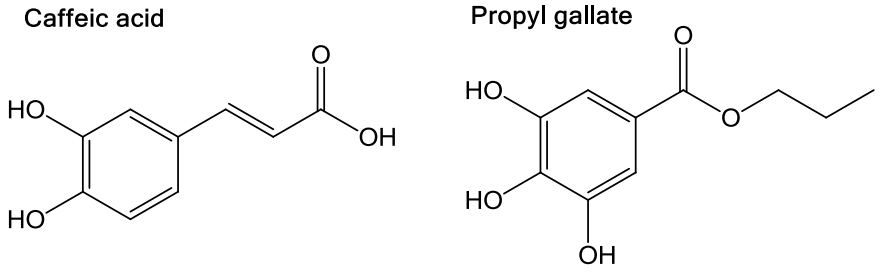

Figure 1.4.1: Chemical structures of the naturally occurring phenolic compound caffeic acid, and the synthetic phenolic compound propyl gallate.

The catechol and galloyl group of caffeic acid and propyl gallate can also function as a binding site for metal ions making these compounds possible metal chelators (Andjelković et al., 2006). Caffeic acid has been found to work as a prooxidant in the presence of iron which is explained by the ability caffeic acid has to reduce Fe^{3+} to the more catalytically active Fe^{2+} (Kristinová et al., 2009, Sørensen et al., 2008).

Tocopherols are monophenolic compounds and the most commonly naturally occurring antioxidants which are used in foods (Reische et al., 2008). They constitute

a group of compounds with a chromanol ring with varying extent of methylation (α, β, γ, δ), bound to a phytol chain. Tocotrienols differ from tocopherols by containing three double bonds in their phytol chain (McClements and Decker, 2008). α-Tocopherol is generally considered to be the most potent antioxidant of the tocopherols (Kamal-Eldin and Appelqvist, 1996). The chemical structure of this compound is shown in Figure 1.4.2.

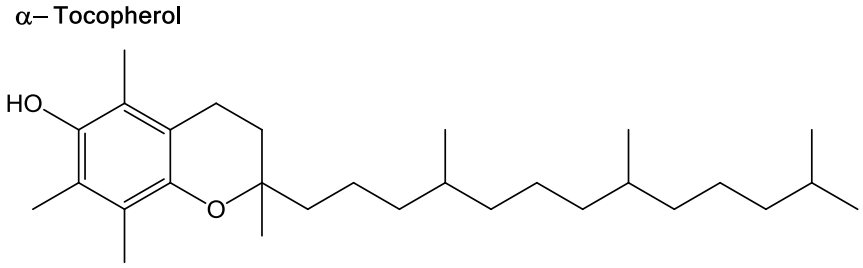

Figure 1.4.2: Chemical structure of α-tocopherol.

The antioxidant activity of tocopherols is related to their ability to donate hydrogen to lipid peroxyl radicals leading to the formation of a lipid hydroperoxide and several resonance stabilized structures of tocopheroxyl radicals (Decker, 2008). The tocopheroxyl radicals will undergo reactions to form a variety of products depending on the conditions in the system. Tocopheroxyl radicals are very reactive towards other radicals, and in the presence of sufficient amounts of lipid alkoxyl, peroxyl and alkyl radicals will adducts between these and tocopheroxyl radicals be formed. The radicals formed by tocopherols can sometimes also partition in prooxidative reactions (Kamal-Eldin and Appelqvist, 1996).

1.4.2 Carotenoids

Carotenoids constitute a group of naturally occurring antioxidants which are found in all photosynthetic organisms where they function as accessory pigments and impart protection of tissue through their ability to quench singlet oxygen and free radical species (Schwartz et al., 2008). Carotenoids consist of two classes of compounds; carotenes which are pure hydrocarbons and xanthophylls which contain oxygenated functional groups (Laguerre et al., 2007). The chemical structures of the carotene β-carotene and the xanthophyll astaxanthin are shown in Figure 1.4.3.

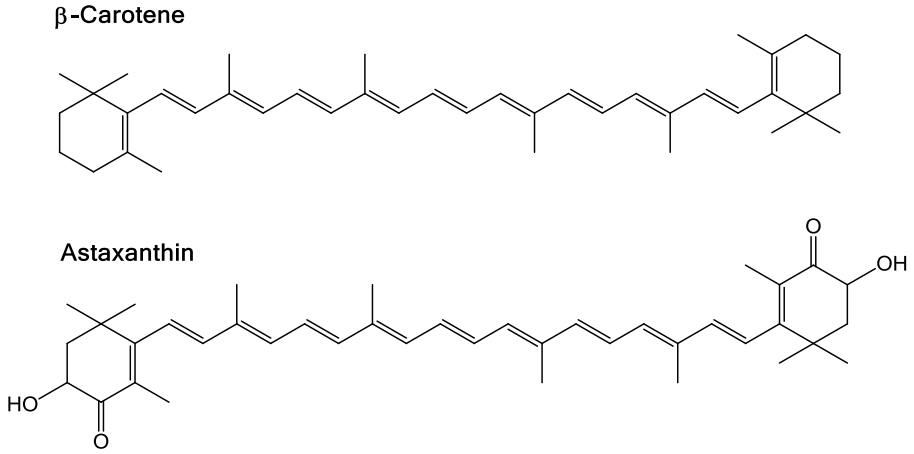

Figure 1.4.3: Chemical structures of the carotenoids β-carotene and astaxanthin.

The primary mechanism by which carotenoids quench singlet oxygen is by physical quenching where energy transfer from oxygen to the carotenoid produces an excited state of the carotenoid and convert oxygen to its ground state, as shown in equation (10). Singlet oxygen can, unlike normal triplet oxygen, react directly with lipids to produce free radicals (Reische et al., 2008). Dissipation of energy from the excited carotenoid to the environment in form of heat, equation (11), returns the carotenoid to the ground state where it can start a new quenching cycle (Laguerre et al., 2007). The ability of carotenoids to quench singlet oxygen is influenced by the number of double bonds and the presence of functional groups such as keto and hydroxyl groups in the structure (Hirayama et al., 1994).

$$^1O_2 + \beta - Carotene \rightarrow {}^3O_2 + \beta - Carotene^* \quad (10)$$

$$\beta - Carotene^* \rightarrow \beta - Carotene + Heat \quad (11)$$

Carotenoids can also function as chain-breaking antioxidants by reactions with lipid peroxyl radical resulting in the formation of a carotenoid radical stabilized by delocalization of electrons (Reische et al., 2008). The carotenoid radical can react further with lipid peroxyl radicals to form nonradical products, or reversibly with oxygen to form a carotenoid peroxyl radical, as shown in equation (12) (Liebler, 1993). High oxygen concentration favours autoxidation of the carotenoid making it function as a prooxidant rather than an antioxidant at these conditions (Decker, 2008).

$$Carotenoid^{\cdot} + O_2 \leftrightarrow Carotenoid - OO^{\cdot} \quad (12)$$

1.4.3 Metal Chelators

Compounds that chelate metals can be efficient inhibitors of lipid oxidation in foods since transition metals are present in foods as inherent constituents of the raw material or in the water, ingredients or packing material of the foods (Hu et al., 2004). Metal chelators can inhibit lipid oxidation by preventing the redox cycling of the metal ions, occupation of all metal coordination sites, formation of insoluble metal complexes or steric hindrance of interaction between the metals and lipids (Decker, 2008). Commonly used chelating agents in foods are polyphosphates and the multiple carboxylic acids ethylenediaminetetraacetic acid (EDTA) and citric acid. The chemical structures of EDTA and citric acid are shown in Figure 1.4.4.

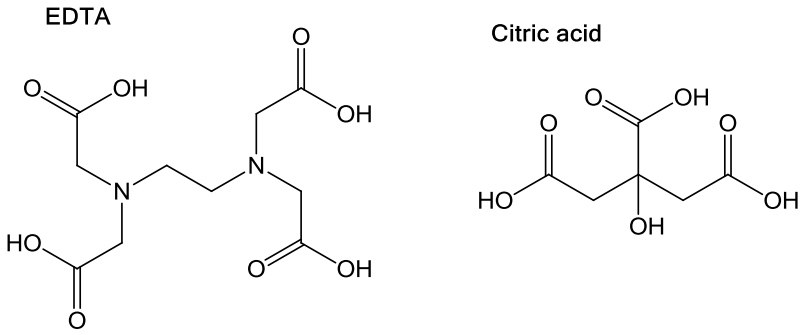

Figure 1.4.4: Chemical structures of the chelating agents ethylenediaminetetraacetic acid (EDTA) and citric acid.

The activity of metal chelators is dependent on pH since the chelators need to be in their ionized forms to be able to bind metals. Some metal chelators can increase the prooxidant activity of transition metals by increasing their solubility or alteration of their redox potential (Decker, 2008).

1.4.4 Ascorbic Acid

Ascorbic acid is known for its complex and multi-functional effects regarding lipid oxidation. The antioxidant properties of ascorbic acid are related to its ability to donate hydrogen to lipid radicals, act as a metal chelator and to scavenge singlet oxygen (Reische et al., 2008). Ascorbic acid can also act as a prooxidant, especially in the presence of trace metals as it is a strong reducing agent and can reduce Fe^{3+} to Fe^{2+} (Miller, 2008).

Oxidation of ascorbic acid to dehydroascorbic acid takes place either as one single two-electron transfer process or as two one-electron transfer processes via an intermediate ascorbate radical (Gregory, 2008). Ascorbic acid is highly susceptible to oxidation, especially in the presence of transition metals where the oxidation process has been proposed to occur through the formation of a ternary complex of ascorbate monoanion, oxygen and iron to yield dehydroascorbic acid as product (Gregory, 2008, Khan and Martell, 1967). The mechanisms for oxidation of ascorbic acid are shown in Figure 1.4.5.

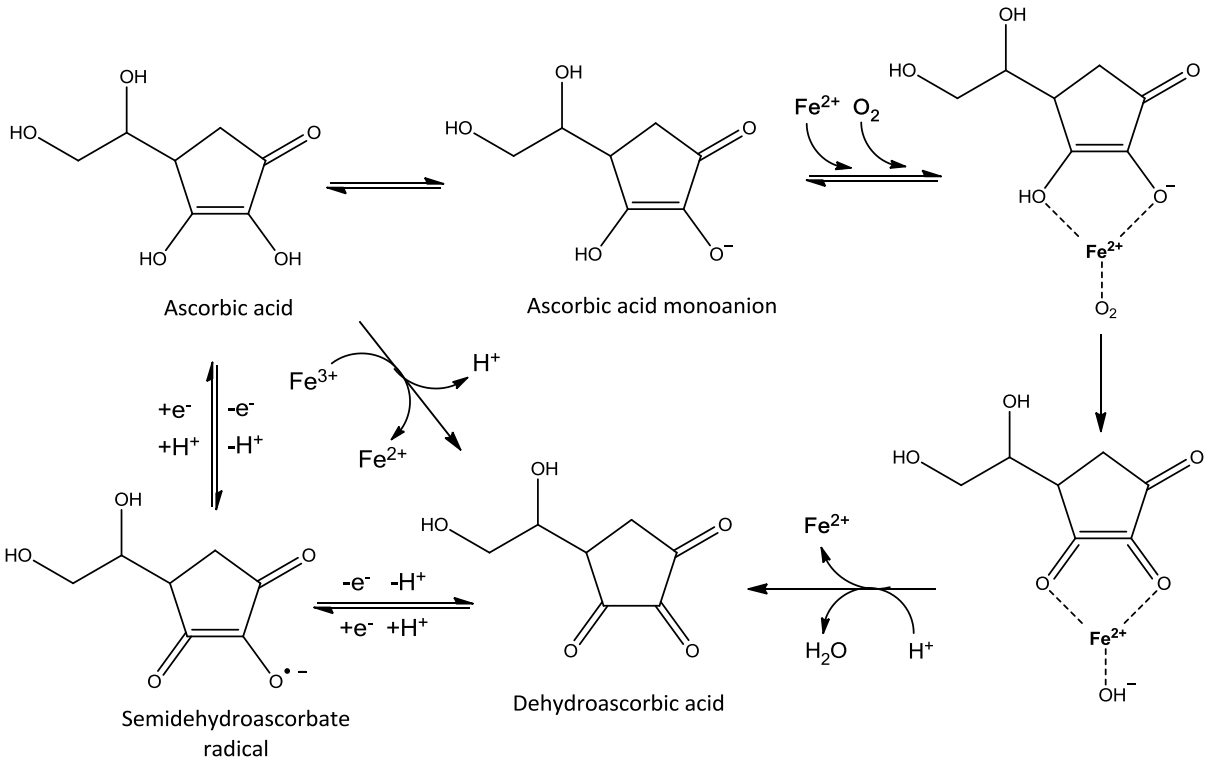

Figure 1.4.5: Oxidation reactions of ascorbic acid (Fisher and Naughton, 2004, Miller, 2008, Gregory, 2008).

The reducing behaviour of ascorbic acid makes it able to regenerate antioxidants (Frankel, 2005). The antioxidant activity of tocopherols has been shown to increase when tocopherols and ascorbic acid are used together, which has been explained by the ability of ascorbic acid to regenerate tocopherol from the tocopheroxyl radical. The interaction between the two compounds is believed to take place at the surface of the oil droplets in emulsions where ascorbic acid and tocopherol reside in the aqueous and lipid phase, respectively (Niki, 1991). The interaction between lipid peroxyl radical, α-tocopherol and ascorbic acid is shown in Figure 1.4.6.

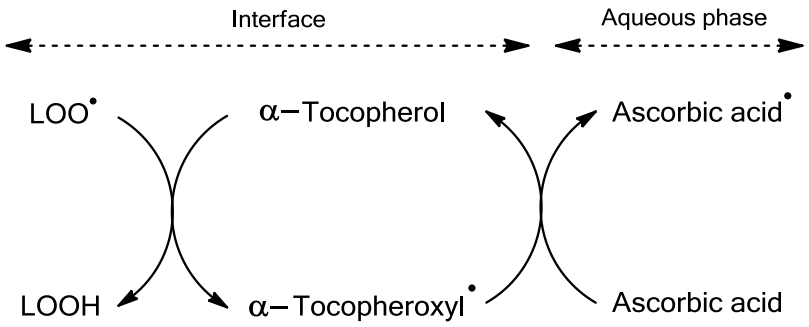

Figure 1.4.6: Recycling mechanism of α-tocopherol by ascorbic acid in emulsions (Laguerre et al., 2007).

1.5 Emulsions

Most foods are in the form of dispersed systems where discrete particles exist in a continuous phase. Dispersions where one liquid is dispersed in another liquid in the form of small droplets are known as emulsions. Emulsions can either be classified as oil-in-water emulsions or as water-in-oil emulsions, where oil-in-water emulsions are most common in foods (Walstra and Vliet, 2008). Examples of foods that are oil-in-water emulsions are milk, cream, mayonnaise, sauces, soups, and dressings (Coupland and McClements, 1996). Formation and stabilization of oil-in-water emulsions require the use of emulsifiers which are surface active molecules that adsorb to the surface of oil droplets in emulsions. Commonly used emulsifiers in foods are amphiphilic proteins, phospholipids and small molecule surfactants (Damodaran, 2005). The most essential role of the emulsifier is to form a protective membrane around newly formed droplets in the emulsion to prevent them from coalescing (Dickinson, 2009). Emulsifiers also have an ability to lower the interfacial tension of the droplets and thereby reduce the amount of energy needed to deform and break up the droplets (Walstra, 1993).

1.5.1 Stability of Emulsions

A system consisting of oil droplets dispersed in water can never exist in a true thermodynamic equilibrium, but it may appear to be stable if it does not show significant changes in properties during the observation time (Walstra and Vliet, 2008). Physical forces that affect the kinetic stability of emulsions are related to density difference between the dispersed and continuous phase, interactions between the droplets, and the properties of the emulsifier membrane. The forces will

have influence on the rate of creaming, flocculation and coalescence of the emulsion droplets (Damodaran, 2005).

Creaming refers to the tendency of oil droplets in an emulsion to rise to the top against gravity and is related to the density difference between the dispersed and continuous phase (Damodaran, 2005). The rate of creaming, v, can be predicted from Stokes law, given in equation (13), where d is the radius of the oil droplets, ρ_D and ρ_C are the densities of the dispersed and continuous phase respectively, g is the gravitational acceleration and η_C is the viscosity of the continuous phase (Walstra and Vliet, 2008).

$$v = \frac{g(\rho_D - \rho_C)d^2}{18\eta_C} \tag{13}$$

As can be seen from Stokes law, the rate of creaming can be greatly reduced if the density difference between the dispersed and continuous phase is reduced, if the diameter of the droplets is reduced, or if the viscosity of the continuous phase is increased. For oil-in-water emulsions, the only parameters that are commonly manipulated are the size of the oil droplets and the viscosity of the continuous phase, as the density difference between the oil and water phase is usually invariable (Damodaran, 2005). The viscosity of the continuous phase can be increased by adding thickening agents such as hydrocolloids. One such biopolymer is xanthan gum which has an ability to stabilize emulsions due to formation of a gel-like structure between the gum molecules in the continuous phase which prevents creaming of the oil droplets (Dickinson, 2009).

Loose association of oil droplets due to attraction between them results in flocculation. The major interactions between oil droplets in emulsions are van der Waals forces which are attractive and electrostatic and steric forces which are repulsive (Damodaran, 2005). Coalescence is unlike flocculation and creaming an irreversible process which occurs when two oil droplets merge to form one single droplet, and is induced by rupture of the emulsifier film between the droplets (Damodaran, 2005). The probability of coalescence increases with the time the droplets are close together, thus coalescence is more likely to occur in creamed or flocculated emulsions (Walstra and Vliet, 2008).

1.5.2 Lipid Oxidation in Emulsions

The mechanisms for lipid oxidation in oil-in-water emulsions differs from those in bulk oils due to the presence of an interfacial membrane between the oil and water which allows for interaction between the lipids and compounds in the aqueous phase (Frankel, 2005). Lipid oxidation in oil-in-water emulsions is influenced by the nature of the interfacial membrane such as its thickness, charge, composition and permeability. The size, concentration and physical state of the oil droplets may also affect the oxidation events (Waraho et al., 2011). Lipid oxidation in water-in-oil emulsions has been suggested to occur by similar mechanisms as oxidation in bulk oils, although water soluble components located within water droplets in the emulsion can affect the oxidation (McClements and Decker, 2000).

Ionic emulsifiers will provide a charge to the interfacial membrane surrounding the oil droplets which will lead to repulsion or attraction of charged components in the system (Mei et al., 1998). The attraction of oppositely charged ions to the oil droplets cause formation of an electrical double layer consisting of an inner layer of tightly bound ions, the Stern layer, and an outer region where the ions are more mobile, as shown in Figure 1.5.1. Only the most strongly bound ions will move with the droplets when they move through a solution. The boundary layer for where the ions no longer move with the oil droplets is called the shear or slipping plane, and the potential that exists in this plane is called the zeta potential. The zeta potential is not a direct measurement of the surface charge, but it gives an approximation of the charge which will determine the interaction with other particles in the solution (Hunter, 1993).

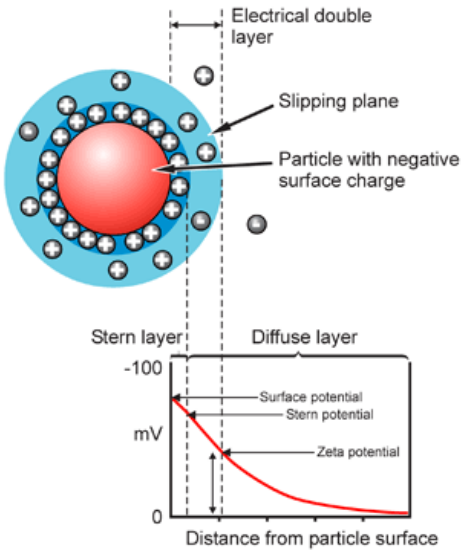

Figure 1.5.1: Illustration of the electrical double layer surrounding an oil droplet in an emulsion (Malvern Instruments Ltd.).

Association of iron with negatively charged oil droplets has been shown to accelerate lipid oxidation, whereas positively charged oil droplets can decrease the oxidation of the lipids due to repulsion of iron (Mei et al., 1998). The electrostatic properties of the oil droplets will also affect the location and hence the activity of charged antioxidants (Mei et al., 1999).

The abilities of antioxidants to retard lipid oxidation in emulsions will depend on their physical location in the emulsions as well as their chemical interaction with other components and the physical conditions of the system (Waraho et al., 2011). Non-polar antioxidants are found to be more effective in oil-in-water emulsions since they are retained in the oil droplets or accumulate at the oil-water interface where oxidation is most prevalent. Polar antioxidants, on the other hand, are most effective in bulk oils since they accumulate at the air-oil interface or in reverse micelles within the oil where lipid oxidation reactions are prominent. The greater efficiency of non-polar antioxidants in polar system and vice versa is known as the polar paradox (Frankel, 2005).

1.6 Measurement of Lipid Oxidation

There are various methods available for measuring lipid oxidation including determination of changes in chemical, physical and sensory properties (Shahidi and Wanasundara, 2002). Sensory analysis is the only technique that directly monitors off-flavours and off-odours resulting from oxidation of lipids, but the analyses are time-consuming and expensive, thus unsuitable for routine analyses. Methods for measuring lipid oxidation are generally divided into those involving primary and secondary changes of the lipids. Lipid hydroperoxides are primary oxidation products present in all lipids to some extent. They can be quantified by determination of peroxide value (PV) which relies on the ability of lipid hydroperoxides to oxidize an indicator compound, commonly iodide or ferrous ion (McClements and Decker, 2008). Peroxide values are useful for samples that are oxidized to relatively low levels and under sufficiently mild conditions so that hydroperoxides are not markedly decomposed (Frankel, 2005). Abstraction of hydrogen from a fatty acid in the initiation step of lipid oxidation results in a shift in the position of the double bonds which leads to formation of conjugated dienes, and in the case of fatty acids with at least three double bonds, formation of conjugated trienes. Conjugated dienes and trienes exhibit intense absorption and can be quantified by absorbance measurements at particular wavelengths (McClements and Decker, 2008).

Measurement of secondary lipid oxidation products has a stronger correlation with sensory attributes of the oil as they are directly responsible for the off-flavours and off-odours in the rancid oil. Decomposition of primary oxidation products results in a variety of products including aldehydes, ketones, hydrocarbons and alcohols, and the methods to analyze them usually focus on a single compound or a class of compounds (McClements and Decker, 2008). Carbonyls can be determined by reaction of the lipid with *p*-anisidine reagent under acidic conditions, which gives the *p*-anisidine value (AV) of the oil. Thibarbituric acid reactive substances (TBARS) refer to compounds that react with thiobarbituric acid (TBA) under acidic conditions. The test was originally attributed to the reaction of TBA with malondialdehyde, but other decomposition products such as alkenals and alkadienals, and nonlipid carbonyls can react with TBA as well (Shahidi and Wanasundara, 2002). Secondary oxidation products are also commonly measured by different chromatography techniques (Frankel, 1993).

The methods for determination of lipid oxidation can be used to study lipid oxidation in both bulk oils and emulsions, but for analyses of lipid oxidation in emulsions it is often necessary to extract the oil phase from the emulsions before the analyses can be carried out (Coupland and McClements, 1996). An alternative approach to study lipid oxidation is to monitor the consumption of oxygen during lipid oxidation, thus focus on the loss of substrate in the oxidation reactions. This can be done by continuous measurement of the oxygen concentration with an oxygen meter in a closed system with lipids. An advantage of this method is that oxidation in emulsions can be studied directly without extracting the oil phase before analysis. Continuous monitoring of the oxygen concentration in the system makes it easier to evaluate the kinetics of the oxidation reactions. The method allows for easy changes of environmental conditions such as light, temperature and pH, as well as addition of prooxidants and antioxidants to the system during the oxidation process.

Oxidation in liposomes prepared from phospholipids from cod roe was studied by Mozuraityte (2007) by measurement of oxygen consumption, and Kristinová et al. (2009) investigated the influence of antioxidants on lipid oxidation in liposomes by this method. In the project work by Aaneby (2011), phospholipids from herring roe were used for preparation of liposomes and studies of lipid oxidation by oxygen uptake measurements. It is of interest to find out whether lipid oxidation in emulsions can be studied by the same method, and to investigate possible differences between lipid oxidation in emulsions and in liposomes. It is also desirable to evaluate the influence of antioxidants on lipid oxidation in emulsions and to see if this can be achieved by measurement of oxygen consumption in emulsions. The objective of this study was to prepare oil-in-water emulsions with herring oil and herring phospholipids

as emulsifier to be used for studies of iron catalyzed lipid oxidation by oxygen consumption measurements. The oxidation of lipids in the emulsions was compared to previous studies of lipid oxidation in liposomes and the influence of several antioxidants was evaluated.

2 Materials and Methods

2.1 Washing of Crude Oil

Crude herring oil was produced by Sintef Mobile Plant by thermal processing of fresh herring rest raw material including heads, guts, muscle trims, bones and skin. The raw material was obtained from Grøntvedt Pelagic (Uthaug, Norway). Oil from two different production batches was used, one produced in November 2010 and one in January 2010. The oil was stored at -30 °C until use.

Crude oil generally contains impurities such as proteins, carbohydrates, free fatty acids, phospholipids, minerals, pigments, sterols and antioxidants and some of these components may have a negative impact on the quality and stability of the oil. Crude oil therefore normally undergoes a refinement process to obtain purer oil (McClements and Decker, 2008). Crude herring oil (produced in Nov. 2010) was washed as described by Crexi et al. (2010) to remove water soluble impurities from the oil. The oil was heated to approximately 50 °C and added 10% boiling water in relation to the oil mass. The oil and water mixture was kept at approximately 60 °C for 10 minutes under manual stirring before the phases were separated by centrifugation for 10 minutes at 40 °C with a Jouan KR22i centrifuge (7000 rpm, DJB Labcare LTD, UK). The washing procedure was repeated three times to determine the influence of the washing on the purity and oxidation of the oil. Samples of the oil and water phases were collected after each washing for further analyses.

The oil produced in January 2012 was used for preparation of emulsions and was washed once.

2.2 Primary and Secondary Oxidation Products

The extent of oxidation of the crude herring oil and the oil samples collected after each washing was determined by analysing primary and secondary lipid oxidation products. More detailed descriptions of the procedures and calculations of the oxidation values can be found in Appendix A.

2.2.1 Peroxide Values

The peroxide values in the oil samples were determined according to ISO 3960 (2001). The iodometric method for determination of peroxide values is based on the reduction of iodide to iodine by lipid hydroperoxides, as shown in equation (14). The amount of iodine formed is proportional to the amount of peroxides in the lipids and is quantified by titration with standardized sodium thiosulphate, as shown in equation (15).

$$LOOH + 2I^- + 2H^+ \rightarrow 2LOH + I_2 \quad (14)$$

$$I_2 + 2S_2O_3^{2-} \rightarrow 2I^- + S_4O_6^{2-} \quad (15)$$

The method was carried out by dissolving a sample of oil in acetic acid/iso-octane solution. Saturated potassium iodide solution was added to the mixture and it was stirred on magnetic stirrer for one minute before addition of distilled water. The amount of iodine was determined by titration with sodium thiosulphate using a TitraLab, TIM 980 Titration Manager (Radiometer Analytical SAS, Copenhagen, Denmark). Sodium dodecyl sulphate was added to the mixture close to the endpoint of the titration to decrease the surface tension of the oil-water interface and thus promote movement of iodine to the water phase where the measurements took place. A blank sample analysis was performed according to the same procedure only without oil. The use of a titrator reduces the uncertainty in the determination of the endpoint of the titration as the disappearance of the pale violet colour produced by the iodine and starch reaction in the manual titration method often is difficult to discern.

The sodium thiosulphate solution needs to be standardized before use. This is achieved by using a solution of potassium iodate as standard. Iodate reacts with iodide to give iodine, as shown in equation (16) which reacts with the thiosulphate ion, as shown in equation (17).

$$IO_3^- + 5I^- + 6H^+ \rightarrow 3I_2 + 3H_2O \quad (16)$$

$$3I_2 + 6S_2O_3^- \rightarrow 6I^- + 3S_4O_6^- \quad (17)$$

The standardization of the sodium thiosulphate solution was performed by PhD student Ana Caravajal and researcher Revilija Mozuraityte.

2.2.2 *p*-Anisidine Values

The *p*-anisidine value of a lipid is defined as 100 times the optical density measured at 350 nm in a solution of 1.0 g of lipid in 100 mL of a mixture of solvent and reagent. The method determines the amount of carbonyls present in lipids (Frankel, 2005). The *p*-anisidine values of the oil samples were determined according to the AOCS Official Method Cd 18-90 (1993). The absorbance of a sample of oil dissolved in ico-octane and of pure iso-octane was measured at 350 nm against iso-octane before and after addition of *p*-anisidine reagent, and the anisidine value was determined according to the differences in absorbance. The measurements were performed with an Ultrospec 2000 UV/Visible Spectrophotometer (Pharmacia Biotech).

2.2.3 Thiobarbituric Acid Reactive Substances

Thiobarbituric acid reacts with malondialdehyde and other secondary lipid oxidation products to form coloured complexes under acidic conditions (McClements and Decker, 2008). Thiobarbituric acid reactive substances in the oil samples were determined according to the spectrophotometric method described by Ke and Woyewoda (1979). A sample of oil was dissolved in TBA working solution and incubated in water bath with almost boiling water for 45 minutes. Trichloroacetic acid was added to the mixture before centrifugation for 10 minutes (2500 rpm) to separate the water and chloroform phase. The absorbance of the water phase was measured at 538 nm against a blank sample with an Ultrospec 2000 UV/Visible Spectrophotometer (Pharmacia Biotech). The amount of TBARS in the oil samples was calculated according to a standard curve made by replacing the oil sample with tetraethoxypropane in the range 0 to 20 nmol.

2.3 Carotenoids

The conjugated double bonds of carotenoids cause them to absorb light in the visible spectrum, thus they can be quantified by spectrophotometric analysis. The content of carotenoids in the oil samples was determined by the spectrophotometric method described by Tolasa et al. (2005). A sample of oil was dissolved in *n*-hexane and the absorbance was measured at 472 nm against pure solvent with an Ultrospec 2000 UV/Visible Spectrophotometer (Pharmacia Biotech). The carotenoid content was calculated using an absorption coefficient E=2100 which is the standard absorbance of 1% (v/w) astaxanthin in *n*-hexane measured at 470 nm. The calculation is shown in Appendix B.

2.4 Absorption Spectra

Crude oil contains various compounds which can be measured by absorption in the visible and ultra violet spectra, such as proteins and pigments, and conjugated dienes and trienes which are formed in oxidized oils. The absorption spectra of crude oil, and of oil and water samples collected after each washing were determined by measuring the absorbance at wavelengths from 200 to 800 nm with an Ultrospec 2000 UV/Visible Spectrophotometer (Pharmacia Biotech). The absorbance measurements of the oil were performed on samples of pure oil and on samples of oil dissolved in iso-octane to a concentration of 0.001 g/mL. This solvent was chosen since it dissolves lipids easily and it is the solvent used for determination of conjugated dienes and trienes in lipids (Pegg, 2001).

2.5 Preparation of Emulsions

Oil-in-water emulsions with a total lipid content of 10% (w/w) were prepared for studies of lipid oxidation in emulsions. Herring oil (produced in Jan. 2011) was used as oil phase and phospholipids isolated from herring roe and soy lecithin (20% L-α-phosphatidylcholine, Sigma) were used as emulsifiers. The phospholipids were isolated from herring roe as a part of the project work performed by Aaneby (2011). The phospholipids were stored in chloroform at -20 °C until use. The concentration of phospholipids in chloroform was determined during the isolation procedure and preparation of liposomes in the project work. Soy lecithin was dissolved in chloroform to a known concentration. A 1:10 (w/w) emulsifier-oil mixture was prepared by mixing appropriate amounts of emulsifier dissolved in chloroform with oil. Chloroform was evaporated from the mixture by nitrogen gas and the mixture was kept frozen at -20 °C until use. To prepare emulsions, oil-emulsifier mixture was mixed with distilled water in a ratio 1:10 (w/w) and emulsified with an Ultra Turrax T10 Basic Disperser (Janke & Kunkel, IKA, Staufen, Germany) gradually increasing the speed from 8000 to 30000 rpm. Emulsification times of 15 and 30 seconds, and 1, 2, 3, 4 and 8 minutes were tested for emulsions with herring phospholipids as emulsifier. Emulsions used for oxidation experiments were emulsified for 30 seconds.

Emulsions where the aqueous phase contained xanthan gum were also prepared. Solutions with 0.1% and 0.2% (w/v) xanthan gum in distilled water were made and mixed with oil-emulsifier mixture with herring phospholipids. The emulsions were prepared by emulsification for 4 minutes.

2.6 Characterization of Emulsions

2.6.1 Droplet Size

The size of the oil droplets in the emulsions were measured with a Mastersizer 3000 (Malvern Instruments Ltd., Worcestershire, UK) which uses the technique of laser diffraction to measure the size of particles in a solution. A laser beam passes through the solution with the dispersed particles and the intensities of the entering and scattered light are measured. The measured intensities are used to calculate the concentration of particles by use of scattering theory and optical properties of the particle and dispersant media. The droplet size distributions obtained by this measurement technique are volume based.

The droplet size measurements were performed by adding a few droplets of emulsion to a circulating water bath until an obscuration of 6-12% was reached. The emulsions were gently shaken before the measurements to limit the influence of creaming and flocculation on the droplet size distributions. The refractive indices of cod liver oil (1.481) and water (1.330) were used for particle and dispersant index, respectively.

2.6.2 Zeta Potential

The zeta potential of the oil droplets was determined by electrophoretic mobility measurements where the velocity of the droplets in an electric field is measured. The zeta potential is obtained by applying the Henry equation (18) which relates the electrophoretic mobility to the zeta potential.

$$u_e = \frac{2\varepsilon\zeta}{3\eta} f(ka) \tag{18}$$

In equation (18), u_e is the electrophoretic mobility of the droplets, ε and η are the dielectric constant and viscosity of the medium, respectively, and *f(ka)* is the Henry's function. For an aqueous medium at moderate ionic strength the value of the Henry function is set to 1.5, known as the Smoluchowski approximation (Hunter, 1993). The zeta potential measurements were performed with a Zetasizer Nano ZS (Malvern Instrument Ltd., Worcestershire, UK). The analyses were performed at 30 °C.

2.6.3 Creaming Stability

Creaming of oil droplets in an emulsion will cause formation of a clearer layer at the bottom of the emulsion, thus the creaming can be evaluated by measuring the change in absorbance in the emulsion with time.

The absorbance of diluted samples of emulsions was measured at 600 nm with an Ultrospec 2000 UV/Visible Spectrophotometer (Pharmacia Biotech). The emulsions were diluted with the same solvent used to prepare the emulsion (water or xanthan gum solution) in a ratio 1:150 (v/v), and 2.5 mL of solution was transferred to three separate plastic cuvettes (1.0 cm). The absorbance was measured shortly after preparation of the emulsions and after approximately two, five and twenty hours of storage.

2.7 Measurement of Lipid Oxidation in Emulsions

Oxidation of lipids in emulsions was determined by measuring oxygen consumption in emulsions in a closed chamber by an Oxygraph system (Hansatech Instruments Ltd., Norfolk, U.K.). The oxidation was induced by either Fe^{2+} or Fe^{3+}, and the influence of citric acid, EDTA, ascorbic acid, propyl gallate, caffeic acid, α-tocopherol, β-carotene and astaxanthin on oxygen consumption in the emulsions were evaluated.

2.7.1 Oxygraph System

The Oxygraph system provides a convenient method for studying oxygen consumption in emulsions. A scheme for the set up of the system is shown in Figure 2.7.1.

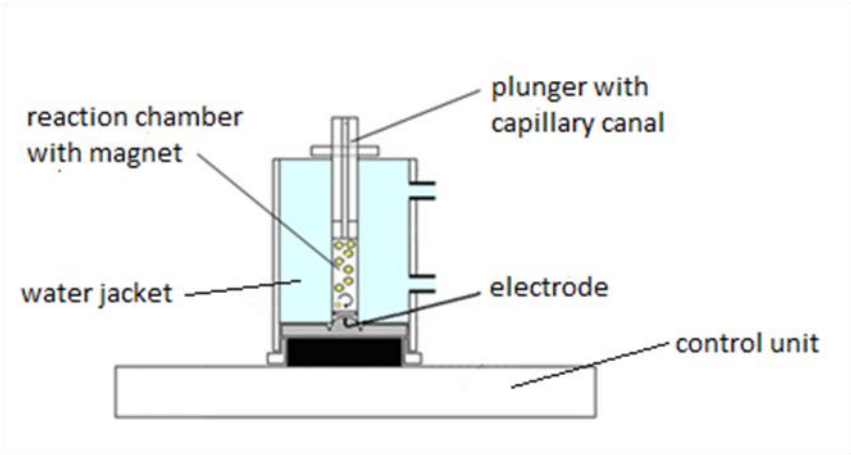

Figure 2.7.1: Schematic presentation of the Oxygraph system used for measurements of oxygen consumption in emulsions.

The oxygen electrode is a specialised form of an electrochemical cell known as a Clark type polarographic sensor consisting of a resin bound central platinum cathode and a concentric silver anode forming the electrode disc. The anode and the cathode are linked by an electrolyte solution of potassium chloride (3 M) during the measurements. Practically this is achieved with the aid of a fine paper and a fine layer of PFTE membrane which is selectively permeable to oxygen molecules. The electrode disc is mounted onto the base of the reaction chamber so the dome section of the disc forms the floor of the reaction chamber. The electrode disc is connected to a control unit supplying voltage and generates a current proportional to the oxygen concentration in the reaction chamber during measurements. The current is converted to a voltage, conditioned and digitised before it is displayed. Continuous oxygen concentration in the chamber is maintained by using a small magnet combined with a magnetic stirrer. A plunger is applied to the top of the reaction chamber to avoid diffusion of oxygen from the atmosphere. A small capillary canal through the plunger allows for additions during the measurements by the use of a Hamilton type syringe. The chamber is surrounded by a water jacket connected to a thermo regulated circulating water bath for temperature control of the sample during measurements. Connection of three separate devices to a computer allows for the monitoring of oxygen concentration in three separate experiments simultaneously.

2.7.2 Preparation of Solutions of Prooxidants and Antioxidants

Stock solutions of Fe^{2+} and Fe^{3+} were prepared by dissolution of $FeSO_4 \cdot 7H_2O$ (99.5%, Merck) and $FeCl_3$ (>98%, Riedel-de Haën) in HCl (0.5 M) to a concentration

of 20 mM. The solutions were made in HCl to avoid precipitation of $Fe(OH)_2$. Working solutions of Fe^{2+} and Fe^{3+} were prepared daily by dilution of the stock solutions with distilled water to a concentration of 1.0 mM.

Stock solutions of propyl gallate (98%, Fluka Analytical), ascorbic acid (purity not stated, Sigma) and caffeic acid (≥98%, Sigma) were prepared in 96% ethanol to a concentration of 100 mM. The compounds were dissolved in ethanol due to poor solubility in water. Citric acid (99.5%, Merck) and EDTA (99.5%, Fluka Analytical) were dissolved in distilled water to a concentration of 50 mM and 0.75 mM, respectively. The stock solution of EDTA was used directly for additions to emulsions during the oxidation experiments. Working solutions of the other antioxidants were prepared daily by dilution of the stock solutions with distilled water. The concentration of the working solutions varied between 2.5 and 20 mM, depending on the desired concentration of the antioxidant in the emulsions.

Stock solutions of DL-α-tocopherol (98.2%, Calbiochem), β-carotene (98.4%, Calbiochem) and astaxanthin (≥92%, Sigma) were prepared in chloroform to a concentration of approximately 5 mM. The antioxidants were added to the oil-emulsifier mixture prior to preparation of the emulsions. A volume of stock solution corresponding to the desired concentration of antioxidant in the emulsion was transferred to a test tube and the chloroform was evaporated from the solution to almost dryness with nitrogen gas. Oil-emulsifier mixture was added to the test tube to dissolve the antioxidants, and remaining chloroform was evaporated with nitrogen gas before the emulsions were prepared as usual.

2.7.3 Oxidation Experiments

All the oxidation experiments were performed in 10% (w/w) oil-in-water emulsions at a temperature of 30 °C and at the natural pH of the emulsions. The pH was measured after preparation of the emulsion and again after the oxidation experiments. Oxidation was studied in emulsions with both herring phospholipids and soy lecithin as emulsifiers, and also in emulsions with 0.2% xanthan gum. The volume of emulsion in each reaction chamber was 1.0 mL.

Lipid oxidation in emulsions was studied with Fe^{2+} (5, 10, 15, 20, 25 and 30 μM) and Fe^{3+} (25 μM) as prooxidants. The concentrations of antioxidants that were investigated are shown in Table 2.7.1. The concentrations were chosen based on previous experiments (Kristinová et al., 2009, Mozuraityte et al., 2007) and on observations done during the present study. All the oxidation experiments with antioxidants were performed with a concentration of prooxidant of 25 μM. The

influence of antioxidants was only investigated in emulsions with herring phospholipids as emulsifier (without xanthan gum).

Table 2.7.1: Concentrations of antioxidants in the emulsions in the oxidation experiments. The concentration of Fe^{2+} and Fe^{3+} was 25 µM in all the experiments.

Antioxidant	Prooxidant	Concentration of antioxidant in emulsion (µM)
EDTA	Fe^{2+} Fe^{3+}	7.5, 15, 25, 50 25
Citric acid	Fe^{2+} Fe^{3+}	7.5, 12.5, 25, 50 25
Caffeic acid	Fe^{2+} Fe^{3+}	10, 25, 50, 100, 200, 500 25
Propyl gallate	Fe^{2+} Fe^{3+}	25, 100, 200, 500 100
Ascorbic acid	Fe^{2+} Fe^{3+}	25, 50, 100, 200 50
α-Tocopherol	Fe^{2+}	100, 200, 300
β-Carotene	Fe^{2+}	100, 200, 300
Astaxanthin	Fe^{2+} Fe^{3+}	100, 200, 300 100, 200, 300

In addition to the experiments given in Table 2.7.1 combinations of α-tocopherol (100, 200 and 300 µM) and ascorbic acid (50, 100 and 200 µM) and combination of EDTA (50 µM) and ascorbic acid (50 µM) were investigated with Fe^{2+} as prooxidant. The influence of addition of water (50 µL) and ethanol (~5%, 50 µL) was also investigated since all but the lipid soluble antioxidants were added to the emulsions dissolved in water or ethanol.

The oxygen electrodes were calibrated before the oxidation experiments. This was done by measuring the oxygen concentration in distilled water saturated with oxygen, and in distilled water where the oxygen had been removed by addition of a small amount of dithionate. The measurement in water saturated with oxygen was repeated after the measurement in water without oxygen. The measurements were performed until constant oxygen uptake rates (OUR) were obtained.

The oxygen consumption in the emulsions was observed during the oxidation experiments. Figure 2.7.2 shows a representative curve for the consumption of oxygen in emulsion added antioxidant and thereafter prooxidant. The background OUR (r_0) was observed for 5-10 minutes before addition of antioxidant, and for another 5-10 minutes before addition of prooxidant (r_1). Prooxidant was added to initiate oxidation and the decrease in oxygen concentration was followed for 10-30 minutes depending on the progress of the oxidation. The oxidation rates were found by subtracting the background OUR from the OUR after addition of prooxidant, $r = r_2 - r_0$. The rates were found by using the oxygraph software Oxyg32 where the rate between a start- and end-point chosen by the user is determined. The oxygraph software was also used to determine the oxygen concentration at the top and bottom of the drop observed immediately after addition of prooxidant.

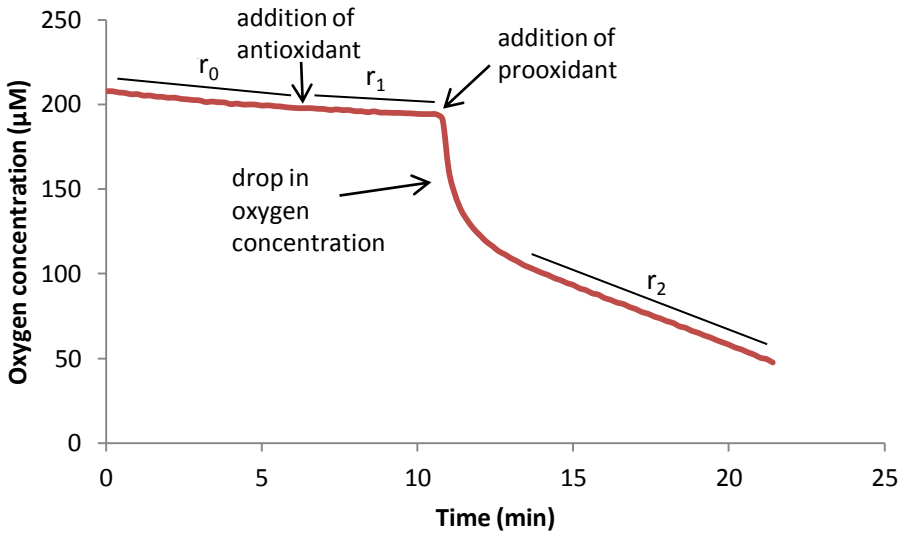

Figure 2.7.2: Representative curve for oxygen concentration in emulsion added antioxidant and thereafter prooxidant.

The effects of the antioxidants were determined by comparison of the oxidation rates and the magnitude of the drops in emulsions with antioxidants to those in emulsions without antioxidants. The comparison was done for experiments with the same prooxidant, and for oxidation in emulsions added water or ethanol in the cases where the antioxidants were dissolved in water or ethanol. The influence of the antioxidants was calculated as shown in equation (19) for oxidation rates and in equation (20) for initial drop in oxygen concentration.

$$Inhibition(\%) = 100 - \left[\left(\frac{r_{with\ \ antioxidant}}{r_{without\ \ antioxidant}} \right) \cdot 100 \right] \quad (19)$$

$$Inhibition(\%) = 100 - \left[\left(\frac{drop_{with\ \ antioxidant}}{drop_{without\ \ antioxidant}} \right) \cdot 100 \right] \quad (20)$$

If the oxygen concentration in the chamber reached zero during the measurements, oxygen was supplied to the reaction chamber by opening the plunger and blowing air into the solution with a Pasteur pipette. In these cases the oxidation curves were processed to give one continuous curve by combining the parts of the curve before and after addition of oxygen and removing the part in between, as illustrated in Figure 2.7.3.

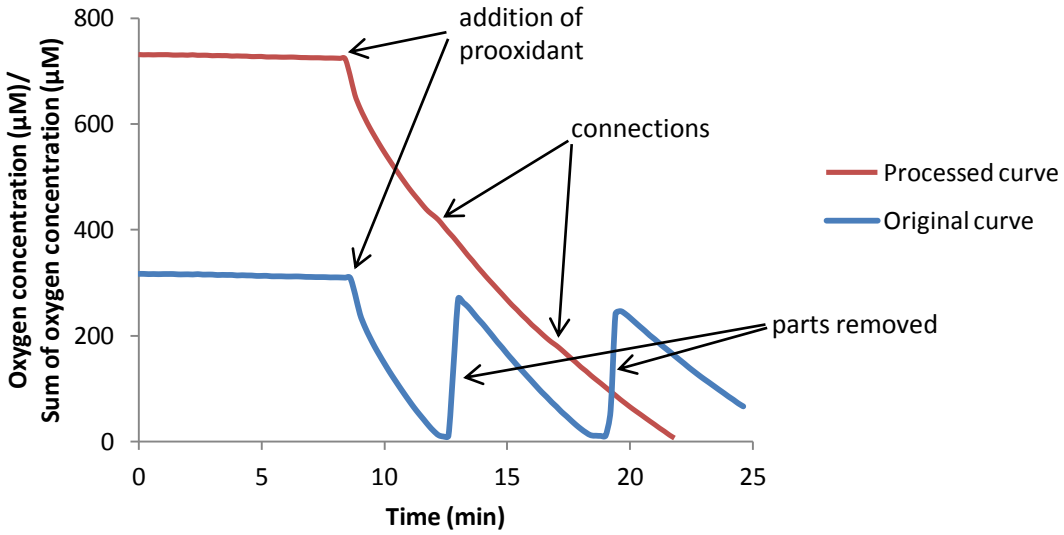

Figure 2.7.3: Original and processed curve for concentration of oxygen in emulsion. The processed curve is made by removing the parts of the curve corresponding to the time period where oxygen was added, and combining the remaining parts.

2.8 Statistical Analyses

Microsoft Excel was used for processing of data and statistical analyses. Student-*t* distribution was used as the probability distribution, and the level of significance was set to 95% (p = 0.05).

3 Results and Discussion

Before the oxidation experiments in emulsions could be carried out, it was necessary to improve the purity of the crude herring oil by washing. The first part of this chapter describes the influence of the washing on the purity and oxidation of the oil. The oil was later used for preparation of emulsions, and the preparation method had to be optimized to obtain emulsions with adequate stability and physical properties for oxidation experiments. This is described in the second part of this chapter. Finally, the results of iron catalyzed lipid oxidation in the emulsions analyzed by oxygen uptake measurements and the influence of antioxidants on this process are presented and discussed.

3.1 Influence of Washing on Purity and Oxidation of Herring Oil

The herring oil had not gone through any form for treatment after processing, and it was expected to contain impurities such as proteins, free fatty acids, phospholipids, minerals, antioxidants, pigments and sterols which are commonly present in crude oil (Chen et al., 2011). It was desirable to remove some of the impurities by washing the oil as described in section 2.1. To determine the influence of the washing treatment on the purity and oxidation of the oil the washing procedure was repeated three times, and the oil and water phases were collected for analyses. The analyses of the oil included determination of primary and secondary oxidation products and the content of carotenoids. The absorption spectra of the oil and water phases were analysed to get an indication of the purity of the phases and what type of compounds that were present.

3.1.1 Primary and Secondary Oxidation Products

The peroxide values, *p*-anisidine values and thiobarbituric acid reactive substances determined in the crude and washed oils are given in Table 3.1.1. The values are based on measurement data given in Appendix A.

Table 3.1.1: Oxidative status of crude and washed herring oil determined as PV, AV and TBARS. The results are the mean values ± SD (n=3-5).

	PV (meq peroxide/kg lipid)	AV	TBARS (µM/g lipid)
Crude oil	20.7 ± 0.7	3.3 ± 0.4	1.0 ± 0.2
Washed oil #1	21.32 ± 0.10	1.11 ± 0.09	0.90 ± 0.13
Washed oil #2	21.7 ± 0.4	1.5 ± 0.2	0.87 ± 0.09
Washed oil #3	24.25 ± 0.18	1.77 ± 0.07	1.05 ± 0.06

The peroxide values of the oils increased for each washing treatment. There was a significant decrease in the anisidine value after the first washing treatment, followed by an increase in the value for the following washing treatments. No significant differences between the amount of TBARS in the oil samples were found.

The increase in peroxide value for each washing treatment reveals that oxidation of the oil had taken place during the washing. This is as expected considering the exposure of the oil to high temperature, light and oxygen which promotes lipid oxidation. It is likely that decomposition of some lipid hydroperoxides took place during the washing as well, but the conditions of the washing treatment was probably not harsh enough to markedly decompose lipid hydroperoxides. The decrease in anisidine value after the first washing treatment could be due to removal of water soluble carbonyl compounds which react in the anisidine test. The increase in anisidine value for the following washing treatments can be explained the formation of new carbonyl compounds arising from lipid oxidation of the oil, which is likely to occur at the prevailing conditions. The similar values for TBARS for the different oil samples could be due to low influence of the washing treatment on the secondary oxidation products measured by this method.

3.1.2 Carotenoids

The carotenoid content in the crude and washed oils was analyzed by spectrophotometry and the determined values are given in Table 3.1.2. The values are based on measurement data given in Appendix B.

Table 3.1.2: Carotenoid content in crude and washed herring oil. The results are based on three measurements and are the mean values ± SD.

	Total carotenoid content (µg/g)
Crude oil	3.8 ± 0.4
Washed oil #1	1.64 ± 0.07
Washed oil #2	2.7 ± 0.4
Washed oil #3	2.8 ± 0.8

There was a significant decrease in the carotenoid content in the oil after the first washing treatment. The carotenoid content then increased for the following washing treatment, while the third washing did not result in changes in the carotenoid content. Carotenoids with polar properties, such as xanthophylls, may have been removed during the washing treatment, thus decreasing the carotenoid content in the washed oils. New carotenoids cannot be formed during the following washing treatments, but formation of compounds that absorb light at similar wavelengths as carotenoids could be the reason for the increased values.

3.1.3 Absorption Spectra of Oil and Water

The absorption spectra of the oil and water phases collected after each washing treatment were evaluated. The presence of compounds that absorb light in the visible and ultra violet spectra, such as pigments and conjugated dienes and trienes, can be detected by absorbance measurements. The absorption spectra of samples of pure oil are given in Figure 3.1.1, and the absorption spectra of samples of oil dissolved in iso-octane are given in Figure 3.1.2.

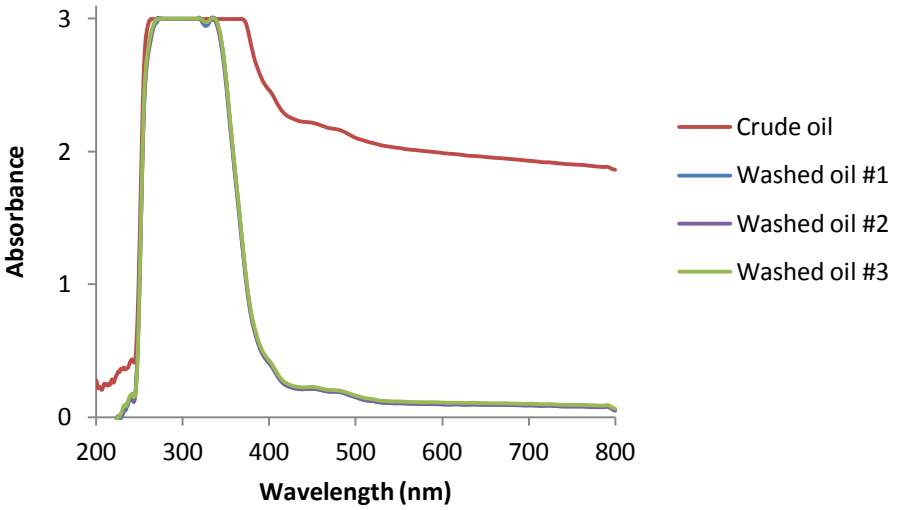

Figure 3.1.1: Absorption spectra of samples of pure crude and washed herring oil.

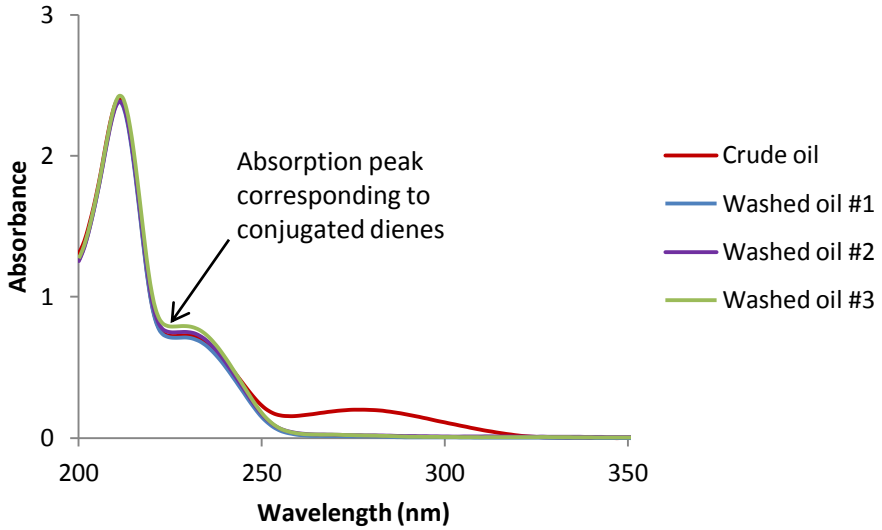

Figure 3.1.2: Absorption spectra of samples of crude and washed herring oil dissolved in iso-octane to a concentration of 0.001 g/mL. The absorbances in the interval 350-800 nm were zero for all samples and are omitted from the figure.

Both the absorption spectra of pure oil and of oil dissolved in iso-octane revealed a significant difference between the crude oil and the oil washed once. Only minor differences were observed between oils that had been washed one or several times. The pure crude oil showed higher absorbance than washed oil in the range 400-800

nm, which is probably due to impurities in the oil. The generally high absorbance at all wavelengths in the crude oil makes it difficult to draw conclusions regarding what type of compounds that were present in the oil, but crude oil normally contain several impurities as previously mentioned. The absorption spectra of oil dissolved in iso-octane showed an absorption maximum around 210 nm for both crude and washed oil. The identity of the compound this peak corresponds to is not known, but it could correspond to triacylglycerols, as triacylglycerols and their oxidation products are commonly measured at this wavelength (Okagami and Terui, 1996, Endo et al., 1997). An absorption peak around 230 nm were observed for all the samples and is likely to be due to the presence of conjugated dienes which have an absorption maximum at 234 nm (McClements and Decker, 2008). A slight increase in the intensity of the absorption peak at this wavelength can be observed for oils that had been washed an increasing number of times. This indicates formation of conjugated dienes in the oil during the washing treatment which indicates oxidation of the oil. Absorbance at 270 nm, corresponding to the absorption of conjugated trienes (McClements and Decker, 2008), was not observed in any of the washed oil samples. Conjugated trienes can only be formed in unsaturated lipids with at least three double bonds, and the amount of conjugated trienes in the oil could be too low to be observed by absorbance measurements in the diluted oil samples.

The absorption spectra of the water phases collected after each washing treatment are given in Figure 3.1.3.

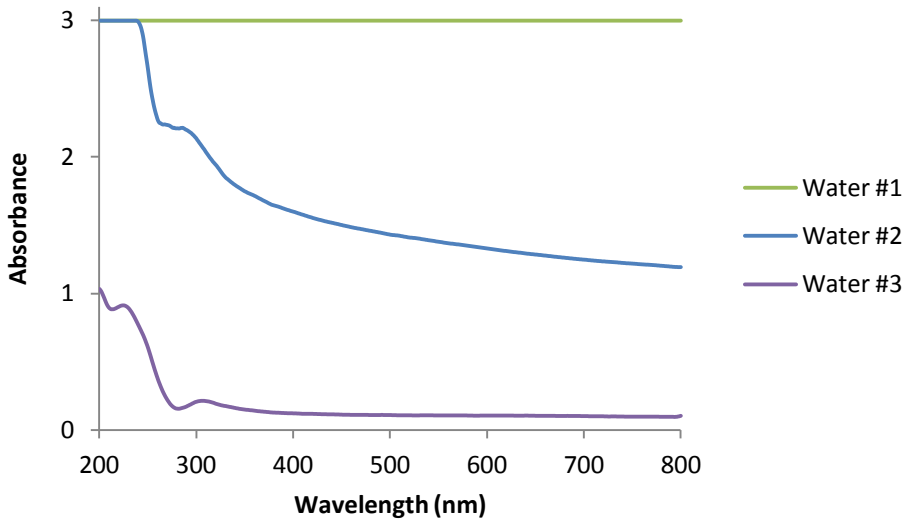

Figure 3.1.3: Absorption spectra of the water phases collected after each washing treatment of the oil.

The absorbance of the water phase collected after the first washing treatment was too high to be measured, as indicated by the invariable line at the absorbance value 3 for all wavelengths. A significant decrease in the absorbance over virtually the whole range of wavelengths was observed for the water phases from each following washing. The high absorbance of the water phase collected from the first washing treatment is likely to be due to impurities removed from the crude oil during the washing. This is in accordance with the high absorbance of the crude oil compared to the washed oils shown in Figure 3.1.1. The absorption spectra for the water phases after the second and third washing treatment showed peaks similar to the absorption spectra of the oils, and are probably due to the presence of oil in the water phases. The absorption spectra of the water phases showed a greater difference between each washing treatment than the absorption spectra of the oils.

Based on the analyses of the oil described in this section it was concluded that the first washing treatment had the greatest impact on the purity of the oil. This was especially evident from the absorption spectra of the oil and water phases, which revealed a significant difference after the first washing, whereas the changes for the following washing treatments were less pronounced. Also, the analyses of the anisidine value and content of carotenoids indicated removal of water soluble carotenoids and carbonyls from the oil after the first washing. The following washing treatments resulted in increasing oxidation of the oil, which was undesirable for the following oxidation experiments. One single washing treatment was considered to be sufficient for the oil used for preparation of emulsions. Due to the relatively high degree of oxidation of the herring oil used for the washing treatment experiments, it was decided to use herring oil from another production batch for the preparation of emulsions.

3.2 Herring Oil Used for Preparation of Emulsions

3.2.1 Primary and Secondary Oxidation Products

The oxidation status of the herring oil used to prepare emulsions was determined by measuring peroxide values, *p*-anisidine values and thiobarbituric acid reactive substances. The results are shown in Table 3.2.1. The values are based on measurement data given in Appendix A.

Table 3.2.1: Oxidation status of crude and washed herring oil determined as PV, AV and TBARS. The values are the mean values ± SD (n=3-4).

	PV (meq peroxide/kg lipid)	AV	TBARS (µM/g lipid)
Crude oil	3.15 ± 0.02	1.15 ± 0.18	0.39 ± 0.05
Washed oil	3.73 ± 0.05	1.61 ± 0.14	0.44 ± 0.05

The determined values for PV, AV and TBARS were higher for the washed than for the crude oil indicating that oxidation of the lipids had taken place during the washing process. This is as expected and similar to what was observed for the oil in the washing treatment experiment. The anisidine value of this oil was found to increase after the washing, which is in contrast to what was observed for the oil used in the washing treatment experiments, where the anisidine value decreased after the first washing. It is possible that the newer oil did not contain water soluble carbonyls that could be removed by washing.

The oxidation values for this oil were considerably lower than for the oil used in the washing treatment experiment, which can be explained by the more recent production date and consequently shorter storage time of this oil. The oils were also produced at different times of the year and seasonal changes in the lipid composition of herring oil is expected since the fish goes through a maturing cycle (Aidos et al., 2002). This can influence the amount of polyunsaturated fatty acids in the oil which will affect its susceptibility to oxidation.

3.2.2 Carotenoids

The content of carotenoids in the crude and washed oil was analyzed by spectrophotometry and the results are given in Table 3.2.2. The values are based on measurement data given in Appendix B.

Table 3.2.2: Carotenoid content in crude and washed herring oil. The results are based on three measurements and are the mean values ± SD.

	Total carotenoid content (µg/g)
Crude oil	3.2 ± 0.8
Washed oil	1.80 ± 0.11

The determined carotenoid content was higher for the crude than the washed oil indicating that some carotenoids were removed during the washing process, as was also observed for the oil in the washing treatment experiment.

3.3 Preparation and Characterization of Emulsions

Emulsions were prepared by emulsification of oil, water and phospholipids as described in section 2.5. Different approaches were tried out in order to obtain stable emulsions with small droplets and narrow droplet size distributions. Emulsions with small droplets are nearly always more stable against creaming, coalescence and often also flocculation (Walstra, 1993) and a narrow size distribution is important as variation in the size of the droplets may influence oxidation of the lipids (McClements and Decker, 2000).

The influence of addition of small amounts of xanthan gum to emulsions is described in section 3.3.1 and the influence of variation of the emulsification time is described in section 3.3.2. The emulsions were evaluated according to their droplet size distribution and creaming stability. Measurement data can be found in Appendix C.

3.3.1 Influence of Xanthan Gum on Emulsion Stability

Small amounts of xanthan gum (0.1 and 0.2% (w/v)) were added to the aqueous phase of the emulsions before emulsification, and the droplet size distributions of these emulsions compared to emulsion without xanthan gum are presented in Figure 3.3.1.

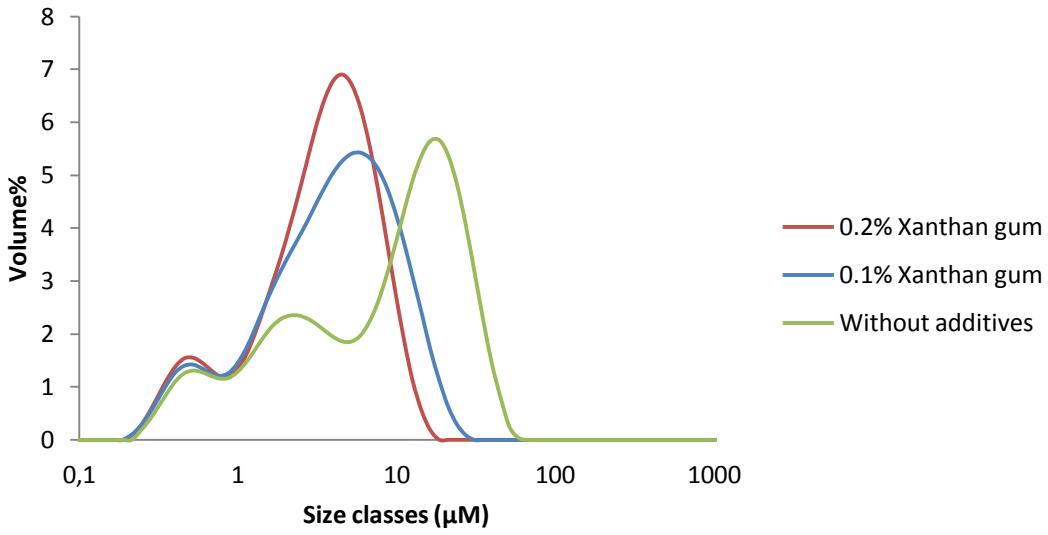

Figure 3.3.1: Size distribution of oil droplets in emulsions with xanthan gum (0.1 and 0.2%) and in emulsion without additives. The curves are based on data from five separate measurements performed on one sample of the emulsions.

Emulsions with xanthan gum showed a narrower droplet size distribution with generally smaller droplets than the emulsion without xanthan gum. Increasing concentration of xanthan gum resulted in a narrower distribution, but the average size of the droplets was only marginally different in the two emulsions, 4.60 ± 0.05 µM and 4.42 ± 0.00 µM for emulsions with 0.1% and 0.2% xanthan gum, respectively.

During the emulsification process oil droplets are deformed and possibly broken up, and contact between oil droplets can result in coalescence (Walstra, 1993). Addition of xanthan gum to the emulsions results in higher viscosity of the continuous phase which could prevent the droplets from coalescing during the emulsification process. Other studies have shown that xanthan gum did not have an influence on the average droplet size in emulsions, but rather induced flocculation and decreased creaming stability at low concentrations (Hemar et al., 2001, Sun et al., 2007). In these studies the emulsions were prepared with a homogenizer instead of a dispersing tool, which could be a reason for the different impact of xanthan gum.

The creaming stability measurements performed on emulsions with and without xanthan gum are given in Figure 3.3.2 shown as change (%) in absorbance with time.

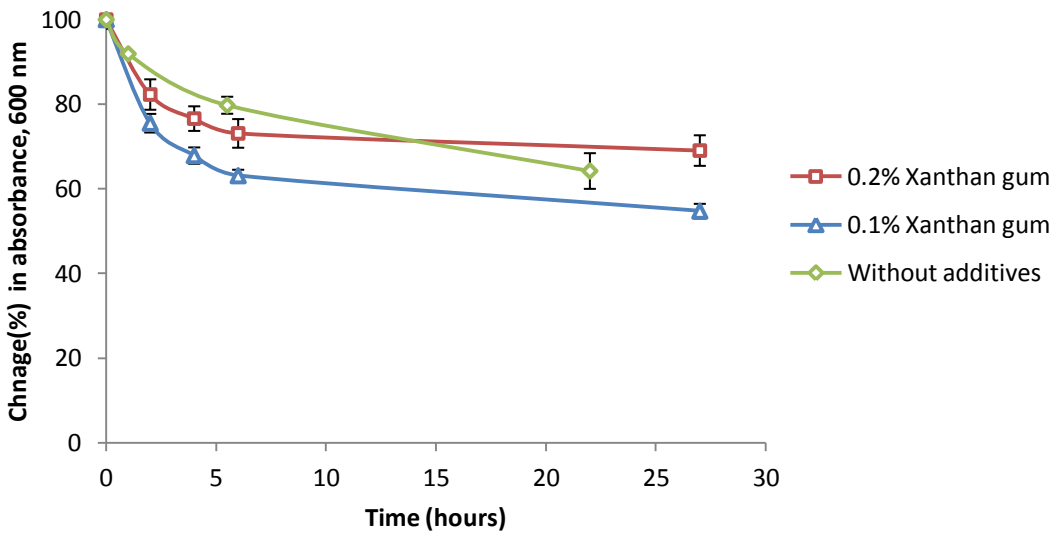

Figure 3.3.2: Effect of xanthan gum (0.1 and 0.2%) on creaming stability in emulsions shown as percentage decrease in absorbance with time. The values are the mean values of two to three measurements ± SD.

There was a decrease in absorbance with time for both the emulsions with and without xanthan gum which indicates creaming of the oil droplets the emulsions. The decrease was largest for emulsions with xanthan gum which could be due to increased flocculation of the droplets by a depletion mechanism causing more rapid creaming (Hemar et al., 2001). Increased concentration of xanthan gum resulted in decreased creaming tendency which is probably due to increased viscosity slowing down the upward movement of the droplets (Sun et al., 2007).

To investigate whether the use of emulsions stabilized with xanthan gum was suitable for the study of lipid oxidation in oil-in-water emulsions by oxygen uptake measurements, oxidation experiments in emulsions with and without xanthan gum were performed with Fe^{2+} (30 µM) as prooxidant. The curves for consumption of oxygen in the emulsions with time are shown in Figure 3.3.3.

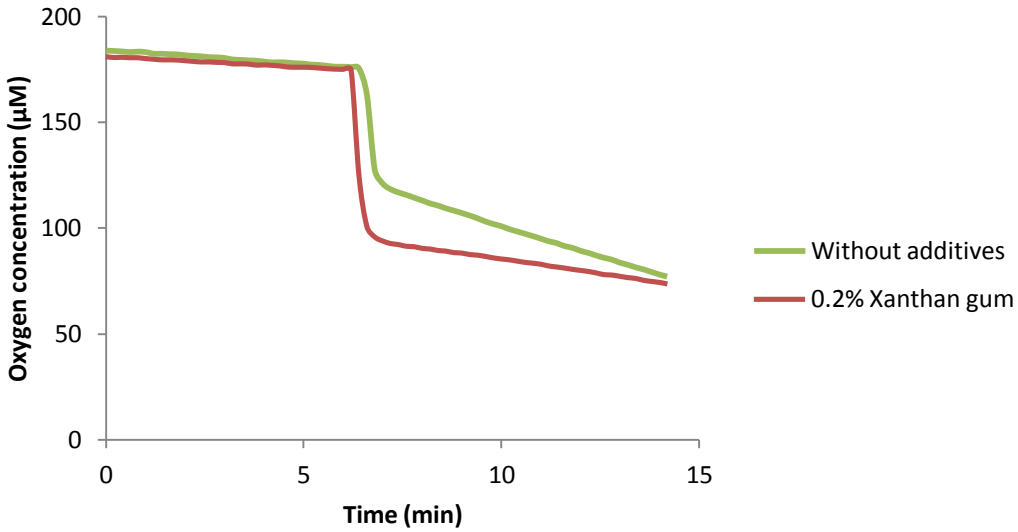

Figure 3.3.3: Comparison of oxygen consumption in emulsions with and without xanthan gum (0.2%). The oxidation was induced by Fe^{2+} (30 µM).

The oxidation curves in Figure 3.3.3 reveal a clear difference between Fe^{2+} induced oxidation in emulsions with xanthan gum compared to emulsions without xanthan gum. The drop in oxygen concentration immediately after addition of iron was greater in emulsions with xanthan gum, while the following linear oxygen uptake rate was significantly lower in emulsions with xanthan gum. The reason for the lower oxidation rates in emulsions with xanthan gum could be due to binding of Fe^{2+} by xanthan gum (Shimada et al., 1994). The reason for the larger initial drop in oxygen concentration in emulsions with xanthan gum is unknown.

The pronounced effect of xanthan gum on oxygen consumption in the emulsions was undesirable when the emulsions were going to be used to study lipid oxidation and the influence of antioxidants. It was therefore chosen not to use xanthan gum in the emulsions for this study, although it would be interesting to investigate the effect of xanthan gum on lipid oxidation and use in oxygen uptake measurements further.

3.3.2 Optimization of Emulsification Time

Emulsification times of 15 and 30 seconds, and 1, 2, 3, 4 and 8 minutes were tested and the droplet size distributions of some of these emulsions are given in Figure 3.3.4. The droplets size distributions for emulsification time of 1 and 3 minutes are not included in the figure as they did not provide any additional information. The droplets size distributions can be found in Appendix C.

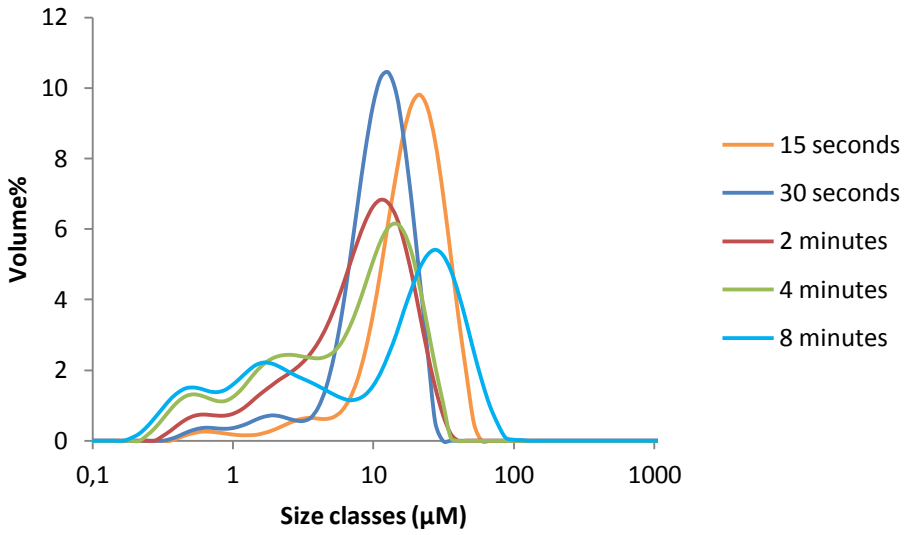

Figure 3.3.4: Size distribution of oil droplets in emulsions where the emulsification time was varied from 15 seconds to 8 minutes. The curves are based on data from five separate measurements performed on one sample of the emulsions.

The graphs in Figure 3.3.4 show that a shorter emulsification time resulted in smaller droplets and a narrower droplet size distribution, except for the shortest emulsification time of 15 seconds which resulted in larger droplets than the emulsification time of 30 seconds. Longer emulsification time could result in increased coalescence of droplets which explains the unsymmetrical distributions and larger droplets in the emulsions where the emulsification time was prolonged. The larger size of the droplets for the emulsification time of 15 seconds than for 30 seconds could be due to insufficient supply of energy to break up the droplets for the shortest emulsification time.

The creaming stability measurements performed on emulsions prepared by emulsification times of 2 and 4 minutes, and 30 seconds are presented in Figure 3.3.5. The results are shown as change (%) in absorbance with time.

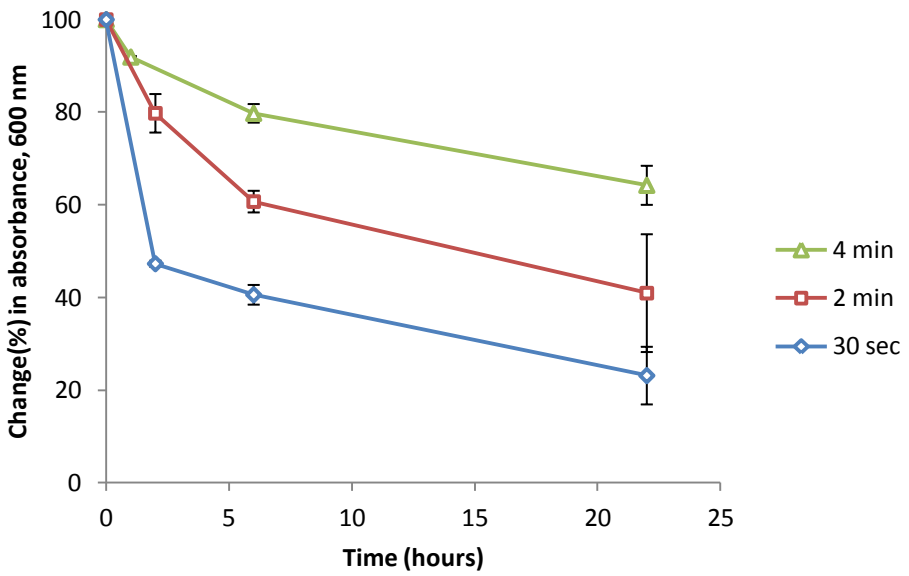

Figure 3.3.5: Creaming in emulsions prepared by emulsification for 2 and 4 minutes, and 30 seconds shown as percentage decrease in absorbance with time. The values are mean values of three measurements ± SD.

Emulsions prepared by longer emulsification times creamed at a slower rate than emulsions prepared by shorter emulsification times. Although emulsions prepared by longer emulsification times had an average larger droplet size, they also contained fewer large droplets and more small droplets than the emulsions prepared by shorter emulsification times. Creaming stability is usually poorer for emulsions with large droplets as they tend to rise to the top at an increased rate (Damodaran, 2005). Increased creaming rate for emulsions prepared by shorter emulsification times can be explained by more large droplets in these emulsions. Creaming is a reversible process and can be reversed by gentle shaking of the emulsions. The creaming stability measurements provide information about the stability and size of the droplets in the emulsion, but creaming will not be of great importance during the oxidation experiments where the emulsions are continuously stirred.

Based on the droplet size distributions, it was chosen to prepare emulsions emulsified for 30 seconds for the oxidation experiments as this emulsion had the smallest variation in droplet size. To verify that the droplet size distribution of the emulsions did not change significantly during the time it took to carry out the oxidation experiments, the droplet size distribution was determined four hours after preparation of the emulsion and compared to the distribution obtained shortly after the emulsion was made. The droplet size distributions for the different times are given in Figure 3.3.6.

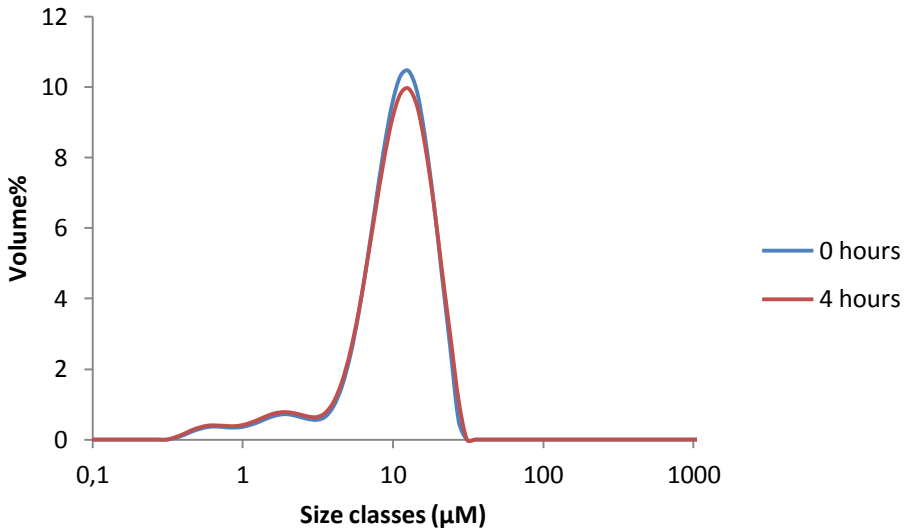

Figure 3.3.6: Droplet size distribution in emulsions shortly after emulsification (0 hours) and approximately 4 hours after emulsification. The emulsification time was 30 seconds. The curves are based on data from five separate measurements performed on one sample of the emulsions.

The graphs in Figure 3.3.6 reveal only minimal changes in the droplet size distribution four hours after the emulsion was made. Four hours were considered to be sufficient time to carry out oxidation experiments for one batch of emulsion.

3.4 Iron Catalyzed Lipid Oxidation in Emulsions

Lipid oxidation catalyzed by Fe^{2+} and Fe^{3+} was analyzed in emulsions with herring phospholipids and soy lecithin as emulsifiers. The oxidation was evaluated by monitoring oxygen consumption in emulsions over time as described 2.7.3. Both the determined oxidation rates and the initial drop in oxygen concentration after addition of Fe^{2+} were used to evaluate the oxidation. The initial drops and oxidation rates are based on measurement data given in Appendix D.

3.4.1 Emulsions with Herring Phospholipids as Emulsifier

Representative curves for the consumption of oxygen in emulsions with herring phospholipids as emulsifier when Fe^{2+} and Fe^{3+} were used to initiate oxidation are shown in Figure 3.4.1.

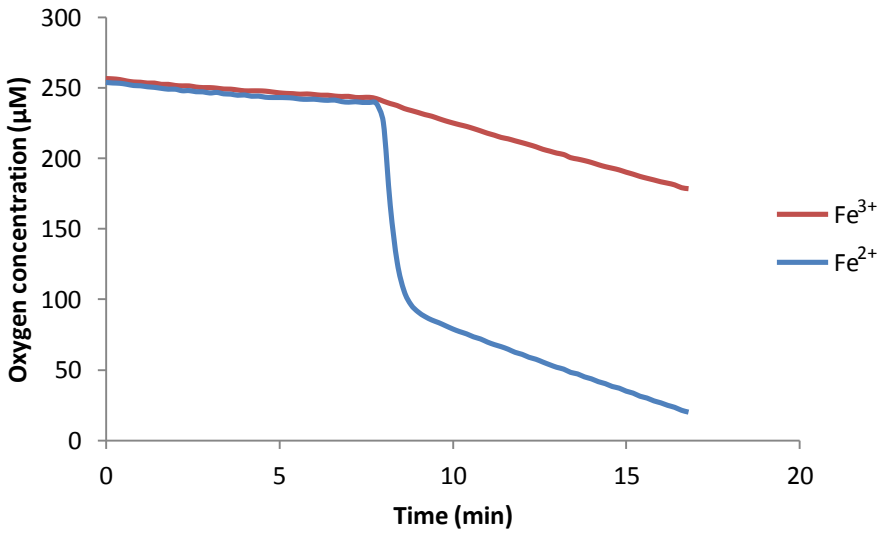

Figure 3.4.1: Representative curves for consumption of oxygen in emulsions added Fe^{2+} (25 µM) or Fe^{3+} (25 µM).

Addition of Fe^{2+} to the emulsions resulted in a rapid drop in the oxygen concentration immediately after addition of the prooxidant, followed by a linear decrease in the oxygen concentration. When Fe^{3+} was used as prooxidant, only the linear decrease in the oxygen concentration was observed. Mozuraityte et al. (2007) explained the drop in oxygen concentration after addition of Fe^{2+} with the rapid oxidation of Fe^{2+} to Fe^{3+} by pre-existing lipid hydroperoxides in the system. The reaction generates

alkoxyl radicals which react further to produce lipid alkyl radicals which react with oxygen. The constant linear oxygen uptake rate begins once all Fe^{2+} has reacted and the slower reaction between Fe^{3+} and lipid hydroperoxides becomes rate-limiting. The mechanism for iron catalyzed lipid oxidation proposed by Mozuraityte et al. (2007) is given in Figure 3.4.2.

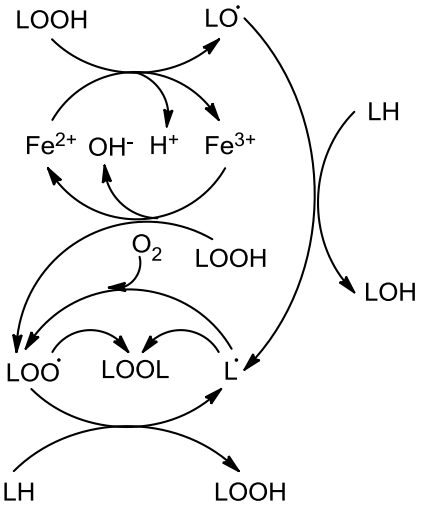

Figure 3.4.2: Mechanism for iron catalyzed oxidation of lipids (Mozuraityte et al., 2007).

Oxidation experiments with different concentrations of Fe^{2+} were performed and the influence on the initial drop in oxygen concentration and oxidation rates for the different concentrations are shown in Figure 3.4.3 and Figure 3.4.4, respectively.

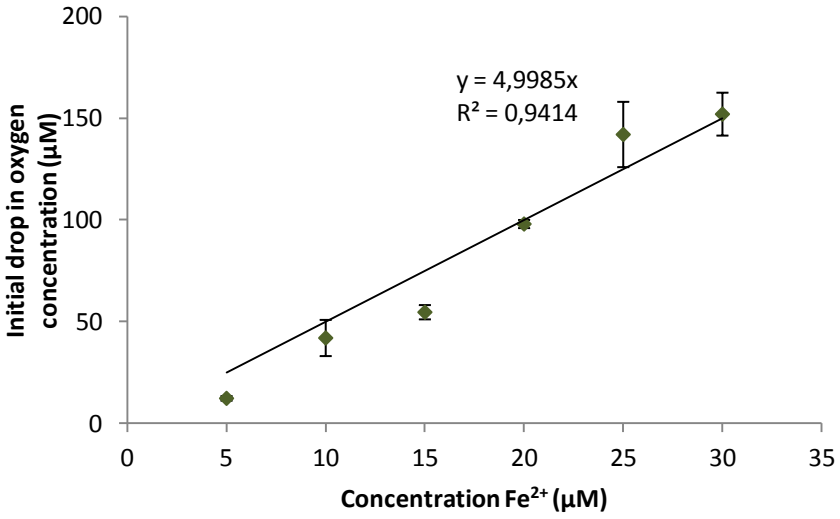

Figure 3.4.3: Drop in oxygen concentration observed immediately after addition of Fe^{2+} to emulsions for different concentrations of Fe^{2+}. The results are the mean values of three (except for 25 µM Fe^{2+} where n=15) parallel experiments ± SD.

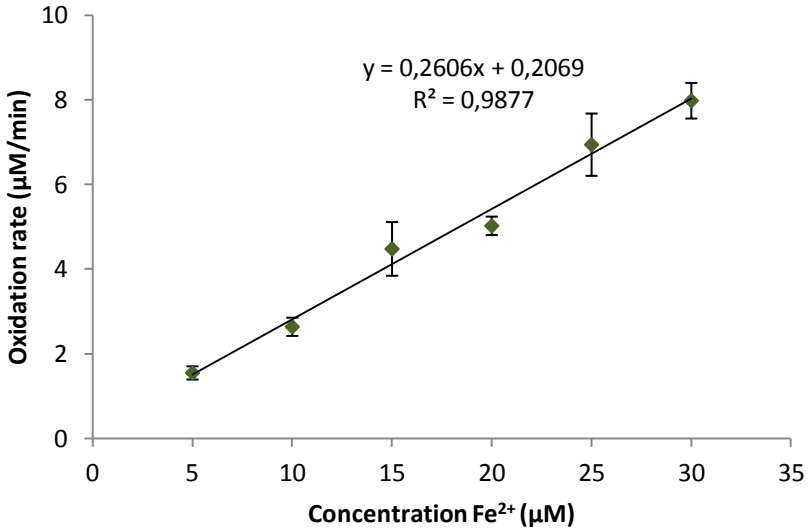

Figure 3.4.4: Oxidation rates for different concentrations of Fe^{2+}. The results are the mean values of three (except for 25 µM Fe^{2+} where n=15) parallel experiments ± SD.

There was a significant linear correlation ($p < 0.05$) between the amount of oxygen consumed in the initial drop and the concentration of Fe^{2+}. The initial drop in oxygen concentration was 5.0 ± 0.2 times higher than the concentration of Fe^{2+}, which means that one ion of Fe^{2+} is responsible for the consumption of several oxygen molecules. Similar trends were found for liposomes made from cod phospholipids,

5.6 ± 0.5 (Mozuraityte et al., 2007), and liposomes made from the same herring phospholipids used as emulsifier in these emulsions, 4.7 ± 0.2 (Aaneby, 2011). The amount of lipids was different in the three systems. The emulsions contained 10% lipids including 1% phospholipids, whereas the liposome solutions prepared from cod and herring phospholipids contained 0.6% and 1.5% phospholipids, respectively. The oxygen consumed in the initial drop as a function of concentration of iron was significantly lower for emulsions than liposomes when considering the total amount of lipids in the systems. A significant correlation ($p < 0.05$) was also found between the oxidation rates and the concentration of Fe^{2+} in the emulsions. A linear correlation between the oxidation rates and concentration of Fe^{2+} was also found for liposomes prepared from the herring phospholipids, but the oxidation rates were significantly lower in the emulsions, 0.261 ± 0.015 µmol O_2/µmol Fe^{2+}, than in the liposomes, 0.62 ± 0.07 µmol O_2/µmol Fe^{2+}. There are several differences between these model systems which could explain their different susceptibility to lipid oxidation.

The liposomes were prepared in a buffer solution adjusted to pH 5.5 before the oxidation experiments, and pH measurements performed after the oxidation experiments revealed only a minor decrease in the pH during the experiments. The emulsions, on the other hand, were prepared in distilled water and the oxidation experiments were carried out at the natural pH of the emulsions which varied between 5.2 and 5.8. The pH measured after the oxidation experiments was considerably lower with values varying between 4.4 and 3.3 depending on the amount of added iron because the iron was dissolved in acid. The measured pH values are given together with the oxidation rates in Appendix D. The lack of buffer capacity in the emulsions probably makes them more susceptible to changes in pH even for addition of small amounts of acid.

The pH is likely to affect the oxidation of the lipids in the system. Mozuraityte et al. (2006) found that liposomes made from cod phospholipids oxidized fastest at pH 4-5, whereas Sørensen et al. (2008) found that lipids in emulsions oxidized faster at pH 3 than at pH 6. The increased oxidation at lower pH was explained by increased solubility of iron at low pH. The charge of the surface of the oil droplets will also be affected by changes in pH, which could have influence on the interaction between the oil droplets and iron, and thus the oxidation rates (Mei et al., 1998). Emulsions stabilized with ionic emulsifiers have been found to be more oxidatively stable at low pH due to a positive surface charge of the emulsifier at lower pH which causes repulsion of iron (Donnelly et al., 1998). The zeta potential of the surface of the oil droplets in the emulsions was determined to -15 ± 5 mV at pH 5.5 ± 0.2 (Appendix C). The zeta potential typically becomes less negative or even positive when the pH is decreased, thus it can be expected that the zeta potential of the oil droplets was

less negative during the oxidation experiments. This was observed in the project work by Aaneby (2011) where the zeta potential of the liposomes made from herring phospholipids was determined was to be less negative at pH 3.5 (-5.3 ± 0.3 mV) than at pH 5.5 (-26 ± 5 mV). The lower oxidation rates in the emulsions than in the liposome solutions could be due to decreased association of iron with the lipids because of a less negative zeta potential of the oil droplets compared to the liposomes.

Different structural properties of emulsions and liposomes are likely to influence the oxidation of the lipids in the systems. Emulsions differ from liposomes by having the majority of the lipids in the interior core of the droplet so prooxidants, free radicals and oxygen need to diffuse into the core to initiate oxidation of these lipids (Waraho et al., 2011). Structures of a liposome and an emulsion oil droplet stabilized by phospholipids are shown in Figure 3.4.5.

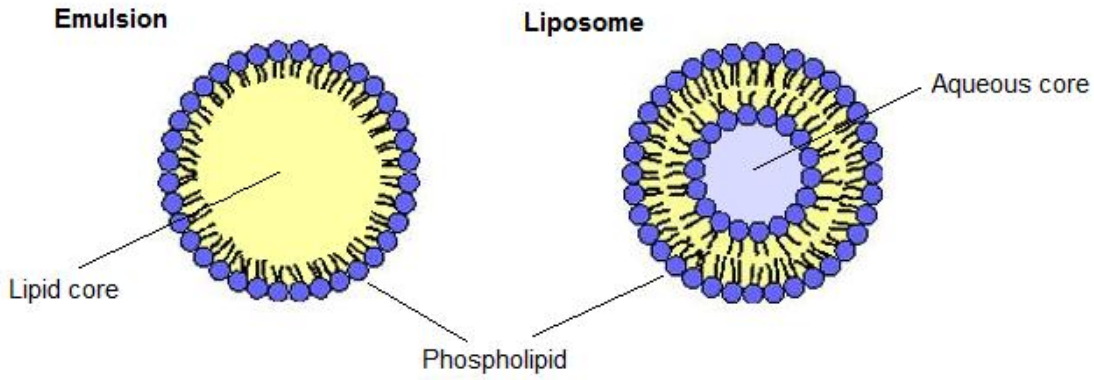

Figure 3.4.5: Structures of an emulsion oil droplet where a phospholipid monolayer enclose a core of lipids, and a liposome consisting of a bilayer structure of phospholipids enclosing an aqueous core.

The interface of the oil droplets in the emulsions consisted of unsaturated phospholipids which are themselves oxidizable. The concentration of phospholipids was higher in the liposome solutions (1.5%) than in the emulsions (1%), but as shown in Figure 3.4.5, a significant amount of phospholipids in liposomes does not face the continuous phase. The average size of the oil droplets in the emulsions was determined to 10.9 ± 0.6 µM (Appendix C) which is generally bigger than the size of liposomes (100-200 nm). This means that the total surface area is larger for liposomes, and a greater amount of lipids will be exposed to the aqueous phase where oxidation is initiated which could result in increased oxidation rates of the lipids

in the liposomes. However, several studies have found that oxidation rates do not change significantly with surface area as the surface in most cases is large enough not to limit the reaction rates (Waraho et al., 2011).

Lipid oxidation is believed to be initiated at the oil-water interface where lipid hydroperoxides accumulate and react with compounds, such as iron, in the aqueous phase (McClements and Decker, 2000). The almost identical initial drop in oxygen concentration found for the liposomes prepared from herring phospholipids and the emulsions, could indicate that primarily lipid hydroperoxides located in phospholipid layer at the surface of the oil droplets are responsible for the initial reaction with Fe^{2+}. The significantly lower oxidation rates in the emulsions than in the liposomes could be due to faster propagation of oxidation in liposomes since a larger amount of the lipids in liposomes are directly available for interactions with prooxidants in the aqueous phase, compared to the majority of the lipids in the emulsions which are located in the interior of the oil droplets so that radicals need to diffuse into the interior of the droplets to propagate oxidation of the lipids (Coupland et al., 1996).

According to the mechanism given in Figure 3.4.2, the linear decrease in oxygen concentration should be the same when Fe^{2+} and Fe^{3+} are used to initiate oxidation. The oxidation rates were however found to be lower when Fe^{3+} was used as prooxidant (5.4 ± 0.5 µM/min) compared to when Fe^{2+} was used as prooxidant (6.9 ± 0.7 µM/min). The considerably lower solubility of Fe^{3+} (K_{sp} $2 \cdot 10^{-39}$) compared to Fe^{2+} (K_{sp} $4 \cdot 10^{-15}$) could result in precipitation of Fe^{3+} as a hydroxide in the emulsions, thus making it unavailable for initiating oxidation of lipid hydroperoxides. The difference between the oxidation rates when the oxidation was induced by Fe^{3+} compared to Fe^{2+} was greater in the emulsions than what have been found for liposomes (Kristinová et al., 2009, Mozuraityte et al., 2007, Aaneby, 2011). The reason for this can be that a higher concentration of iron was used to initiate oxidation in the emulsions which makes precipitation more likely. The generally lower oxidation rates in the emulsions could make the oxidation more sensitive to changes in the concentration of iron.

3.4.2 Emulsions with Soy Lecithin as Emulsifier

To investigate the impact of the properties of the emulsifier interface on lipid oxidation in emulsions, emulsions with soy lecithin as emulsifier were prepared. Oxygen consumption in emulsions with soy lecithin as emulsifier compared to oxygen consumption in emulsion with herring phospholipids as emulsifier is shown in Figure 3.4.6.

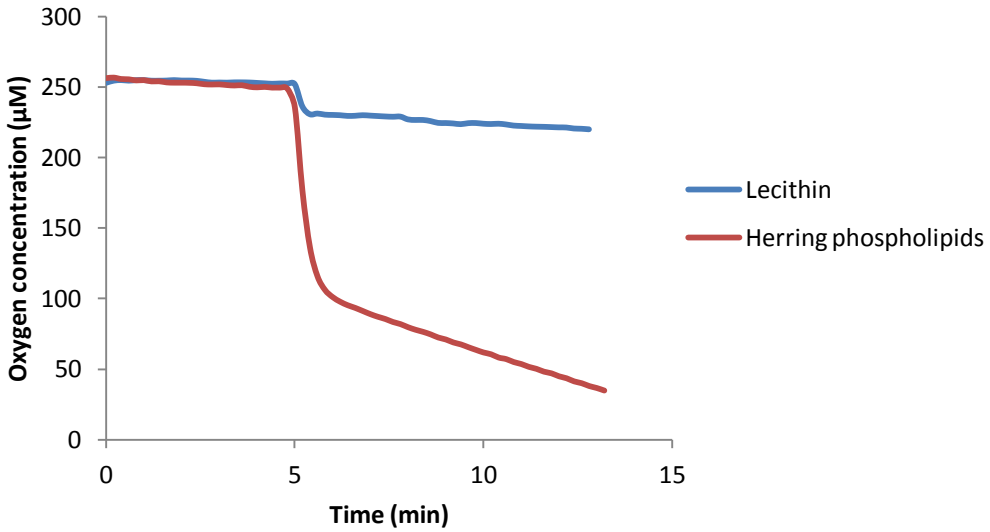

Figure 3.4.6: Oxygen consumption in emulsions with soy lecithin and herring phospholipids as emulsifier when Fe^{2+} (25 µM) was used as prooxidant.

The initial drop in oxygen concentration and the following linear oxygen uptake rate was significantly lower in emulsions with soy lecithin as emulsifier compared to in emulsions with herring phospholipids as emulsifier. The oxidation rates and initial drop in oxygen concentration in emulsions with soy lecithin as emulsifier for different concentrations of Fe^{2+} are given in Table 3.4.1.

Table 3.4.1: Oxidation rates and initial drops in oxygen concentration for different concentrations of Fe^{2+} in emulsions with soy lecithin as emulsifier. The results are the mean values of three parallel experiments ± SD.

Concentration Fe^{2+} (µM)	Oxidation rate (µM/min)	Initial drop in oxygen concentration (µM)
10	-0.2 ± 0.2	6 ±1
20	-0.5 ± 0.7	10 ± 2
25	-0.6 ± 0.5	17 ± 5
30	-0.6 ± 0.3	17 ± 2

The initial drop in oxygen concentration when Fe^{2+} was added to emulsions with soy lecithin as emulsifier only slightly increased with increasing concentration of iron, and was significantly lower than in emulsions with herring phospholipids as emulsifier. The following linear oxygen consumption was completely inhibited in emulsions with soy lecithin for all concentrations of Fe^{2+}, as indicated by the negative oxidation rates in Table 3.4.1. Faster oxidation of lipids in emulsions with herring phospholipids as

emulsifier was also observed by sensory analyses of the emulsions without added iron. Discolouration and development of off-odours were observed after a few days of storage in room temperature of the emulsion with herring phospholipids as emulsifier, while the sensory appearance of the emulsion with soy lecithin not was observed to change during this time.

The pH of the emulsions with soy lecithin was initially around 6.1 to 6.2, and decreased to between 5.7 and 5.1 after the oxidation experiment depending on the amount of added iron. Thus, the emulsions with soy lecithin as emulsifier showed better pH stability regarding additions of acid. Different composition of phospholipid classes in the two emulsifiers could be the reason for different susceptibility to changes in pH. It is possible that the different susceptibility to oxidation of emulsions with soy lecithin and herring phospholipids was due different pH of the emulsions, but other aspects of the emulsions are considered to be important for influences on the oxidation rates as well. Soy lecithin contains different classes of phospholipids with varying fatty acid composition including both saturated and unsaturated fatty acids (Scholfield, 1981). Long chain polyunsaturated fatty acids (i.e. EPA and DHA) are commonly not present in soy lecithin, hence soy phospholipids are expected to be less susceptible to oxidation. It is possible that the soy phospholipids formed a protective unoxidizable layer around the emulsion droplets so initiation and propagation of oxidation of lipids in the core of the emulsion droplets was inhibited.

The amount of lipid hydroperoxides in the emulsifier has been shown to influence oxidation of lipids in emulsions. In studies by Horn et al. (2012) were emulsions with milk phospholipids as emulsifier found to oxidize faster than emulsions with lecithin, despite a higher content of unsaturated fatty acids in lecithin. This was explained by the higher peroxide value of the milk phospholipids compared to the lecithin. The herring phospholipids was determined to contain 8.9 ± 0.9 meq peroxide/kg lipid in the project work by Aaneby (2011). It is possible that emulsions with soy lecithin did not oxidize due to low amounts of lipid hydroperoxides in the interfacial layer. Also, different saturation of the phospholipids used as emulsifier could have influence on the structure of the interfacial layer and thus interaction between lipids and transition metals (Horn et al., 2012). It can be assumed that the oil within the core of the emulsion droplets in emulsions with soy lecithin as emulsifier was not oxidized since the oxygen consumption in the emulsions was virtually completely inhibited. Whether the oil in the interior of the oil droplets in emulsions with herring phospholipids as emulsifier was oxidized, or if the oxygen consumption was due to oxidation of the phospholipids at the interface is not know.

3.5 Influence of Antioxidants on Iron Catalyzed Lipid Oxidation

Iron catalyzed lipid oxidation was analyzed in emulsions with EDTA, citric acid, caffeic acid, propyl gallate, α-tocopherol, ascorbic acid, β-carotene, astaxanthin and combinations of α-tocopherol and ascorbic acid. All but the lipid soluble antioxidants were added to the emulsions dissolved in water or ethanol, and the influence of addition of water or ethanol alone was therefore investigated first. The change (%) in background oxygen uptake rate, initial drop in oxygen concentration and oxidation rates for Fe^{2+} and Fe^{3+} catalyzed oxidation compared to emulsions without any additives are shown in Figure 3.5.1.

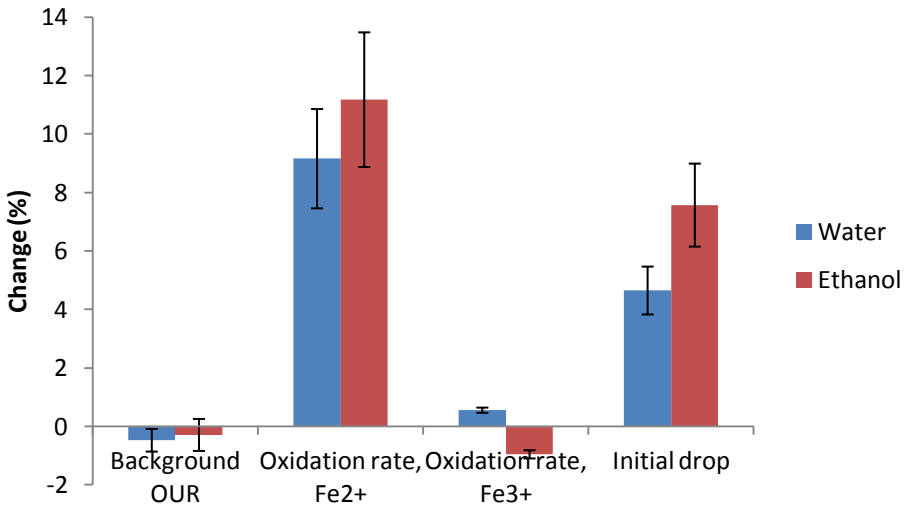

Figure 3.5.1: Change (%) in background OUR, initial drop in oxygen concentration and oxidation rates when Fe^{2+} (25 µM) and Fe^{3+} (25 µM) were used as prooxidants in emulsions added water (50 µL) or ethanol (5%, 50 µL) compared to in emulsions without additives. The results are the mean values ± SD (n=6-12).

The background oxygen uptake rates showed a slight decrease when water or ethanol was added to the emulsions. The oxidation rates for Fe^{3+} catalyzed oxidation only showed a minor change, while the oxidation rates and initial drop in oxygen concentration in Fe^{2+} catalyzed oxidation were higher compared to in emulsions without added water or ethanol. The increase in oxidation rates and initial drop in oxygen concentration could be due to dilution of the emulsions and higher solubility of iron.

Oxidation in emulsions with antioxidants was compared to oxidation in emulsions without antioxidants, and the effects of the antioxidants were calculated as described in section 2.7.3. The antioxidants were evaluated both by their influence on the

oxidation rates and on the initial drop in oxygen concentration after addition of Fe^{2+}. The oxidation rates and initial drop in oxygen concentration were compared to those in emulsions with water or ethanol, respectively. The calculations are based on measurement data given in Appendix D.

3.5.1 Citric Acid and EDTA

Oxidation curves for emulsions with citric acid and EDTA compared to oxidation in emulsions without antioxidant when the oxidation was induced by Fe^{2+} are shown in Figure 3.5.2.

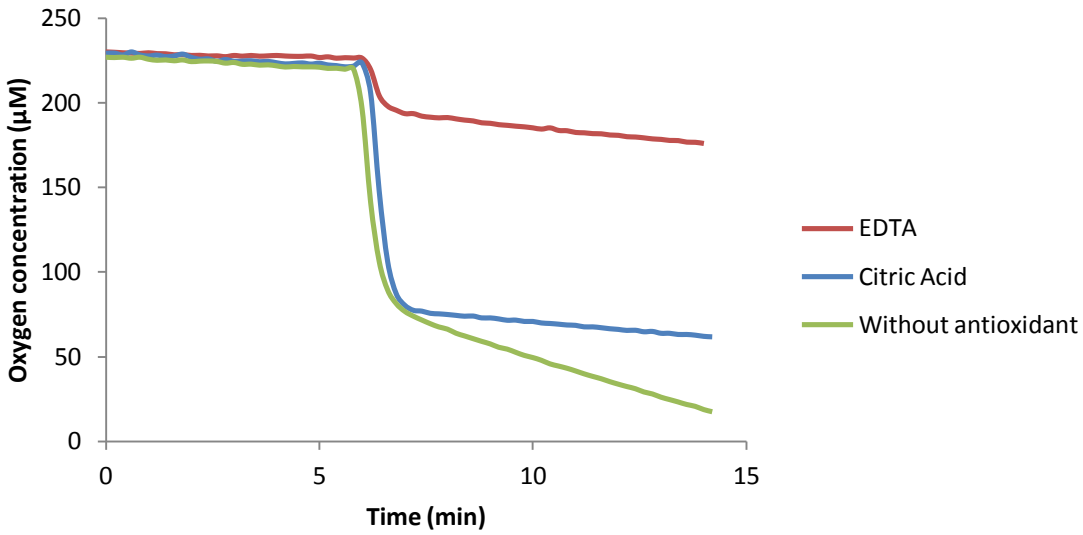

Figure 3.5.2: Oxidation curves showing the consumption of oxygen in emulsions with EDTA (25 µM), citric acid (25 µM) and without antioxidant when Fe^{2+} (25 µM) was used to initiate the oxidation.

The oxidation curves in Figure 3.5.2 show that both EDTA and citric acid reduced the oxidation rates compared to in emulsions without antioxidant, but only EDTA reduced the initial drop in oxygen concentration after addition of Fe^{2+}. Oxidation experiments with different concentrations of the antioxidants were performed and the effects on the oxidation rates and initial drop in oxygen concentration for the different concentrations are given in Figure 3.5.3.

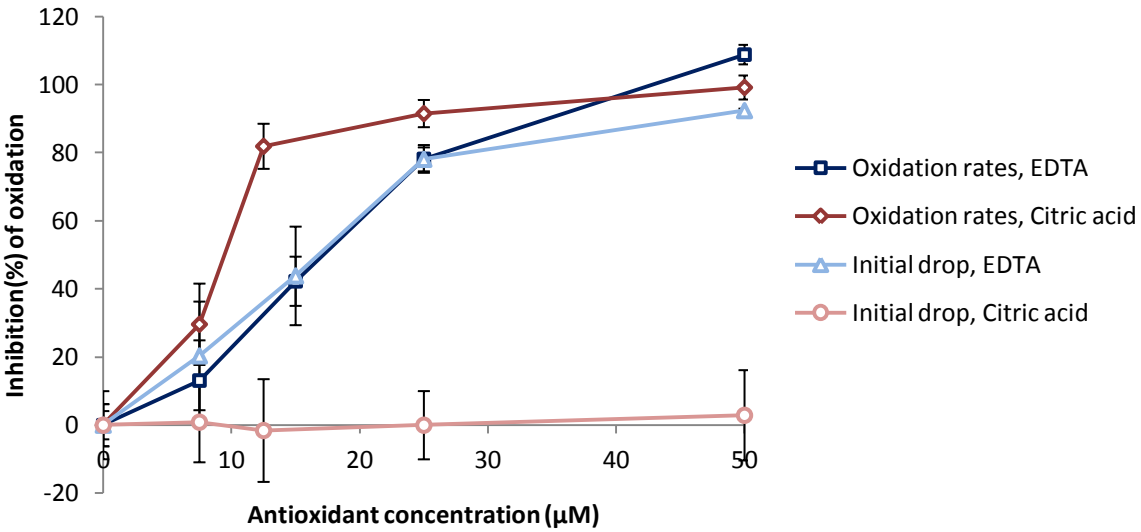

Figure 3.5.3: Inhibition (%) of oxidation rates and initial drop in oxygen concentration in emulsions with different concentrations of EDTA and citric acid when Fe^{2+} (25 µM) was used as prooxidant. The results are the mean values ± SD (n=3).

The graphs in Figure 3.5.3 show that increasing concentrations of the antioxidants lead to greater inhibition of the oxidation rates, and complete inhibition was observed at an antioxidant concentration twice as high as the concentration of iron. Citric acid did not have any significant influence on the initial drop in oxygen concentration for any of the concentrations investigated, whereas increasing concentrations of EDTA resulted in decreasing amount of oxygen consumed in the initial drop. Citric acid seemed to inhibit the oxidation rates to a larger extent than EDTA at the lower concentrations. The inhibitory effect of EDTA was greatly improved when the concentration of EDTA was greater than that of iron, which is similar to results found by Hu et al. (2004). Only small amounts of iron associated with the emulsions droplets are needed to accelerate lipid oxidation (Mei et al., 1998), which could explain why the oxidation rates were not markedly reduced until EDTA was added in equal ratio to iron. Hu et al. (2004) did not find citric acid to have an impact on lipid oxidation induced by Fe^{2+} in emulsions at pH 3.0, which is in contrast to the results found in these oxidation experiments. Lipid oxidation was in the studies by Hu et al. (2004) evaluated by formation of lipid hydroperoxides and aldehydes. It is possible that some oxidation products were formed in the emulsions with citric acid since the initial reaction between Fe^{2+} and lipid hydroperoxides was not inhibited by citric acid.

The pH of the emulsions has influence on the ionization of the chelators and their ability to chelate metal ions. Only one of the four ionizable groups of citric acid (pK_1 3.13, pK_2 4.76, pK_3 6.40 and $pK_4 \approx 11$ (hydroxyl group) (Pierre and Gautier-Luneau,

2000)) will be ionized at pH 3.5, whereas four of the ionizable groups of EDTA (pK_1 0.0, pK_2 1.5, pK_3 2.00, pK_4 2.69, pK_5 6.13 and pK_6 10.37 (Harris, 2010)) will be ionized at this pH. The more negative charge of EDTA is likely to make it more reactive towards positively charged iron ions. Citric acid has a possibility of binding more than one ion of Fe^{3+} (Pierre and Gautier-Luneau, 2000), which could explain why citric acid is more efficient than EDTA in inhibiting the oxidation rates when iron is in excess.

The initial drop in oxygen concentration was almost undetectable when the emulsion contained EDTA in twice the ratio to iron. The very rapid reaction between Fe^{2+} and lipid hydroperoxides probably makes complete inhibition of the drop difficult, and some free Fe^{2+} will still be present even though the emulsion contains more EDTA than iron. It is also possible that iron can decompose lipid hydroperoxides even when it is complexed with EDTA (Schaich, 1992). The lack of influence of citric acid on the initial drop in oxygen concentration indicates that citric acid did not form a nonreactive complex with Fe^{2+} in the emulsions. Francis and Dodge (1993) found that citric acid formed a tridentate complex with Fe^{3+}, $[Fe(III)(OH)\ Cit]^-$, at pH 3.5, while a tridentate complex between Fe^{2+} and citric acid, $[Fe(II)\ Cit]^-$, was not formed until pH 5. This can explain why citric acid was not able to inhibit the drop in the emulsions with pH around 3.5.

The inhibitory effects of citric acid and EDTA when the oxidation was induced by Fe^{3+} compared to Fe^{2+} are presented in Figure 3.5.4. The percentage inhibitions are based on uninhibited oxidation induced by Fe^{3+} and Fe^{2+}, respectively.

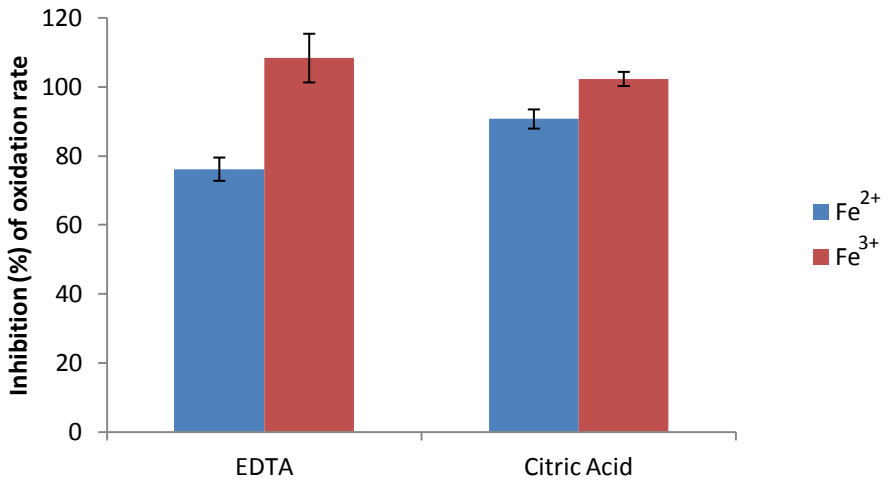

Figure 3.5.4: Inhibition (%) of oxidation rates when Fe^{2+} (25 µM) and Fe^{3+} (25 µM) were used as prooxidants in emulsions containing EDTA (25 µM) or citric acid (25 µM). The results are the mean values ± SD (n=3).

Both citric acid and EDTA were able to inhibit oxidation at lower concentrations when the oxidation was induced by Fe^{3+} compared to Fe^{2+}. The oxidation was completely inhibited when the concentration of the chelating agent was equal to that of iron, rather than twice to that of iron which was observed for Fe^{2+} induced oxidation. EDTA is known to chelate Fe^{3+} (stability constant $1.3 \cdot 10^{25}$) more favourably than Fe^{2+} (stability constant $2.0 \cdot 10^{14}$). This explains the larger effect of EDTA on lipid oxidation induced by Fe^{3+} compared to Fe^{2+}. In contrast to oxidation induced by Fe^{2+}, EDTA was more efficient than citric acid in inhibiting oxidation induced by Fe^{3+}. This can be explained by the higher binding constant EDTA has for Fe^{3+} compared to what citric acid has for Fe^{3+} (stability constant $1.5 \cdot 10^{11}$) (Hu et al., 2004).

3.5.2 Phenolic Compounds

Comparison of oxidation curves for emulsions with the phenolic compounds caffeic acid, propyl gallate, α-tocopherol and emulsion without antioxidant when the oxidation was induced by Fe^{2+} are given in Figure 3.5.5.

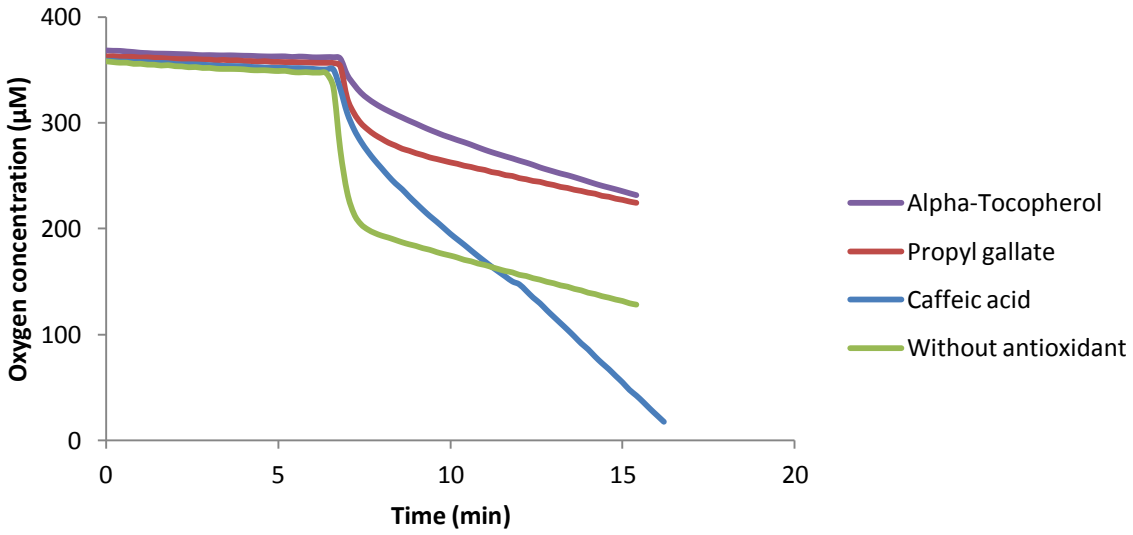

Figure 3.5.5: Oxidation curves for emulsions with α-tocopherol (100 µM), propyl gallate (100 µM), caffeic acid (100 µM) and without antioxidant when the oxidation was induced by Fe^{2+} (25 µM).

The initial drop in oxygen concentration was clearly reduced in emulsions containing α-tocopherol and propyl gallate. A decrease in the initial drop in emulsions with caffeic acid was also observed, but the linear oxygen uptake rate was greatly enhanced. Emulsions with propyl gallate showed a slight reduction in the following linear oxygen uptake rate, whereas α-tocopherol increased the oxygen uptake rate. Different concentrations of the phenolic compounds were investigated, and the effect on oxidation rates and initial drop in oxygen concentration were determined.

Caffeic acid

The increase (%) in the oxidation rates as a function of concentration of caffeic acid is plotted in Figure 3.5.6.

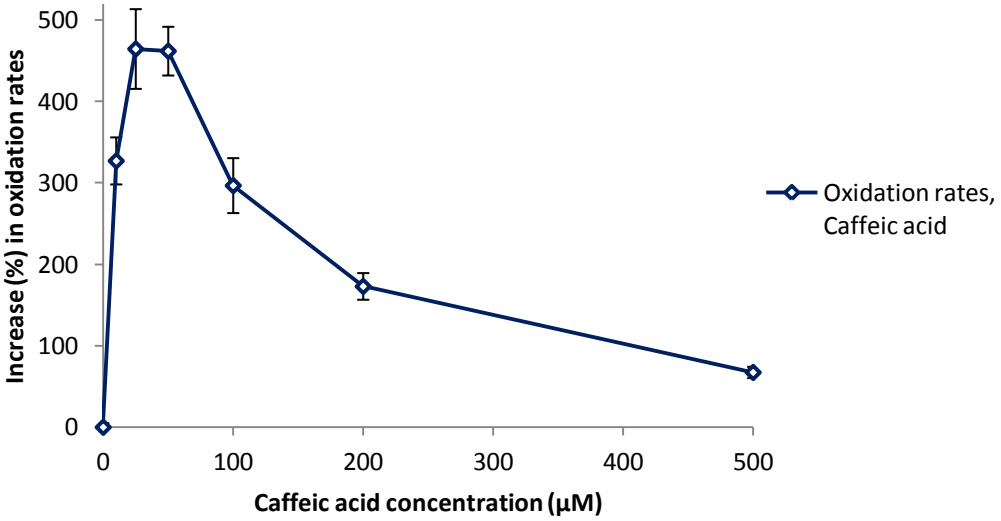

Figure 3.5.6: Increase (%) in oxidation rates by different concentrations of caffeic acid when Fe^{2+} (25 µM) was used as prooxidant. The results are the mean values ± SD (n=3).

Caffeic acid strongly enhanced the oxidation rates at all tested concentrations, with a maximum prooxidative effect observed at 25-50 µM caffeic acid. Above this concentration, the oxidation rates decreased with increasing concentration of caffeic acid, but none of the tested concentrations reduced the oxidation rates. Prooxidative behaviour of caffeic acid was also observed in oil-in-water emulsions in studies performed by Sørensen et al. (2008) who evaluated formation of radicals, hydroperoxides and secondary lipid oxidation products, and in liposomes studied by oxygen uptake measurements by Kristinová et al. (2009). The prooxidative behaviour was explained by the ability of caffeic acid to reduce Fe^{3+} to the more catalytically active Fe^{2+}. Caffeic acid forms a complex with Fe^{3+} which subsequently decays through an electron transfer reaction which involves the reduction of Fe^{3+} to Fe^{2+} (Hynes and O'Coinceanainn, 2004). The mechanism for reduction of Fe^{3+} to Fe^{2+} by caffeic acid is shown in Figure 3.5.7.

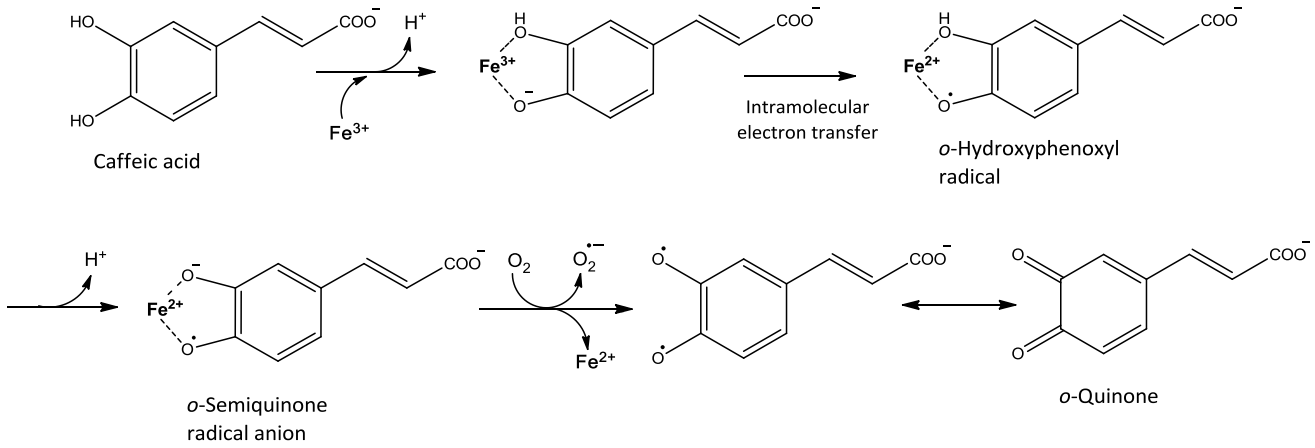

Figure 3.5.7: Mechanism for reduction of Fe^{3+} to Fe^{2+} by caffeic acid (Kristinová et al., 2009).

The maximum prooxidative effect of caffeic acid was observed at a ratio of caffeic acid to iron of about 1-2, which indicates that excess amount of caffeic acid did not result in increased rates of the reduction of Fe^{3+} to Fe^{2+}. This is in contrast to what was observed in the studies of iron catalyzed lipid oxidation in liposomes by Kristinová et al. (2009) where a maximum prooxidative activity of caffeic acid was observed at a ratio of caffeic acid to iron of about 20 at pH 3.0. The maximum increase in the oxidation rates by caffeic acid was lower in the emulsions (< 500%) than in the liposomes (> 600%). The different prooxidative activity of caffeic acid in the two systems could be due to different susceptibility of lipids to be oxidized in the systems as described in section 3.4.1. The activity of caffeic acid has been shown to depend on the physical state of the lipids and the system in which they are studied, and also on the type of prooxidant present (Medina et al., 2011)

The decreasing prooxidative effect of caffeic acid when it was present at concentrations greater than 50 µM, could be due to chelation of iron or scavenging of free radicals by caffeic acid. The interaction between iron and caffeic acid was found to be prooxidative as it resulted in reduction of iron, but it is possible that increased concentration of caffeic acid resulted in a more stable complex between iron and caffeic acid. To function as a chain-breaking antioxidant caffeic acid needs to be in vicinity of the free radicals generated in the lipid phase. Caffeic acid has a polar character due to its carboxylic acid group, but the group will be protonated at pH 3.5 making the compound less polar which might facilitate accessibility of caffeic acid at the interface of the emulsions droplets (Kristinová et al., 2009).

Caffeic acid reduced the oxygen concentration consumed in the initial drop, and reduction (%) of the drop for the different concentrations of caffeic acid are plotted in Figure 3.5.8.

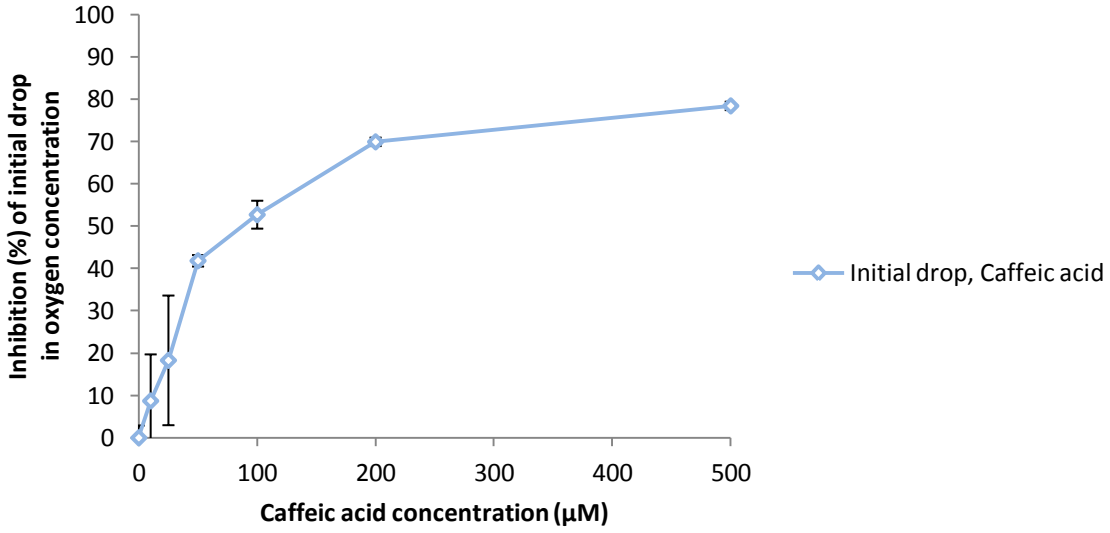

Figure 3.5.8: Inhibition (%) of the initial drop in oxygen concentration by different concentrations of caffeic acid when Fe^{2+} (25 µM) was used as prooxidant. The results are the mean values ± SD (n=3).

Increasing concentrations of caffeic acid resulted in reducing magnitude of the initial drop in oxygen concentration. The inhibitory effect of caffeic acid on the initial drop is probably related to its metal chelating and free radical scavenging abilities. The drop was rapidly converted to a very fast oxygen uptake rate, as shown in Figure 3.5.5, which demonstrates the predominant prooxidative behaviour of caffeic acid in the emulsions.

Comparison of the effect of caffeic acid on lipid oxidation induced by Fe^{2+} and Fe^{3+} is illustrated by oxidation curves in Figure 3.5.9.

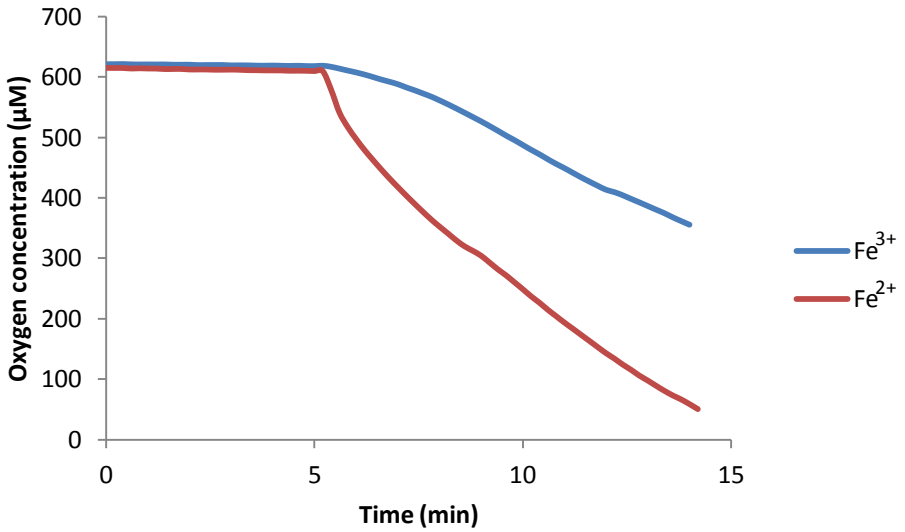

Figure 3.5.9: Comparison of oxidation curves for oxidation induced by Fe^{2+} (25 µM) and Fe^{3+} (25 µM) in emulsions with caffeic acid (25 µM).

The initial drop in oxygen concentration was absent when the oxidation was induced by Fe^{3+}, but the immediate oxygen uptake rate was very fast. The average oxidation rates were somewhat higher when the oxidation was induced by Fe^{2+} (43 ± 7 µmol/min) compared to Fe^{3+} (34 ± 3 µmol/min) for the same concentration of caffeic acid, but caffeic acid strongly enhanced the oxidation rates in both cases. Caffeic acid will reduce the added Fe^{3+} to Fe^{2+} thus increase the oxidation rates. The lower oxidation rates found for oxidation induced by Fe^{3+} compared to Fe^{2+} could be due precipitation of Fe^{3+} due to its low solubility. Lower oxidation rates for Fe^{3+} catalyzed oxidation is similar to what was observed in emulsions without antioxidants.

Propyl gallate

The influence of propyl gallate on the oxidation rates and the initial drop in oxygen concentration for the different concentrations of propyl gallate are shown in Figure 3.5.10.

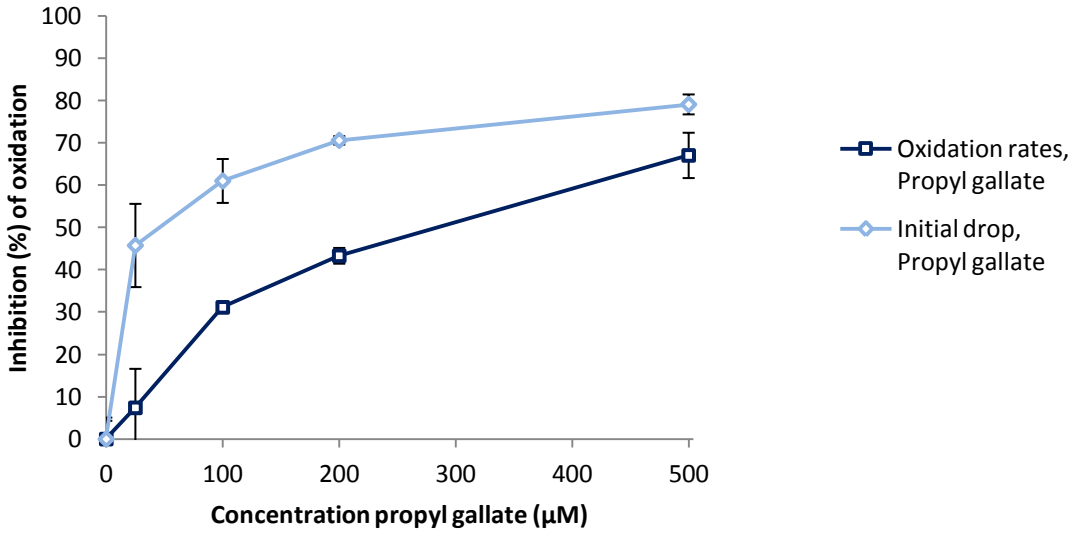

Figure 3.5.10: Inhibition (%) of oxidation rates and initial drop in oxygen concentration by different concentrations of propyl gallate when Fe^{2+} (25 µM) was used as prooxidant. The results are the mean values ± SD (n=3).

All tested concentrations of propyl gallate were found to inhibit both the initial drop in oxygen concentration and the oxidation rates, and the degree of inhibition increased with increasing concentration of propyl gallate. The reduction of the initial drop in oxygen concentration was generally greater than the reduction of the oxidation rate for the same concentration of propyl gallate.

The antioxidant activity of propyl gallate is related to its ability to donate hydrogen to lipid radicals, thus terminating the propagation of lipid oxidation. Interactions between propyl gallate and lipid radicals formed in the reaction between iron and lipid hydroperoxides make the radicals unavailable for reaction with oxygen and the drop in oxygen concentration and the oxidation rates are thus reduced. The non-polar character of propyl gallate makes it concentrate at the oil-water interface in the emulsion where lipid oxidation primarily takes place. Propyl gallate also has an ability to chelate iron, but the non polar character of the compound might favour interactions with lipid radicals rather than iron in the aqueous phase.

The oxidation rates were significantly lower when the oxidation was induced by Fe^{3+} (1.9 ± 0.6 µmol/min) than Fe^{2+} (5.30 ± 0.11 µmol/min) in emulsions with propyl gallate (100 µM), which indicates that propyl gallate was more efficient regarding inhibition of Fe^{3+} catalyzed oxidation. This could be due to increased chelation of Fe^{3+} compared to Fe^{2+} by propyl gallate. No difference was observed between the ability of propyl gallate to inhibit Fe^{2+} and Fe^{3+} catalyzed lipid oxidation in liposomes in studies by Kristinová et al. (2009). This could be due to increased concentration of iron in the emulsions (25 µM) compared to the liposomes (10 µM), thus greater susceptibility to precipitation. The antioxidant efficiency of propyl gallate was generally found to be better in the liposomes than in the emulsions. A ratio of propyl gallate to iron of 20 resulted in complete inhibition of oxidation in the liposomes, whereas the same ratio of propyl gallate to iron in the emulsions resulted in about 65% inhibition.

α-Tocopherol

The influence of different concentrations of α-tocopherol on the initial drop in oxygen concentration and oxidation rates when Fe^{2+} was used to initiate the oxidation are shown in Figure 3.5.11.

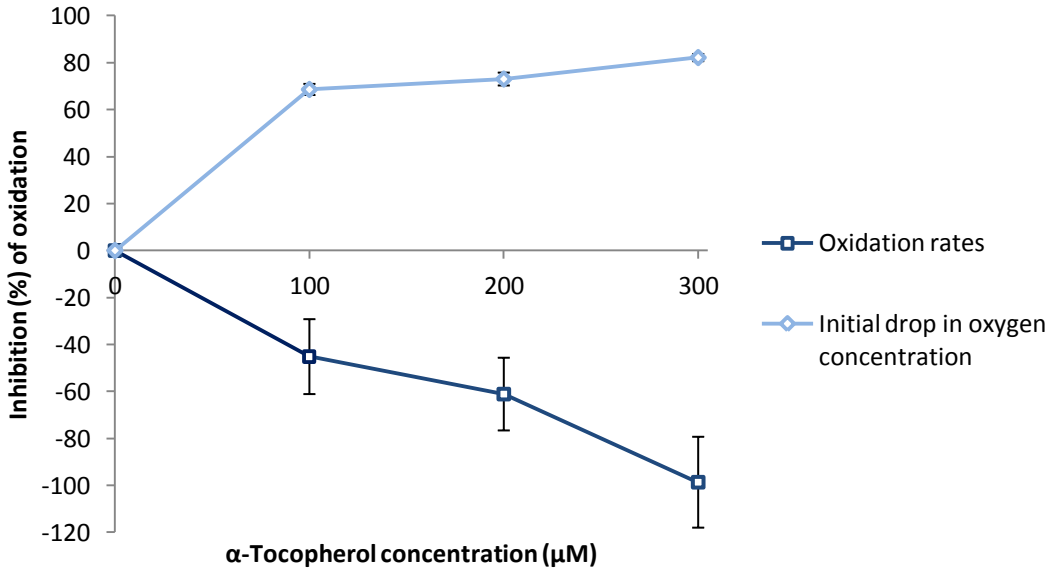

Figure 3.5.11: Influence (%) of different concentrations of α-tocopherol on the initial drop in oxygen concentration and oxidation rates. Positive values indicate inhibition, while negative values indicate increase of oxidation. The oxidation was induced by Fe^{2+} (25 µM). The results are the mean values ± SD (n=3-6).

Increasing concentrations of α-tocopherol lead to increasing oxidation rates and there was a significant linear correlation between the concentration of α-tocopherol in the emulsions and the increase in the oxidation rates. The initial drop in oxygen concentration was significantly reduced in emulsions containing α-tocopherol compared to those without, and the reduction was slightly increased for increasing concentrations of α-tocopherol.

The reason for the increased oxidation rates in emulsions with α-tocopherol could be due to prooxidative reactions of the tocopheroxyl radical formed when α-tocopherol donates hydrogen to a lipid radical. The tocopheroxyl radical may promote oxidation by forming new radicals in reactions with unsaturated lipids and lipid hydroperoxides. This is however not believed to be a major prooxidative pathway of α-tocopherol due to the low rates of these reactions compared to termination reactions between tocopheroxyl radicals (Kamal-Eldin and Appelqvist, 1996). Tocopherols and tocopheroxyl radicals have an ability to reduce transition metals to their more catalytically active state (Chen et al., 2011), and the prooxidative behaviour of α-tocopherol observed in the emulsions could be due to increased reduction rate of Fe^{3+} to Fe^{2+}. The reduction of Fe^{3+} to Fe^{2+} by tocopherol and the tocopheroxyl radical are shown in equation (21) and (22), respectively (Kamal-Eldin and Appelqvist, 1996).

$$Tocopherol + Fe^{3+} \rightarrow Tocopheroxyl^{\cdot} + H^{+} + Fe^{2+} \quad (21)$$

$$Tocopheroxyl^{\cdot} + Fe^{3+} \rightarrow Tocopherol^{+} + Fe^{2+} \quad (22)$$

Yamamoto and Niki (1988) also found α-tocopherol to increase oxidation of lipids when the oxidation was induced by Fe^{3+}. They observed the disappearance of α-tocopherol together with the formation of Fe^{2+}, and any remaining α-tocopherol suppressed the oxidation until it was depleted. Even though α-tocopherol was in great abundance in the oxidation experiments performed in these studies, it was not found to suppress the oxidation, but rather increase the oxidation rates with increasing concentration of α-tocopherol. The redox cycling mechanism between Fe^{2+} and Fe^{3+} by lipid hydroperoxides results in continuous formation of Fe^{3+} which can be reduced back to Fe^{2+} by α-tocopherol and the tocopheroxyl radical at an increased rate.

The reason for the reduced initial drop in emulsions with α-tocopherol could be due to scavenging of lipid radicals by α-tocopherol and termination reactions between tocopherol radicals and lipid radicals. These reactions might occur at an increased

rate during the initial drop due to the high amounts of lipid radicals formed in the initial reaction between Fe^{2+} and lipids hydroperoxides.

3.5.3 Ascorbic Acid

Oxidation curves for emulsions with different concentrations of ascorbic acid and emulsions without antioxidant when the oxidation was catalyzed by Fe^{2+} are given in Figure 3.5.12.

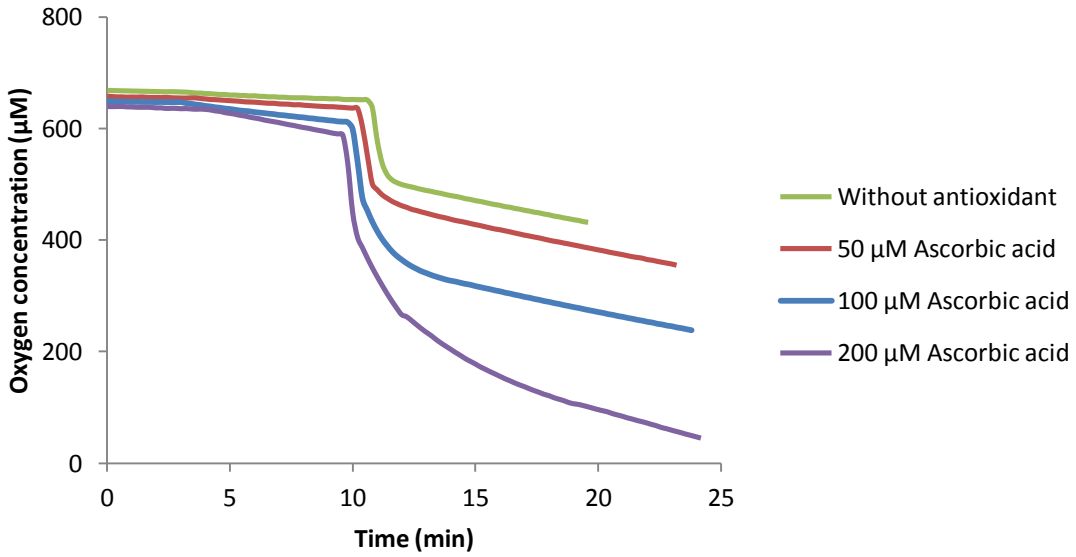

Figure 3.5.12: Oxidation curves in emulsions with different concentrations of ascorbic acid and without antioxidant when Fe^{2+} (25 µM) was used as prooxidant.

Addition of Fe^{2+} to emulsions containing ascorbic acid resulted in large drops in the oxygen concentration followed by a linear decrease in the oxygen concentration. The magnitude of the drops increased with increasing concentration of ascorbic acid, and was greater than for emulsion without antioxidant for all the concentrations of ascorbic acid. The oxygen concentration in the reaction chamber rapidly reached zero after addition of iron in all the experiments with ascorbic acid, and oxygen had to be supplied to the chamber one or several times. The graphs in Figure 3.5.12 are processed as described in section 2.7.3 and it is difficult to make reliable estimates of the magnitude of the drops in oxygen concentration as the reaction continued while oxygen was supplied to the system. The large initial drops in oxygen concentration in emulsions with ascorbic acid is likely to be due to the oxidation of ascorbic acid by iron, as ascorbic acid is highly susceptible to oxidation in the presence of metal ions

(Gregory, 2008). Ascorbic acid is also a strong reducing agent and reduction of Fe^{3+} to Fe^{2+} could possibly give a larger initial drop, but this was not observed for caffeic acid or α-tocopherol which also reduced Fe^{3+} to Fe^{2+}.

The changes in the oxidation rates for different concentrations of ascorbic acid are given in Figure 3.5.13.

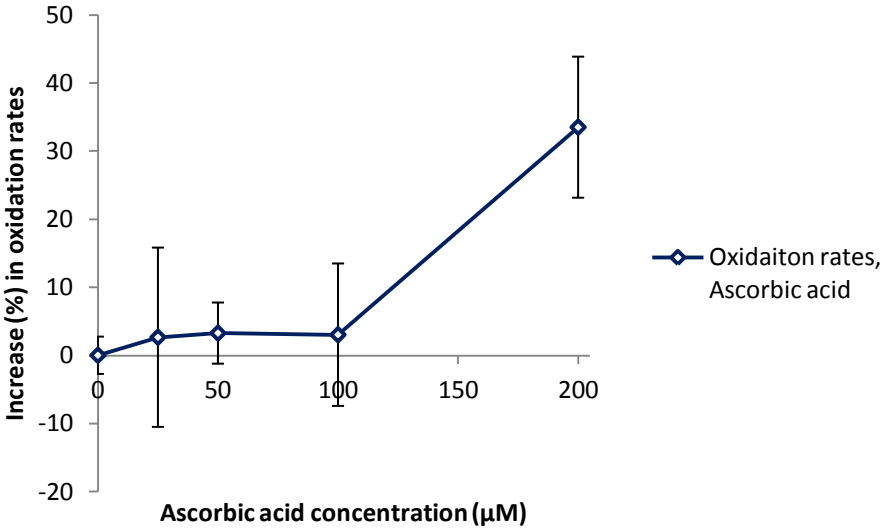

Figure 3.5.13: Increase (%) in oxidation rates by different concentrations of ascorbic acid when Fe^{2+} (25 µM) was used as prooxidant. The results are the mean values ± SD (n=3-6).

For concentrations up to 100 µM, ascorbic acid did not influence the oxidation rates. This could be due to depletion of ascorbic acid from the system as a result of its oxidation by iron. A significant increase in the oxidation rate was found for emulsions with 200 µM ascorbic acid. This could be because ascorbic acid was still present in the system and worked by reducing Fe^{3+} to Fe^{2+} or was itself oxidized.

Addition of ascorbic acid to the emulsions resulted in a distinct increase in the background oxygen uptake rates, which is evident from the oxidation curves in Figure 3.5.12. The increase in the background oxygen uptake rates at different concentrations of ascorbic acid is shown in Figure 3.5.14. The change in background oxygen uptake rate was also determined in emulsions where the iron had been removed by addition of EDTA prior to the addition of ascorbic acid and this result is presented in the same figure.

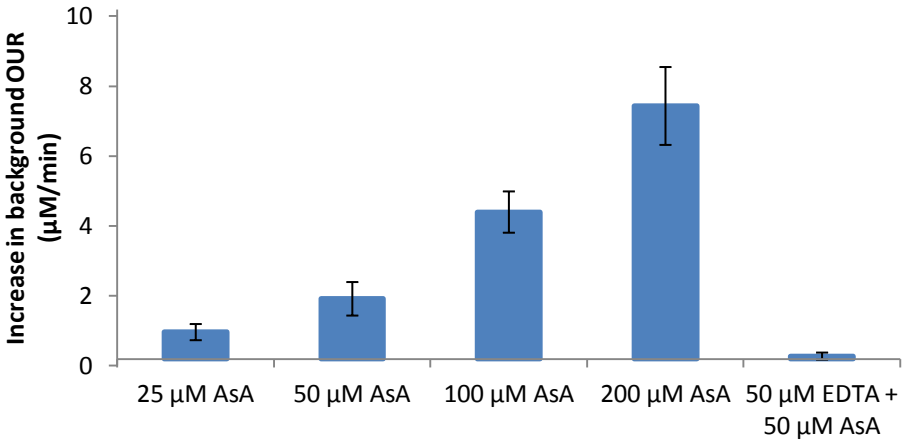

Figure 3.5.14: Increase in background OUR in emulsions with different concentrations of ascorbic acid and in emulsion with ascorbic acid and EDTA. The results are the mean values ± SD (n=3-6).

Increasing concentrations of ascorbic acid resulted in increasing background oxygen uptake rates. The increase in the background oxygen uptake rate is probably due to oxidation of ascorbic acid by traces of iron present in the emulsions. In emulsions where iron had been removed by EDTA, no change in the background oxygen uptake rate was observed when ascorbic acid was added. The influence of addition of EDTA prior to the addition of ascorbic acid on oxidation in emulsions is illustrated by oxidation curves in Figure 3.5.15.

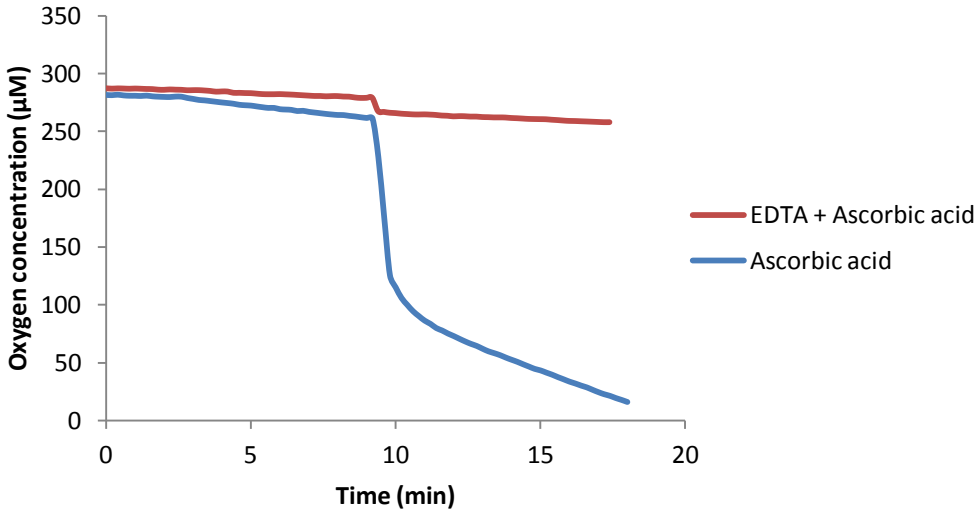

Figure 3.5.15: Oxidation curves illustrating the differences between oxidation in emulsions with and without EDTA (50 µM) when ascorbic acid (50 µM) was added to the emulsions. The oxidation was induced by Fe^{2+} (25 µM).

Addition of Fe^{2+} to emulsion containing both EDTA and ascorbic acid only resulted in a minor drop in oxygen concentration, followed by an oxidation rate similar to the background oxygen uptake rate. These results were similar to the ones where EDTA (50 µM) was used by itself. Both the oxidation of lipids and of ascorbic acid was inhibited when the iron was chelated by EDTA.

Comparison of the oxidation curves when Fe^{2+} and Fe^{3+} were used to catalyze oxidation of lipids in emulsions with ascorbic acid (50 µM) are given in Figure 3.5.16.

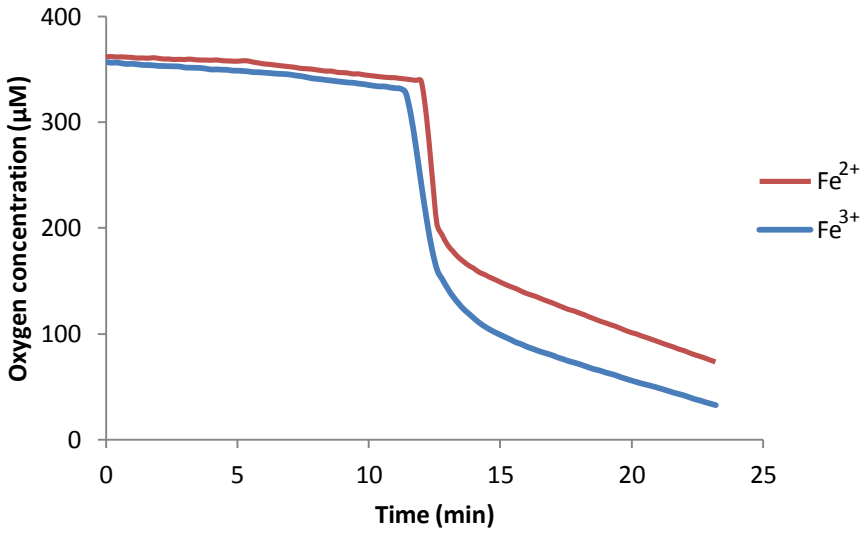

Figure 3.5.16: Oxidation curves for oxidation induced by Fe^{2+} (25 µM) and Fe^{3+} (25 µM) in emulsions with ascorbic acid (50 µM).

In contrast to the other oxidation experiments where Fe^{3+} was used to initiate the oxidation, addition of Fe^{3+} to emulsions containing ascorbic acid resulted in a rapid drop in the oxygen concentration in a similar manner to what was observed when Fe^{2+} was used as prooxidant. This probably means that Fe^{3+} can function as a catalyst for oxidation of ascorbic acid in a similar manner to Fe^{2+}. The magnitude of the drop was actually found to be greater in emulsions added Fe^{3+} than Fe^{2+} which is unexpected since lipid hydroperoxides not will be oxidized by Fe^{3+}. It is possible that ascorbic acid rapidly reduced Fe^{3+} to Fe^{2+}, or Fe^{3+} could be more catalytically active than Fe^{2+} in the oxidation of ascorbic acid.

3.5.4 Combination of α-Tocopherol and Ascorbic Acid

The influence of addition of Fe^{2+} to emulsions with α-tocopherol alone and with ascorbic acid and α-tocopherol is illustrated by oxidation curves in Figure 3.5.17.

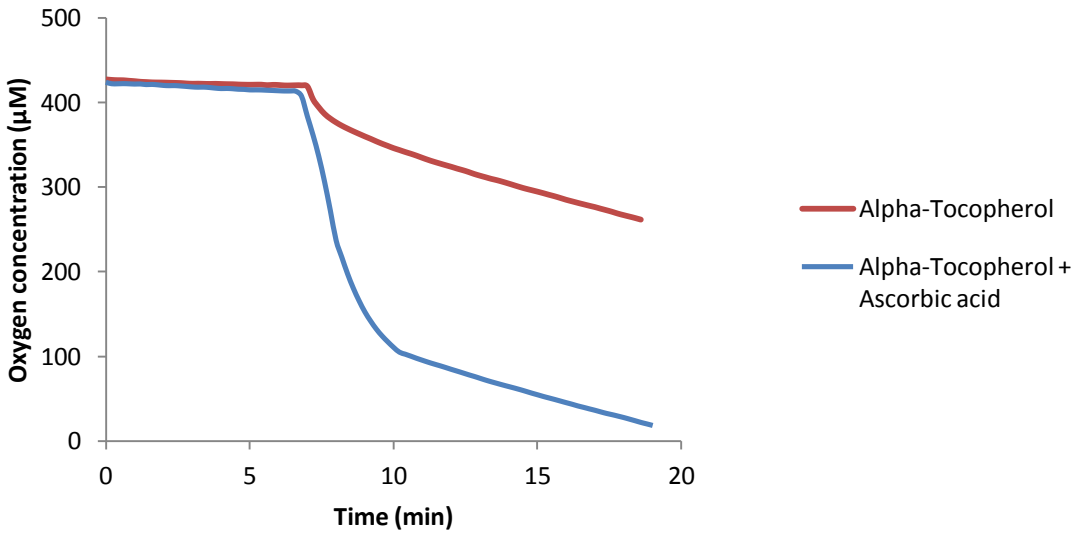

Figure 3.5.17: Oxidation curves for emulsions with α-tocopherol (100 µM) alone and with α-tocopherol (100 µM) and ascorbic acid (100 µM) when Fe^{2+} (25 µM) was used as prooxidant.

Addition of Fe^{2+} to emulsions with ascorbic acid and α-tocopherol resulted in a rapid drop in oxygen concentration similar to what was observed in emulsions with only ascorbic acid. This indicates that the oxidation of ascorbic acid was not influenced by the presence of α-tocopherol in the emulsion. The effect of ascorbic acid on the oxidation rates in emulsions with different concentrations of α-tocopherol compared to the effect of α-tocopherol alone is given in Figure 3.5.18.

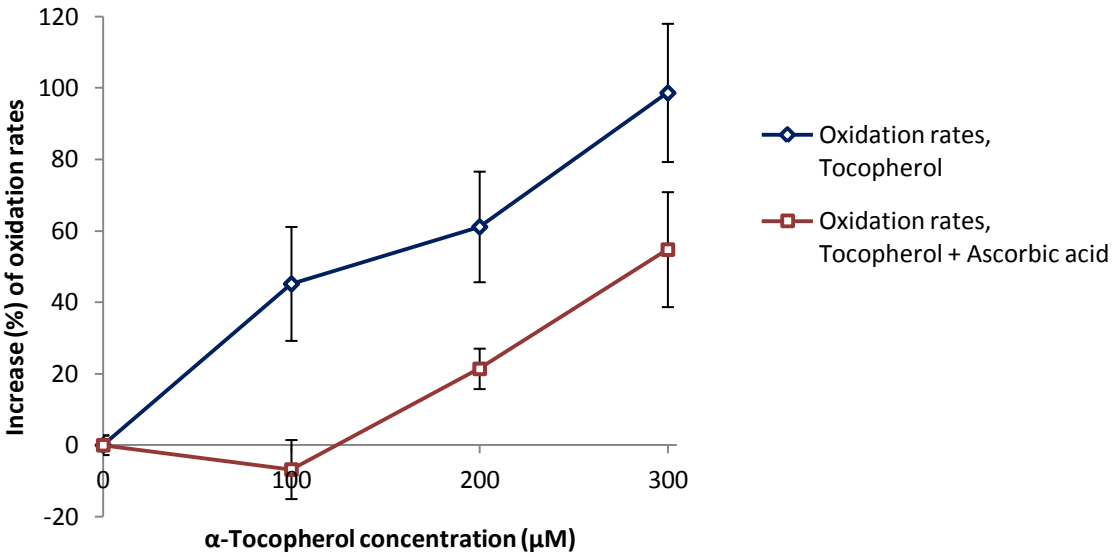

Figure 3.5.18: Increase (%) in oxidation rates in emulsions with different concentrations of α-tocopherol alone, and with ascorbic acid (50 µM) in addition to α-tocopherol when the oxidation was induced by Fe^{2+} (25 µM). The results are the mean values ± SD (n=2-6).

The oxidation rates were reduced when ascorbic acid was added to emulsions containing α-tocopherol compared to emulsions with α-tocopherol alone, as shown by the graphs in Figure 3.5.18. The effect of increasing concentrations of ascorbic acid in emulsions with constant concentration of α-tocopherol (100 µM) is given in Figure 3.5.19.

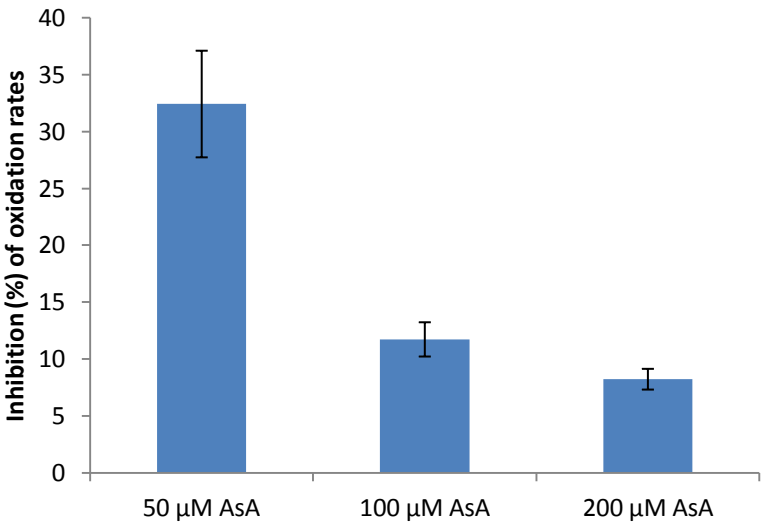

Figure 3.5.19: Inhibition (%) of oxidation rates for different concentrations of ascorbic acid in emulsions with α-tocopherol (100 µM). The results are % inhibition of oxidation rates compared to the oxidation rates in emulsions with α-tocopherol (100 µM) alone. The results are the mean values ± SD (n=2-3).

All tested concentrations of ascorbic acid reduced the oxidation rates in emulsions with α-tocopherol compared to emulsions with α-tocopherol alone, but the extent of the reduction decreased with increasing concentrations of ascorbic acid. The decrease in the oxidation rates in emulsions with both ascorbic acid and α-tocopherol is probably due to regeneration of α-tocopherol from the α-tocopheroxyl radical by ascorbic acid which prolongs the antioxidant activity of α-tocopherol (Frankel, 2005). It has been shown that addition of ascorbic acid to systems with α-tocopherol suppresses lipid oxidation as if more α-tocopherol was present (Niki, 1991). Although the oxidation rates were lower in emulsions with both ascorbic acid and α-tocopherol compared to in emulsions with only α-tocopherol, they were still higher than in emulsions without antioxidant except for emulsions with 50 µM ascorbic acid and 100 µM α-tocopherol. It is likely that both the prooxidative and antioxidative mechanisms of α-tocopherol took place in the emulsions since the initial drop in oxygen concentration was observed to decrease while the oxidation rates were found to increase in emulsions with α-tocopherol (Figure 3.5.5). Ascorbic acid might be able to improve the antioxidative activity of α-tocopherol in the emulsions, although the prooxidative activity is still dominant. The free radical scavenging activity of α-tocopherol will be predominant in the lipid phase or at the interface of the emulsions as these are the sites where lipid radicals are formed. Ascorbic acid will be located in the aqueous phase, but can interact with tocopheroxyl radicals at the interface

(Laguerre et al., 2007). Regeneration of α-tocopherol at this location probably favours the antioxidative reactions of α-tocopherol.

3.5.5 β-Carotene and Astaxanthin

Oxidation curves for emulsions with the carotenoids β-carotene and astaxanthin when Fe^{2+} was used to initiate the oxidation are given in Figure 3.5.20.

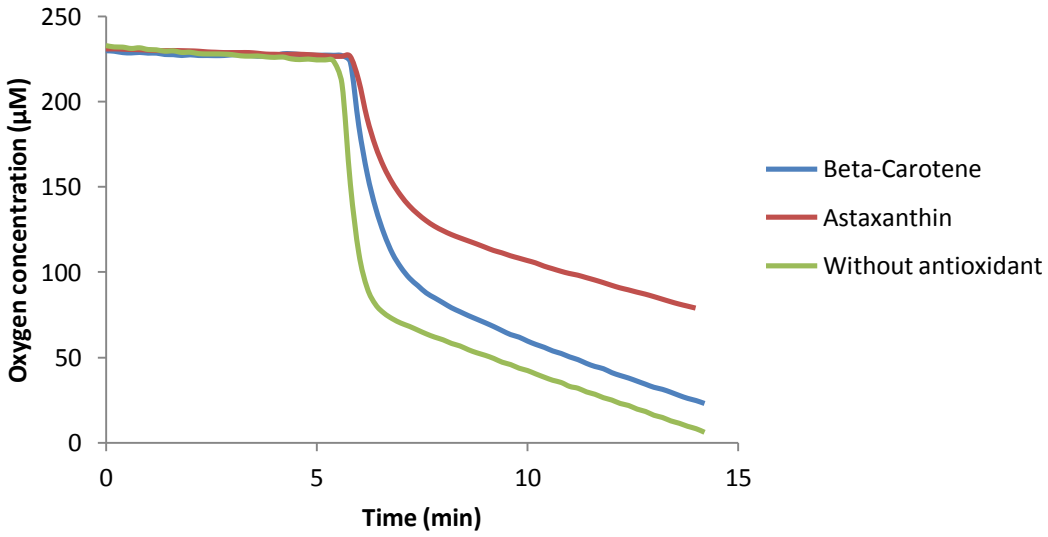

Figure 3.5.20: Comparison of oxygen consumption in emulsions with astaxanthin (200 µM) and β-carotene (200 µM) and emulsions without antioxidant when the oxidation was catalyzed by Fe^{2+} (25 µM).

Both β-carotene and astaxanthin reduced the initial drop in oxygen concentration to some extent. The effect of astaxanthin was more pronounced than that of β-carotene. The effect of the carotenoids on the following linear oxygen uptake rates was less evident. Three different concentrations of the carotenoids were investigated and the influence on the oxidation rates and initial drops in oxygen concentration when the oxidation was induced by Fe^{2+} are shown in Figure 3.5.21.

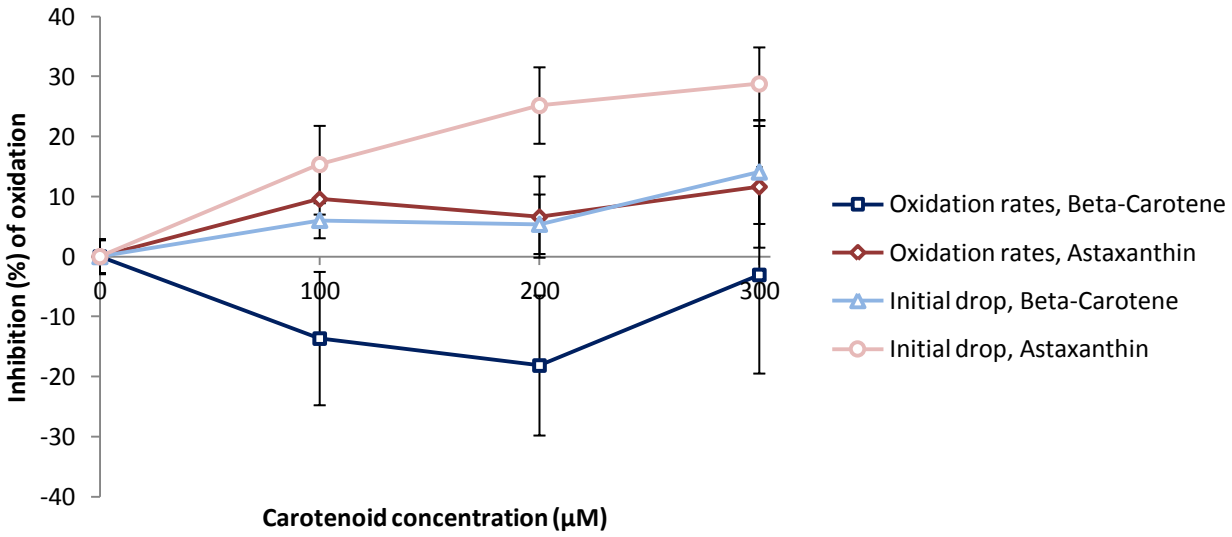

Figure 3.5.21: Influence (%) of different concentrations of β-carotene and astaxanthin on oxidation rates and initial drop in oxygen concentration in emulsions when Fe^{2+} (25 µM) was used as prooxidant. Positive values indicate inhibition of oxidation, while negative values indicate increase in oxidation. The results are the mean values ± SD (n=4-6).

β-Carotene slightly increased the oxidation rates, whereas astaxanthin slightly reduced the oxidation rates in the emulsions. There were no significant variations between the three concentrations of the carotenoids analyzed, nor was the influence the antioxidants had on the oxidation rates significant. Both β-carotene and astaxanthin had an inhibitory effect on the initial drop in oxygen concentration. The effect of astaxanthin was greater than that of β-carotene. The oxidation rates seemed to be independent of the concentration of added astaxanthin, while the initial drop in oxygen concentration decreased with increasing concentration of astaxanthin, as illustrated in Figure 3.5.21.

Carotenoids are known to be able to both inhibit and enhance lipid oxidation depending on the oxygen concentration in the system. The slight increase in oxidation rates in emulsions with β-carotene could be due to reactions with β-carotene radicals and oxygen, a reaction which both consumes oxygen and leads to formation of carotenoid peroxyl radicals which can initiate oxidation.

Astaxanthin was found to work better as an antioxidant in the emulsions than β-carotene. The only difference between the two compounds is the presence of a keto group and a hydroxyl group on the two β-ionone rings of astaxanthin, which makes astaxanthin more polar than β-carotene. This will have influence on the location of the carotenoids in the emulsion. Shibata et al. (2001) found considerable differences between β-carotene and astaxanthin regarding their molecular packing and

orientation in phospholipid layers where astaxanthin showed a greater miscibility in phospholipid layers than β-carotene. A tighter packing of astaxanthin around the emulsion droplets could make it more efficient in inhibiting lipid oxidation compared to β-carotene. The different structures of β-carotene and astaxanthin could also influence their reactivity towards other molecules in the emulsion, like lipid radicals and oxygen.

Both carotenoids reduced the magnitude of the initial drop in oxygen concentration. This could be due to reactions between the carotenoids and lipid radicals formed in the initial reaction between lipid hydroperoxides and Fe^{2+}. The large amount of lipid peroxyl radicals formed in the drop might make reactions between carotenoid radicals and lipid peroxyl radicals to termination products more likely than formation of new radicals.

For astaxanthin, lipid oxidation induced by Fe^{3+} was compared to lipid oxidation induced by Fe^{2+}. The inhibition (%) of the oxidation rates are given in Figure 3.5.22.

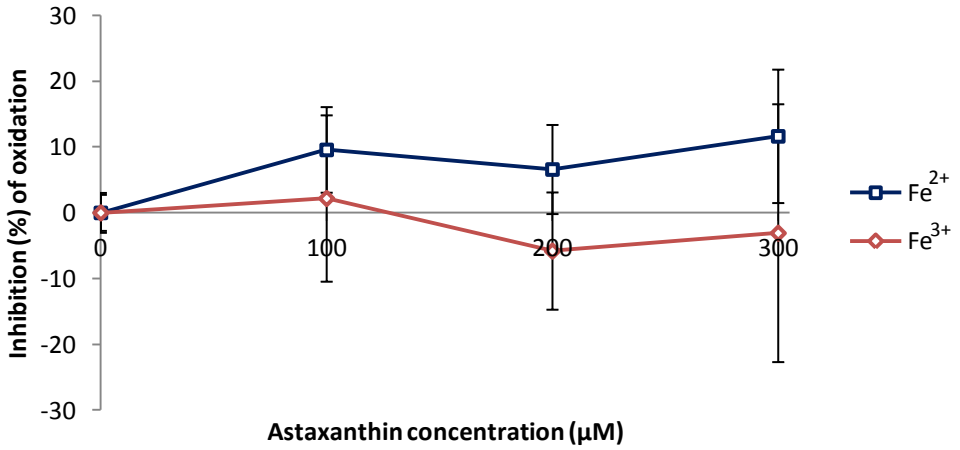

Figure 3.5.22: Inhibition (%) of oxidation catalyzed by Fe^{3+} (25 µM) and Fe^{2+} (25 µM) in emulsions with different concentrations of astaxanthin. The results are the mean values ± SD (n=3-6).

The effect of astaxanthin on Fe^{3+} catalyzed oxidation was lower than that of Fe^{2+} catalyzed oxidation, and the oxidation rates were in the case of Fe^{3+} catalyzed oxidation found to increase rather than to decrease. The use of Fe^{3+} as prooxidant in the emulsions generally resulted in lower oxidation rates than when Fe^{2+} was used as prooxidant, emulsions with astaxanthin therefore showed unusual behaviour. However, the large uncertainties in the measured values make it difficult to conclude that there is any difference between oxidation induced by the two iron species in the

presence of astaxanthin. It is possible that the reaction between the astaxanthin radical and oxygen is preferred over the termination reaction when the reaction is induced by Fe^{3+} instead of Fe^{2+}, as the rapid formation of lipid peroxyl radicals in Fe^{2+} induced oxidation will not take place.

3.5.6 Activities of Antioxidants in Emulsions

The investigated antioxidants influenced lipid oxidation by different mechanisms, and some of the antioxidants showed both prooxidative and antioxidative effects. This illustrates how one antioxidant can act by several different reaction mechanisms. Interactions between iron and the antioxidants seemed to be particularly important.

Caffeic acid, α-tocopherol and β-carotene exhibited both antioxidative and prooxidative effects in the emulsions by having an inhibitory effect on the initial drop in oxygen concentration and an increasing effect on the oxidation rates. This was particularly evident for caffeic acid and α-tocopherol while the influence of β-carotene on the initial drop and oxidation rates was less pronounced. The prooxidative effects of α-tocopherol and caffeic acid are believed to be due to their ability to reduce Fe^{3+} to Fe^{2+}. The prooxidative effect of caffeic acid was greater than that of α-tocopherol which could be due to a greater catalytical activity of caffeic acid. The location of the two compounds in the emulsion might also have affected their abilities to interact with iron. The non polar character of α-tocopherol makes it reside in the lipid phase where iron is less available, thus its prooxidative interaction with iron is likely to be less pronounced. The reason for the lower prooxidative activity of α-tocopherol could also be due to other reactions taking place in the emulsions. α-Tocopherol is considered to be an efficient free radical scavenger (Kamal-Eldin and Appelqvist, 1996) and chain-breaking reactions by α-tocopherol may have taken place in the emulsions so even if the oxidation rates were increased, they were increased to a lower extent. This agrees well with the lower oxidation rates found when ascorbic acid was added to emulsions with α-tocopherol, as ascorbic acid is known to be able to prolong the free radical scavenging activity of α-tocopherol (Niki, 1991).

The phenolic compounds caffeic acid, propyl gallate and α-tocopherol inhibited the initial drop in oxygen concentration to a similar degree. These compounds can all function as free radical scavengers and it is possible that they reduced the oxygen consumption in the initial drop by interaction with the large amounts of radicals formed in the rapid reaction between Fe^{2+} and lipid hydroperoxides. The initial drop can also be reduced by chelation of Fe^{2+}, as was observed in emulsions with EDTA. Both caffeic acid and propyl gallate have metal chelating properties which has been

attributed to their catechol and galloyl group, respectively (Andjelković et al., 2006). α-Tocopherol does not bear any of these functional groups, but its ability to reduce Fe^{3+} to Fe^{2+} shows that it has an ability to interact with iron. The reduction of the initial drop in oxygen concentration could be a result of combination of chelation of iron and scavenging of free radicals.

EDTA was found to be the most efficient inhibitor of iron induced oxidation in the emulsions, as it could inhibit both the initial drop and the following linear oxygen uptake rate very efficiently. When EDTA was added in twice the ratio to iron, the initial drop was almost undetectable. This was significantly better than for propyl gallate and caffeic acid which were able to reduce the drop about 80% when they were added in a ratio of 20 times to iron. α-Tocopherol reduced the drop about 80% when the ratio of α-tocopherol to iron was about 12, thus it was more efficient than the propyl gallate and caffeic acid, but less efficient than EDTA. Citric acid was not able to reduce the initial drop at any of the tested concentration which was thought to be due to its inability to bind Fe^{2+} at the pH of the emulsion, but it efficiently reduced the following linear oxygen uptake rate in a similar manner to EDTA. The inhibition of oxidation by EDTA and citric acid shows how iron induced oxidation of lipids can efficiently be counteracted by removal of iron from the system.

Ascorbic acid was the only compound that increased the magnitude of the initial drop in oxygen concentration, which was thought to be due to oxidation of ascorbic acid itself, and not due to increased oxidation of the lipids. This illustrates how it is important to bear in mind that oxidation of other compounds present in the system may influence the oxidation rates when studying lipid oxidation by measurement of oxygen consumption. It is possible that the increased oxidation rates in emulsions with β-carotene were also due to oxidation of the carotenoid itself rather than increased oxidation of the lipids.

The location of the antioxidants in the multiphase system is also of importance when considering their antioxidative activities. According to the polar paradox, the most efficient antioxidants in oil-in-water emulsions are non-polar antioxidants as they are retained in the oil phase where the interaction between radicals and unsaturated lipids finds place. This principle might be too simple when regarding iron catalyzed oxidation as the interaction between the antioxidant and iron is of great importance. Sørensen et al. (2008) found that some phenolic compounds working as prooxidants in the presence of iron could inhibit oxidation when iron was not added.

The carotenoids showed lower influence on the oxygen uptake in the emulsions compared to the phenolic compounds and chelating agents. Carotenoids are efficient singlet oxygen scavengers but this is probably not of major importance in the

emulsions as singlet oxygen is most commonly formed by photosensitization by photosensitizers such as chlorophyll (McClements and Decker, 2008). Carotenoids can also function as free radical scavengers, but they do this by addition reactions in contrast to phenolic compounds which scavenge free radicals by donation of hydrogen (Tsuchihashi et al., 1995). Studies have shown that β-carotene is a less efficient free radical scavenger than α-tocopherol, which is thought to be because the β-carotene radical is quite reactive towards oxygen in contrast to the α-tocopheroxyl radical which is quite nonreactive (Liebler, 1993). This could be the reason why the initial drop was inhibited to a larger extent in emulsions with α-tocopherol than with the carotenoids.

3.6 Further Work

The emulsions in this work were made in distilled water, and the lack of a buffer system made the emulsions unstable regarding pH. pH is known to have an important influence on iron catalyzed oxidation of lipids, thus it is desirable to have more control of the pH in the system. Implementation of a buffer system in the emulsions would make it easier to control the initial pH of the emulsions, as well as making the system more stable regarding changes in pH during the experiments. This could make it possible to investigate the relationship between pH, zeta potential and oxidation rates further.

Lipid oxidation can be induced by other transition metals than iron, such as copper, and also transition metals associated with pigments such as myoglobin, haemoglobin and chlorophyll. These prooxidants are also commonly found in foods and it would be interesting to investigate their influence on lipid oxidation in emulsions. The activity of some of the studied antioxidants was clearly influenced by the presence of iron in the system, and the activity of these antioxidants in the presence of other prooxidants could improve the knowledge of the functions of these antioxidants. Measurement of oxygen consumption in emulsions provides useful information about oxidation of lipids, but to get a more complete view of the oxidation processes taking place, the measurements could be combined with measurement techniques that determine the formation of oxidation products such as volatiles and peroxides.

4 Conclusions

Washing of crude herring oil with water improved the purity but slightly increased the oxidation level of the oil. Emulsification of herring oil, herring phospholipids and water with a dispersing tool for increasing time resulted in larger droplets and wider droplet size distributions. Addition of xanthan gum to the emulsions gave a narrower droplet size distribution with smaller droplets, but the use of xanthan gum had undesirable influence on the oxidation in the emulsions.

Studies of lipid oxidation by oxygen consumption in emulsions showed that iron catalyzed lipid oxidation in emulsions with herring oil and herring phospholipids as emulsifier occurred at a lower rate than oxidation of liposomes prepared from herring phospholipids analyzed in previous studies. The initial reaction between Fe^{2+} and lipid hydroperoxides was similar for the two systems, which indicated that lipid hydroperoxides in the phospholipid interface of the oil droplets were responsible for the initial reaction. The reason for the lower reaction rates in the emulsions was thought to be related to the majority of the lipids in emulsions being located in the core of the oil droplets making them less available for oxidation. Oxidation in emulsions with soy lecithin as emulsifier was virtually completely inhibited demonstrating the influence of the emulsifier on oxidation of lipids in emulsions. The emulsions with oil and emulsifier from herring were shown to be a suitable system for studies of iron catalyzed lipid oxidation as oxidation occurred at high enough rates to evaluate the influence of antioxidants.

Interactions between iron and antioxidants had a major impact on the oxidation rates in the emulsions. EDTA and citric acid chelated iron and completely inhibited oxidation when they were present in twice the ratio to iron. Citric acid was not able to inhibit the initial reaction of Fe^{2+} with lipid hydroperoxides which was thought to be due to inability of citric acid to bind Fe^{2+}. Propyl gallate was the only phenolic compound which decreased the oxidation rates. Caffeic acid and α-tocopherol both enhanced the oxidation rates by reducing Fe^{3+} to Fe^{2+}. The prooxidative activity of caffeic acid was significantly greater than that of α-tocopherol. Caffeic acid, α-tocopherol and propyl gallate inhibited the initial reaction between lipid hydroperoxides and Fe^{2+} to a similar degree which was thought to be related to their metal chelating and free radical scavenging activities. Ascorbic acid was itself oxidized by Fe^{2+} and Fe^{3+} which resulted in increased initial consumption of oxygen in the emulsions, but not increased oxidation of the lipids. Ascorbic acid was able to decrease the prooxidative activity of α-tocopherol by regeneration of α-tocopherol from the α-tocopheroxyl radical. β-Carotene and astaxanthin showed only minor influences on oxidation in the emulsions.

References

AOCS Official Method Cd 18-90: p-Anisidine Value. IL, USA (1993).

ISO 3960 Determination of peroxide value (2001).

Oxygen measurement products [Online]. Hansatech Instruments Ltd. Available: http://www.hansatech-instruments.com/oxygen_products.htm.

Zeta potential measurement using laser Doppler electrophoresis (LDE) [Online]. Malvern Instruments Ltd. Available: http://www.malvern.com/LabEng/technology/zeta_potential/zeta_potential_LDE.htm.

AANEBY, J. 2011. *Phospholipids from Herring Roe - Suitability for Oxygen Uptake Measurements.* Norwegian University of Science and Technology.

AIDOS, I., VAN DER PADT, A., LUTEN, J. B. & BOOM, R. M. 2002. Seasonal changes in crude and lipid composition of herring fillets, byproducts, and respective produced oils. *Journal of agricultural and food chemistry,* 50**,** 4589-4599.

ANDJELKOVIĆ, M., VAN CAMP, J., DE MEULENAER, B., DEPAEMELAERE, G., SOCACIU, C., VERLOO, M. & VERHE, R. 2006. Iron-chelation properties of phenolic acids bearing catechol and galloyl groups. *Food Chemistry,* 98**,** 23-31.

CHEN, B., MCCLEMENTS, D. J. & DECKER, E. A. 2011. Minor Components in Food Oils: A Critical Review of their Roles on Lipid Oxidation Chemistry in Bulk Oils and Emulsions. *Critical reviews in food science and nutrition,* 51**,** 901-916.

COUPLAND, J., ZHU, Z., WAN, H., MCCLEMENTS, D., NAWAR, W. & CHINACHOTI, P. 1996. Droplet composition affects the rate of oxidation of emulsified ethyl linoleate. *Journal of the American Oil Chemists' Society,* 73**,** 795-801.

COUPLAND, J. N. & MCCLEMENTS, D. J. 1996. Lipid oxidation in food emulsions. *Trends in food science & technology,* 7**,** 83-91.

CREXI, V. T., MONTE, M. L., SOARES, L. A. S. & PINTO, L. A. A. 2010. Production and refinement of oil from carp (Cyprinus carpio) viscera. *Food Chemistry,* 119**,** 945-950.

DAMODARAN, S. 2005. Protein stabilization of emulsions and foams. *Journal of Food Science,* 70**,** R54-R66.

DECKER, E. A. 2008. Antioxidant Mechanisms. *In:* AKOH, C. C. & MIN, D. B. (eds.) *Food Lipids - Chemistry, Nutrition and Biotechnology.* 3rd ed. Boca Raton: CRC Press, Taylor & Francis.

DICKINSON, E. 2009. Hydrocolloids as emulsifiers and emulsion stabilizers. *Food Hydrocolloids,* 23**,** 1473-1482.

DONNELLY, J., DECKER, E. & MCCLEMENTS, D. 1998. Iron-Catalyzed Oxidation of Menhaden Oil as Affected by Emulsifiers. *Journal of food science,* 63**,** 997-1000.

ENDO, Y., HOSHIZAKI, S. & FUJIMOTO, K. 1997. Autoxidation of synthetic isomers of triacylglycerol containing eicosapentaenoic acid. *Journal of the American Oil Chemists' Society,* 74**,** 543-548.

FISHER, A. E. O. & NAUGHTON, D. P. 2004. Iron supplements: the quick fix with long-term consequences. *Nutrition journal,* 3**,** 2.

FRANCIS, A. & DODGE, C. 1993. Influence of complex structure on the biodegradation of iron-citrate complexes. *Applied and environmental microbiology,* 59**,** 109-113.

FRANKEL, E. 1993. In search of better methods to evaluate natural antioxidants and oxidative stability in food lipids. *Trends in Food Science & Technology,* 4**,** 220-225.

FRANKEL, E. N. 2005. *Lipid oxidation,* Bridgewater, Oily Press.

GREGORY, J. F. 2008. Vitamins. *In:* DAMODARAN, S., PARKIN, K. L. & FENNEMA, O. R. (eds.) *Fennema's Food Chemistry.* Boca Raton: Taylor & Francis.

HARRIS, D. C. 2010. *Quantitative Chemical Analysis,* New York, Freeman.

HEMAR, Y., TAMEHANA, M., MUNRO, P. & SINGH, H. 2001. Influence of xanthan gum on the formation and stability of sodium caseinate oil-in-water emulsions. *Food Hydrocolloids,* 15**,** 513-519.

HIRAYAMA, O., NAKAMURA, K., HAMADA, S. & KOBAYASI, Y. 1994. Singlet oxygen quenching ability of naturally occurring carotenoids. *Lipids,* 29**,** 149-150.

HORN, A. F., NIELSEN, N. S. & JACOBSEN, C. 2012. Iron-mediated lipid oxidation in 70% fish oil-in-water emulsions: effect of emulsifier type and pH. *International Journal of Food Science & Technology*.

HU, M., JULIAN MCCLEMENTS, D. & DECKER, E. A. 2004. Impact of chelators on the oxidative stability of whey protein isolate-stabilized oil-in-water emulsions containing ω-3 fatty acids. *Food Chemistry,* 88**,** 57-62.

HUNTER, R. J. 1993. *Introduction to modern colloid science,* Oxford, Oxford University Press.

HYNES, M. J. & O'COINCEANAINN, M. 2004. The kinetics and mechanisms of reactions of iron (III) with caffeic acid, chlorogenic acid, sinapic acid, ferulic acid and naringin. *Journal of inorganic biochemistry,* 98**,** 1457-1464.

HYTTAN, S. & ØSTVIK, S. O. 2009. Biråstoff fra filetering av sild; Kartlegging og analyse av råstoff og utnyttelsesmuligheter. *In:* RUBIN (ed.). Sjøset Pelagic AS, SINTEF Fiskeri og havbruk.

KAMAL-ELDIN, A. & APPELQVIST, L. Å. 1996. The chemistry and antioxidant properties of tocopherols and tocotrienols. *Lipids,* 31**,** 671-701.

KE, P. & WOYEWODA, A. 1979. Microdetermination of thiobarbituric acid values in marine lipids by a direct spectrophotometric method with a monophasic reaction system. *Analytica Chimica Acta,* 106**,** 279-284.

KHAN, M. M. T. & MARTELL, A. E. 1967. Metal ion and metal chelate catalyzed oxidation of ascorbic acid by molecular oxygen. I. Cupric and ferric ion catalyzed oxidation. *Journal of the American Chemical Society,* 89**,** 4176-4185.

KOLANOWSKI, W. & LAUFENBERG, G. 2006. Enrichment of food products with polyunsaturated fatty acids by fish oil addition. *European Food Research and Technology,* 222**,** 472-477.

KRISTINOVÁ, V., MOZURAITYTE, R., STORRØ, I. & RUSTAD, T. 2009. Antioxidant Activity of Phenolic Acids in Lipid Oxidation Catalyzed by Different Prooxidants. *Journal of agricultural and food chemistry,* 57**,** 10377-10385.

LAGUERRE, M., LECOMTE, J. & VILLENEUVE, P. 2007. Evaluation of the ability of antioxidants to counteract lipid oxidation: existing methods, new trends and challenges. *Progress in Lipid Research,* 46**,** 244-282.

LIEBLER, D. C. 1993. Antioxidant Reactions of Carotenoids. *Annals of the New York Academy of Sciences,* 691**,** 20-31.

MCCLEMENTS, D. J. & DECKER, E. A. 2000. Lipid Oxidation in Oil-in-Water Emulsions: Impact of Molecular Environment on Chemical Reactions in Heterogeneous Food Systems. *Journal of Food Science,* 65**,** 1270-1282.

MCCLEMENTS, D. J. & DECKER, E. A. 2008. Lipids. *In:* DAMODARAN, S., PARKIN, K. & FENNEMA, O. R. (eds.) *Fennema's Food Chemistry.* 4th ed. Boca Raton: Taylor & Francis.

MEDINA, I., UNDELAND, I., LARSSON, K., STORRØ, I., RUSTAD, T., JACOBSEN, C., KRISTINOVÁ, V. & GALLARDO, J. M. 2011. Activity of caffeic acid in different fish lipid matrices: A review. *Food Chemistry*.

MEI, L., DECKER, E. A. & MCCLEMENTS, D. J. 1998. Evidence of iron association with emulsion droplets and its impact on lipid oxidation. *Journal of Agricultural and Food Chemistry,* 46**,** 5072-5077.

MEI, L., MCCLEMENTS, D. J. & DECKER, E. A. 1999. Lipid oxidation in emulsions as affected by charge status of antioxidants and emulsion droplets. *Journal of agricultural and food chemistry,* 47**,** 2267-2273.

MILLER, D. D. 2008. Minerals. *In:* DAMODARAN, S., PARKIN, K. & FENNEMA, O. R. (eds.) *Fennema's Food chemistry.* 4th ed. Boca Raton: Taylor & Francis.

MOZURAITYTE, R. 2007. *Oxidation of marine phospholipids in liposomes.* Faculty of Natural Sciences and Technology, Department ofBiotechnology.

MOZURAITYTE, R., RUSTAD, T. & STORRØ, I. 2006. Pro oxidant activity of Fe2+ in oxidation of cod phospholipids in liposomes. *European Journal of Lipid Science and Technology,* 108**,** 218-226.

MOZURAITYTE, R., RUSTAD, T. & STORRØ, I. 2007. The role of iron in peroxidation of polyunsaturated fatty acids in liposomes. *Journal of agricultural and food chemistry,* 56**,** 537-543.

NIKI, E. 1991. Action of ascorbic acid as a scavenger of active and stable oxygen radicals. *The American journal of clinical nutrition,* 54**,** 1119S-1124S.

OKAGAMI, N. & TERUI, K. 1996. Differences in the rates of metabolism of various triacylglycerols during seed germination and the subsequent growth of seedlings of Dioscorea tokoro, a perennial herb. *Plant and cell physiology,* 37**,** 273-277.

PEGG, R. B. 2001. Measurement of Primary Lipid Oxidation Products. *In:* WROLSTAD, R. E., ACREE, T. E., DECKER, E. A., PENNER, M. H., REID, D. S., SCHWARTZ, S. J., SHOEMAKER, C. F., SMITH, D. M. & SPORNS, P. (eds.) *Current Protocols in Food Analytical Chemistry.* John Wiley & Sons, Inc.

PIERRE, J. & GAUTIER-LUNEAU, I. 2000. Iron and citric acid: a fuzzy chemistry of ubiquitous biological relevance. *Biometals,* 13**,** 91-96.

REISCHE, D. W., LILLARD, D. A. & EITENMILLER, R. R. 2008. Antioxidants. *In:* AKOH, C. C. & MIN, D. B. (eds.) *Food Lipids: Chemistry, Nutrition and Biotechnology.* 3rd ed. Boca Raton: CRC Press, Taylor & Francis Group.

RIEDIGER, N. D., OTHMAN, R. A., SUH, M. & MOGHADASIAN, M. H. 2009. A systemic review of the roles of n-3 fatty acids in health and disease. *Journal of the American Dietetic Association,* 109**,** 668-679.

RUXTON, C., REED, S. C., SIMPSON, M. & MILLINGTON, K. 2004. The health benefits of omega-3 polyunsaturated fatty acids: a review of the evidence. *Journal of Human Nutrition and Dietetics,* 17**,** 449-459.

SCHAICH, K. 1992. Metals and lipid oxidation. Contemporary issues. *Lipids,* 27**,** 209-218.

SCHOLFIELD, C. 1981. Composition of soybean lecithin. *Journal of the American Oil Chemists' Society,* 58**,** 889-892.

SCHWARTZ, S. J., ELBE, J. H. V. & GIUSTI, M. 2008. Colorants. *In:* DAMODARAN, S., PARKIN, K. L. & FENNEMA, O. R. (eds.) *Fennema's Food Chemistry.* Boca Raton: Taylor & Francis.

SHAHIDI, F. & WANASUNDARA, U. N. 2002. Method for Measuring Oxidative Rancidity in Fats and Oils.

SHIBATA, A., KIBA, Y., AKATI, N., FUKUZAWA, K. & TERADA, H. 2001. Molecular characteristics of astaxanthin and [beta]-carotene in the phospholipid monolayer and their distributions in the phospholipid bilayer. *Chemistry and physics of lipids,* 113**,** 11-22.

SHIMADA, K., MUTA, H., NAKAMURA, Y., OKADA, H., MATSUO, K., YOSHIOKA, S., MATSUDAIRA, T. & NAKAMURA, T. 1994. Iron-binding property and antioxidative activity of xanthan on the autoxidation of soybean oil in emulsion. *Journal of agricultural and food chemistry,* 42**,** 1607-1611.

SUN, C., GUNASEKARAN, S. & RICHARDS, M. P. 2007. Effect of xanthan gum on physicochemical properties of whey protein isolate stabilized oil-in-water emulsions. *Food Hydrocolloids,* 21**,** 555-564.

SØRENSEN, A. D. M., HAAHR, A. M., BECKER, E. M., SKIBSTED, L. H., BERGENSTÅHL, B., NILSSON, L. & JACOBSEN, C. 2008. Interactions between iron, phenolic compounds, emulsifiers, and pH in omega-3-enriched oil-in-water emulsions. *Journal of agricultural and food chemistry,* 56**,** 1740-1750.

TOLASA, S., CAKLI, S. & OSTERMEYER, U. 2005. Determination of astaxanthin and canthaxanthin in salmonid. *European Food Research and Technology,* 221**,** 787-791.

TSUCHIHASHI, H., KIGOSHI, M., IWATSUKI, M. & NIKI, E. 1995. Action of [beta]-Carotene as an Antioxidant against Lipid Peroxidation. *Archives of biochemistry and biophysics,* 323**,** 137-147.

WALSTRA, P. 1993. Principles of emulsion formation. *Chemical Engineering Science,* 48**,** 333-349.

WALSTRA, P. & VLIET, T. V. 2008. Dispersed Systems: Basic Considerations. *In:* DAMODARAN, S., PARKIN, K. L. & FENNEMA, O. R. (eds.) *Fennema's Food Chemistry.* 4th ed. Boca Raton: Taylor & Francis.

WARAHO, T., MCCLEMENTS, D. J. & DECKER, E. A. 2011. Mechanisms of lipid oxidation in food dispersions. *Trends in Food Science & Technology,* 22**,** 3-13.

YAMAMOTO, K. & NIKI, E. 1988. Interaction of alpha-tocopherol with iron: antioxidant and prooxidant effects of alpha-tocopherol in the oxidation of lipids in aqueous dispersions in the presence of iron. *Biochimica et biophysica acta,* 958**,** 19.

Appendix A: Primary and Secondary Oxidation Products

A.1 Peroxide Values

Peroxide values in crude and washed herring oil were determined according to ISO 3960 (2001). A sample of lipid was dissolved in 3:2 (v/v) acetic acid/iso-octane solution (50 mL). Saturated potassium iodide solution (0.5 mL) was added to the mixture and it was stirred on magnetic stirrer (250 rpm) for 1 minute before addition of distilled water (30 mL). The amount of peroxides in the lipids was quantified by titration with sodium thiosulphate by using a TitraLab, TIM 980 Titration Manager (Radiometer Analytical, SAS, Copenhagen, Denmark). Close to the endpoint of the titration sodium dodecyl sulphate (10%, 1.0 mL) was added to the solution. A blank sample analysis was carried out by following the same procedure but without the lipid sample. The peroxide values were calculated according to equation (A-1).

$$meq\,peroxide\,/\,kg\,lipid = \frac{\left(V_{sample} - V_{blank}\right) \cdot N \cdot 1000}{m} \qquad \text{(A-1)}$$

V_{sample} and V_{blank} are the volumes of titrant used to titrate the lipid sample and blank sample, respectively. N is the normality of the sodium thiosulphate solution, m is the amount of lipids and 1000 is a scaling factor to obtain the results in meq peroxides per kilogram lipid.

Two different solutions of sodium thiosulphate were used for the analyses. The solution used for the analyses of oil samples obtained from the washing experiment was standardized to 0.1078 mol/L, while the solution used for analyses of the oil used for preparation of emulsions was standardized to 0.1060 mol/L. Both solutions were diluted in a ratio 1:10 with distilled water before use.

The consumption of sodium thiosulphate in the blank sample analyses performed before analyses of the oil samples from the washing treatment experiment and before analyses of oil used for preparation of the emulsions are given in Table A.1.1 and Table A.1.2, respectively.

Table A.1.1: Consumption of sodium thiosulphate in the blank sample analyses performed before analyses of the oil samples from the washing treatment experiment.

Parallel	Consumption $Na_2S_2O_3$ (mL)
1	0.16174
2	0.14687
3	0.27854
4	0.21845
5	0.25000
6	0.12223

Table A.1.2: Consumption of sodium thiosulphate in the blank sample analyses performed before analyses of the oil used for preparation of emulsions.

Parallel	Consumption $Na_2S_2O_3$ (mL)
1	0.24067
2	0.24282
3	0.23300

The average values of consumption of sodium thiosulphate in the blank sample analyses were used for calculation of the amount of peroxides in the lipid samples.

The amounts of lipids and the consumptions of sodium thiosulphate together with the calculated peroxide values are given in Table A.1.3 for the oil samples obtained from the washing treatment experiment, and in Table A.1.4 for the oil used for preparation of emulsions.

Table A.1.3: Amount of lipids and consumption of sodium thiosulphate for determination of peroxide values in oil samples obtained from the washing treatment experiment.

Oil sample	Amount of lipids (g)	Consumption $Na_2S_2O_3$ (mL)	Peroxide value (meq peroxide/kg lipid)
Crude oil	1.6912	3.388	20.22
	1.7536	3.563	20.57
	1.7518	3.773	21.89
	1.7815	3.576	20.33
	1.7170	3.461	20.37
Washed oil #1	1.7372	3.638	21.23
	1.7223	3.631	21.37
	1.8199	3.815	21.32
	1.7243	3.609	21.21
	1.7647	3.727	21.45
Washed oil #2	1.7084	3.691	21.93
	1.7398	3.746	21.87
	1.7001	3.687	22.01
	1.7272	3.646	21.41
	1.7263	3.601	21.14
Washed oil #3	1.7104	4.061	24.23
	1.7583	4.172	24.25
	1.7554	4.138	24.08
	1.7346	4.101	24.14
	1.7249	4.145	24.55

Table A.1.4: Amount of lipids and consumption of sodium thiosulphate for determination of peroxide values in the oil used for preparation of emulsions.

Oil sample	Amount of lipids(g)	Consumption $Na_2S_2O_3$ (mL)	Peroxide value (meq peroxide/kg lipid)
Crude oil	4.9421	1.6986	3.13
	4.9907	1.7345	3.18
	5.0407	1.7395	3.16
Washed oil	5.0000	1.9785	3.69
	5.0378	2.0061	3.72
	4.9791	2.0202	3.79

A.2 Anisidine Values

The *p*-anisidine values were determined according to the AOCS Official Method Cd 18-90 (1993). *p*-Anisidine reagent was made by dissolving *p*-anisidine (0.25 g) in acetic acid (100 mL). A sample of lipid was dissolved in ico-octane (10 mL). A sample of this solution (2.5 mL) and iso-octane (2.5 mL) were added to two glass cuvettes and the absorbances of the solutions were measured at 350 nm against iso-octane. *p*-Anisidine reagent (0.5 mL) was then added to both cuvettes, the solutions were mixed and left in the dark for exactly 10 minutes before the absorbances were measured again at 350 nm. The *p*-anisidine value was calculated according to equation (A-2),

$$p-Anisidine\ Value = \frac{V \cdot (1{,}2A_{S2} - A_{B2}) \cdot (A_{S1} - A_{B1})}{m} \qquad \text{(A-2)}$$

where m is the mass of the lipid sample and V is the volume of iso-octane used to dissolve the sample. A_{S1} and A_{S2} are the absorbances of the lipid solution before and after addition of p-anisidine reagent, similarly A_{B1} and A_{B2} are the absorbances of iso-octane before and after addition of *p*-anisidine reagent. The volume of iso-octane was 10 mL for all the analyses.

The amount of lipids and the measured absorbances before and after addition of *p*-anisidine together with the calculated *p*-anisidine values are given in Table A.2.1 for oil samples obtained from the washing treatment experiment, and in Table A.2.2 for the oil used for preparation of emulsions. One blank analysis was performed together with three sample analyses, and these values are also given in Table A.2.1 and Table A.2.2.

Table A.2.1: Amounts of lipids and measured absorbances before and after the addition of *p*-anisidine for the determination of *p*-anisidine values in oil samples obtained from the washing treatment experiment.

Oil sample	Amount of lipids (g)	Absorbance 350 nm		*p*-Anisidine value
		Without *p*-anisidine	With *p*-anisidine	
Crude oil	0.3152	0.107	0.120	2.98
	0.2635	0.090	0.109	3.70
	0.2624	0.094	0.104	3.34
	Blank sample	0.070	0.011	
Washed oil #1	0.2950	0.041	0.067	1.18
	0.2940	0.075	0.091	1.01
	0.2563	0.048	0.068	1.13
	Blank sample	0.005	0.008	
Washed oil #2	0.2027	0.029	0.050	1.29
	0.2107	0.041	0.067	1.64
	0.2139	0.042	0.069	1.68
	Blank sample	0.006	0.009	
Washed oil #3	0.2581	0.070	0.098	1.84
	0.2837	0.078	0.107	1.78
	0.2914	0.086	0.113	1.70
	Blank sample	0.000	0.000	

Table A.2.2: Amounts of lipids and measured absorbances before and after the addition of *p*-anisidine for the determination of *p*-anisidine values in the oil used for preparation of emulsions.

Oil sample	Amount of lipids (g)	Absorbance 350 nm		*p*-Anisidine value
		Without *p*-anisidine	With *p*-anisidine	
Crude oil	0.2634	0.065	0.088	1.31
	0.2712	0.070	0.090	1.18
	0.2623	0.078	0.091	0.96
	Blank sample	-0.006	0.000	
Washed oil	0.2456	0.072	0.098	1.45
	0.2541	0.096	0.125	1.73
	0.2545	0.061	0.094	1.64
	Blank sample	-0.010	0.000	

A.3 Thiobarbituric Acid Reactive Substances

Thiobarbituric acid reactive substances were determined according to the spectrophotometric method described by Ke and Woyewoda (1979). A sample of lipid was mixed with TBA work solution (5 mL) in a short Klimax test tube. The test tubes were closed with a cap and incubated in water bath with almost boiling water for 45 minutes and then cooled with cold water. TCA solution (2.5 mL) was added to the tubes and the solutions were mixed by inverting the test tubes before the tubes were centrifuged (10 minutes, 2500 rpm) to separate the water and chloroform phases. The absorbance of the water phase was measured at 538 nm against a blank sample prepared by the same procedure only without oil. Samples for a standard curve were made by replacing the oil sample with tetraethoxypropane (TEP) work solution (0-200 µL) giving an amount of TEP ranging from 0 to 20 nmol The standard curve was constructed by plotting the absorbance against the corresponding amount of TEP. Details about the reagents and solvents and volumes used in the analyses are given in Table A.3.1.

Table A.3.1: Solvents and reagents used for determination of TBARS.

Solvents/Reagents	Preparation
0.04 M TBA stock solution	2.88 g 2-thiobarbituric acid (>99.5%, Sigma-Aldrich) in 50 mL distilled water + 450 mL glacial acetic acid (96%, Merck)
0.3 M Na_2SO_3 solution	18.91 g Na_2SO_3 (Merck) in 500 mL distilled water
0.28 M TCA solution	22.87 g trichloroacetic acid (>99.5%, Merck) in 500 mL distilled water
0.01 M TEP stock solution	0.22 g 1,1,3,3-tetraethoxypropane (approx. 97%, Sigma) in 100 mL distilled water
0.1 mM TEP work solution	TEP stock solution diluted in distilled water in a ratio 1:100
TBA work solution	TBA stock solution, chloroform and Na_2SO_3-solution in a ratio 12:8:1

The amount of TBARS in the lipid samples were calculated according to equation (A-3).

$$\mu M\,TBARS\,/\,g\,lipid = \frac{A-b}{a \cdot m \cdot 1000} \qquad \text{(A-3)}$$

In equation (A-3), A is the absorbance of the sample, a and b are the slope and intercept of the standard curve, respectively, m is the amount of sample and 1000 is a conversion factor to obtain the results in µM/g.

One standard curve was made for each time the procedure for determination of TBARS was carried out. The standard samples were analyzed in triplicate. Some samples were lost during the preparation due to evaporation of the solution, and for this reason some samples were analyzed in fewer parallels. The absorbance of the standard samples and the corresponding standard curve made when the oil samples from the washing experiment were analyzed are given in Table A.3.2 and Figure A.3.1, respectively. The absorbance of the standard samples and the corresponding standard curve made when the oil used for preparation of emulsions was analysed are given in Table A.3.3 and Figure A.3.2, respectively.

Table A.3.2: Absorbance of TEP used as basis for the standard curve given in Figure A.3.1.

Amount TEP (nmol)	Absorbance, 538 nm		
	1	2	3
0.0	0.015	0.014	
2.5	0.065	0.058	0.062
5.0	0.126	0.120	0.114
10.0	0.253	0.255	0.251
15.0	0.344	0.333	0.332
20.0	0.449	0.441	

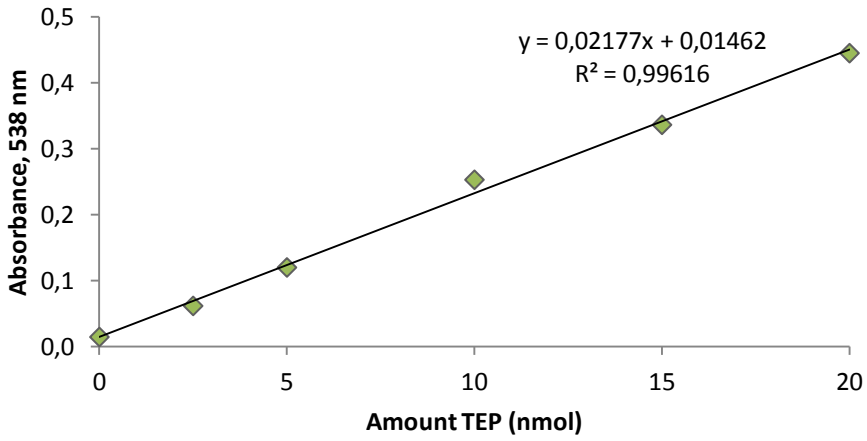

Figure A.3.1: Standard curve for absorbance as a function of amount of TEP.

Table A.3.3: Absorbance of TEP used as basis for the standard curve given in Figure A.3.2.

Amount TEP (nmol)	Absorbance, 538 nm		
	1	2	3
0.0	-0.004	-0.003	-0.002
2.5	0.057	0.058	0.059
5.0	0.116	0.114	0.123
10.0	0.243	0.245	0.237
15.0	0.358	0.359	
20.0	0.473	0.474	0.475

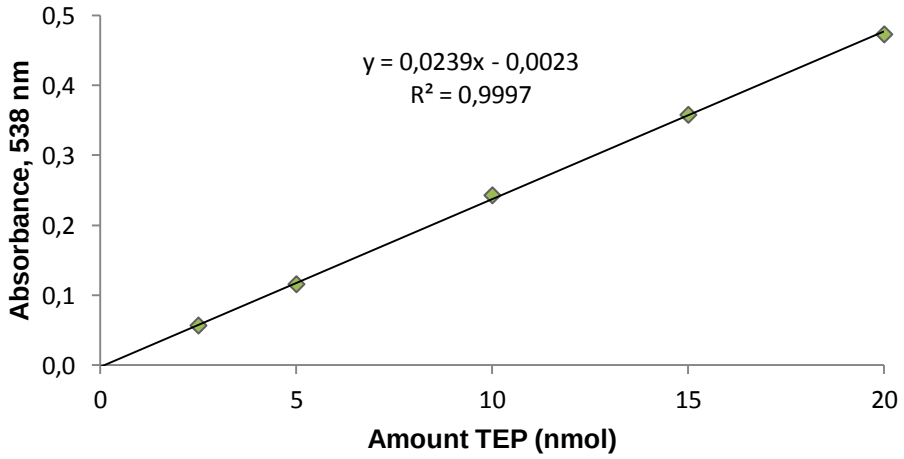

Figure A.3.2: Standard curve for absorbance as a function of amount of TEP.

The amount of lipids, measured absorbances and the calculated values for TBARS for oil samples from the washing treatment experiment are given in Table A.3.4. The values for a and b in equation (A-3) are taken from the standard curve given in Figure A.3.1 (a=0.02177, b=0.01462). For the oil used for preparation of emulsions the amount of lipids, measured absorbances and the calculated values for TBARS are given in Table A.3.5 and the values for a and b in equation (A-3) are taken from the standard curve given in Figure A.3.2 (a=0.0239, b=0.0023).

Table A.3.4: Amounts of lipids and measured absorbances for determination of TBARS in oil samples obtained from the washing treatment experiment.

Oil sample	Amount of lipid (g)	Absorbance, 538 nm	TBARS (μM/g lipid)
Crude oil	0.0112	0.243	0.94
	0.0152	0.420	1.23
	0.0148	0.253	0.74
Washed oil #1	0.0121	0.267	0.96
	0.0138	0.326	1.04
	0.0112	0.197	0.75
	0.0123	0.242	0.85
Washed oil #2	0.0140	0.317	0.99
	0.0148	0.265	0.78
	0.0224	0.434	0.86
	0.0127	0.255	0.87
Washed oil #3	0.0139	0.317	1.00
	0.0174	0.405	1.03
	0.0113	0.288	1.11

Table A.3.5: Amounts of lipids and measured absorbances for determination of TBARS in the oil used for preparation of emulsions.

Oil sample	Amount of lipid (g)	Absorbance, 538 nm	TBARS (μM/g lipid)
Crude oil	0.0122	0.120	0.40
	0.0118	0.090	0.32
	0.0114	0.114	0.42
	0.0128	0.126	0.41
Washed oil	0.0120	0.149	0.47
	0.0135	0.144	0.41
	0.0127	0.131	0.39
	0.0136	0.157	0.48

Appendix B: Carotenoids

The content of carotenoids in crude and washed herring oil was determined by the spectrophotometric method described by Tolasa et al. (2005). A sample of lipid was dissolved in *n*-hexane (5 mL) and the absorbance of the solution was measured at 470 nm. The carotenoid content in the sample was calculated according to equation (B-1), where abs is the absorbance of the solution measured at 470 nm, E=2100 is the standard absorbance of 1% (w/v) astaxanthin solution measured at 472 nm in a 1 cm cuvette, 10000 is a scaling factor to obtain the result in µg/mL and C is the concentration of lipids in the solvent. Division by the concentration of the lipids in the solvent gives the result in µg carotenoids/g lipid.

$$carotenoids\left(\mu g / g\right) = \frac{abs}{E(g/100mL)} \cdot 10000 \cdot \frac{1}{C(g/mL)} \qquad \text{(B-1)}$$

The amount of lipids dissolved in *n*-hexane, the measured absorbances of the solutions and the calculated carotenoid contents in the lipid samples are given in Table B.1.1 for the oil samples obtained from the washing treatment experiment, and in Table B.1.2 for the oil used for preparation of emulsions.

Table B.1.1: Amounts of lipids dissolved in *n*-hexane (5 mL), the absorbance of the solutions and the determined carotenoid contents in lipid samples obtained from the washing treatment experiment.

Oil sample	Lipids (g)	Absorbance, 470 nm	Carotenoid content in sample (µg/g)
Crude oil	0.2548	0.046	4.30
	0.2213	0.033	3.55
	0.2160	0.032	3.53
Washed oil #1	0.3104	0.022	1.69
	0.2139	0.014	1.56
	0.2131	0.015	1.68
Washed oil #2	0.2136	0.026	2.90
	0.2305	0.022	2.27
	0.2176	0.028	3.06
Washed oil #3	0.2315	0.018	1.85
	0.2171	0.028	3.07
	0.2068	0.029	3.34

Table B.1.2: Amounts of lipids dissolved in *n*-hexane (5 mL), absorbance of the solutions and the determined carotenoid contents in the lipid samples used for preparation of emulsions.

Oil sample	Lipids (g)	Absorbance, 470 nm	Carotenoid content in sample (µg/g)
Crude oil	0.2548	0.046	3.57
	0.2213	0.033	2.29
	0.2160	0.032	3.71
Washed oil	0.3104	0.022	1.69
	0.2139	0.014	1.80
	0.2131	0.015	1.92

Appendix C: Emulsion Characteristics

The measurement data for the evaluation of droplet size, creaming stability and zeta potential of the oil droplets in the emulsions are given in this appendix. The size of the oil droplets in the emulsions were measured with a Mastersizer 3000 (Malvern Instruments Ltd., Worcestershire, UK). The zeta potential of the oil droplets in the emulsion was determined with a Zetasizer Nano ZS (Malvern Instrument Ltd., Worcestershire, UK).

C.1 Emulsions with Xanthan Gum

Average droplet diameters in emulsions with 0.1% and 0.2% xanthan gum are given in Table C.1.1

Table C.1.1: Average droplet size in emulsions with 0.1% and 0.2% xanthan gum.

	0.1% Xanthan gum	**0.2% Xanthan gum**
Dv50 (µM)	4.42	4.59
	4.42	4.55
	4.42	4.60
	4.42	4.61
	4.42	4.63

The creaming stability of the emulsions was evaluated by measurements of absorbance at 600 nm in emulsions diluted with xanthan gum solution (0.1% or 0.2%) in a ratio 1:150. The measured absorbances are given in Table C.1.2.

Table C.1.2: Absorbance measured at 600 nm in emulsions with different amount of xanthan gum in the aqueous phase. The emulsions were diluted in a ratio 1:150.

	Absorbance, 600 nm				
Time (Hours)	**0**	**2**	**4**	**6**	**27**
0.1% Xanthan gum	1.381	1.065	0.955	0.884	0.769
	1.401	1.036	0.933	0.872	0.754
0.2% Xanthan gum	1.359	1.081	1.012	1.004	0.950
	1.330	1.132	1.048	0.962	0.907

C.2 Emulsions without Additives

Size distributions of oil droplets in emulsions prepared by emulsification times of 15 seconds, 30 seconds, 1, 2, 3, 4 and 8 minutes are given in Figure C.2.1.

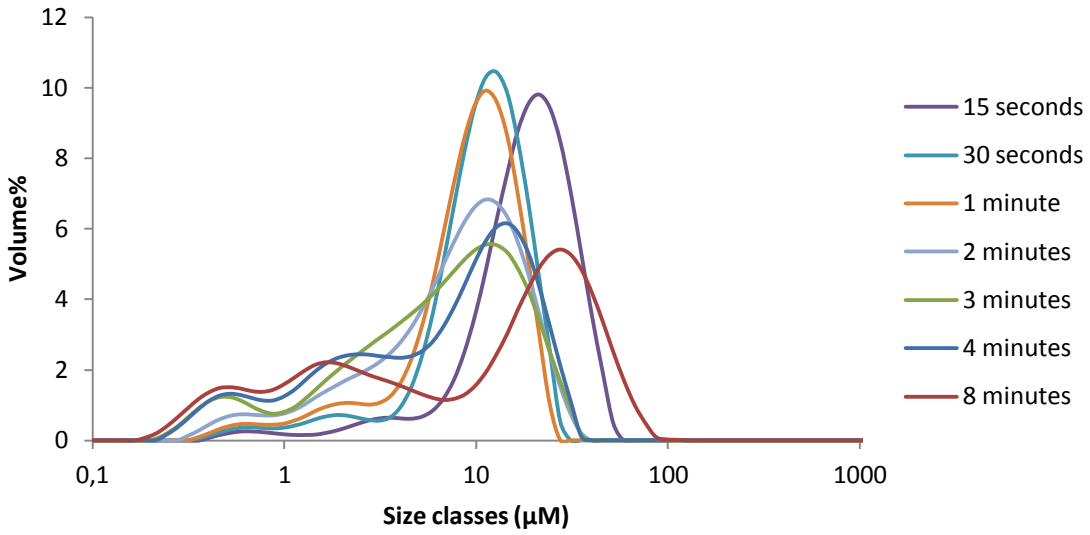

Figure C.2.1: Droplet size distributions of emulsions prepared by different emulsification times.

The creaming stability of the emulsions prepared by different emulsification times was evaluated by measurements of absorbance at 600 nm in emulsions diluted with water in a ratio 1:150. The measured absorbances at different times after preparation of the emulsions are given in Table C.2.1. The decrease (%) in absorbance compared to the first measured absorbance of the sample at time 0 are plotted in Figure C.2.2.

Table C.2.1: Absorbance measured at 600 nm in emulsions made with distilled water. The emulsions were diluted in a ratio 1:150.

Time (hours)	0	2.5	19
15 seconds	0.306	0.102	0.063
	0.305	0.094	0.049
	0.317	0.111	0.055

Time (hours)	0	2	6	22
30 seconds	0.562	0.291	0.230	0.119
	0.560	0.310	0.232	0.122
	0.563	0.287	0.222	0.149
1 minute	0.63	0.371	0.296	0.164
	0.628	0.386	0.29	0.188
	0.626	0.38	0.308	0.189
2 minutes	0.864	0.684	0.516	0.362
	0.863	0.687	0.536	0.328
	0.859	0.692	0.518	0.369
4 minutes	1.003	0.919	0.799	0.615
	1.002	0.922	0.783	0.669
	1.000	0.921	0.815	0.646

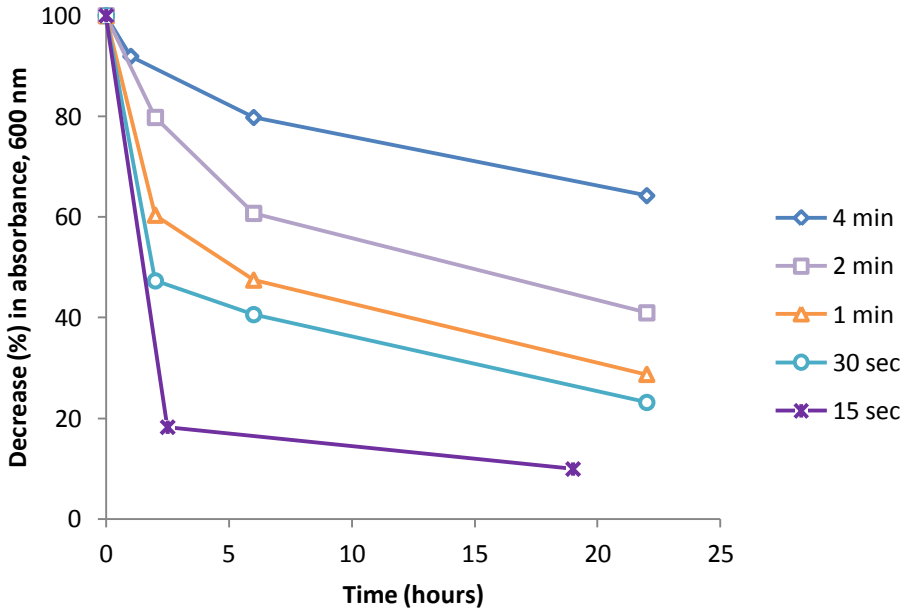

Figure C.2.2: Creaming stability in emulsions prepared by different emulsification times measured as decrease (%) in absorbance at 600 nm.

Droplet size measurements performed in emulsions prepared by emulsification for 30 seconds at five different occasions (named A-E) are given as size distributions in Figure C.2.3 and as average diameters in Table C.2.2.

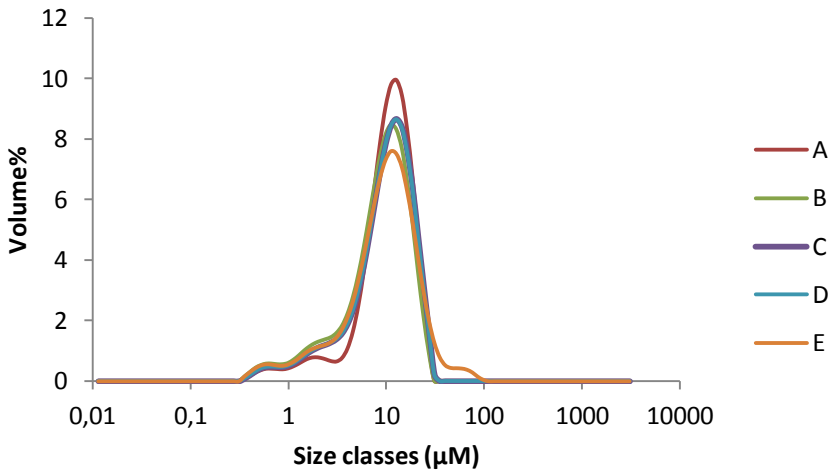

Figure C.2.3: Droplet size distributions for emulsions prepared by emulsification for 30 seconds at five different occasions.

Table C.2.2: Average droplet diameter of oil droplets in emulsions prepared at five different occasions.

	A	B	C	D	E
DV50 (µM)	11.7	10.1	11.1	11.0	10.7
	11.7	10.0	11.0	11.0	10.7
	11.7	10.0	11.0	11.0	10.7
	11.7	10.0	11.0	11.1	10.7
	11.7	10.0	11.0	11.1	10.7

The zeta potential of oil droplets in emulsions prepared at two different occasions are given in Table C.2.3. The measurements were performed at 30 °C.

Table C.2.3: Zeta potential of oil droplets in emulsions prepared at two separate occasions.

pH	Zeta potential (mV)
5.29	-8,86
	-12
	-16,1
5.74	-11,9
	-14,8
	-24,3

Appendix D: Measurement Data from Oxidation Experiments

The oxygen uptake rates (OUR) and oxygen concentrations at the top and bottom of the drop when Fe^{2+} was used as prooxidant were determined by using the Oxygraph software Oxyg32 and are given in this appendix.

The oxidation rates are calculated by subtracting the background oxidation rate (before addition of antioxidant) from the oxygen uptake rate after addition of prooxidant (Fe^{2+} or Fe^{3+}). The drops in oxygen concentration are calculated by subtracting the oxygen concentration at the top of the drop (initial oxygen concentration) from the oxygen concentration at the bottom of the drop (final oxygen concentration). The calculated oxidation rates and drops in oxygen concentration are given in the tables together with the values obtained from the oxygraph software.

The pH measured in the emulsion before (pH_1) and after (pH_2) the oxidation experiments are given in the tables with the oxidation rates.

The measurement data for emulsions without additives are given in section D.1, and in section D.2 and D.3 for emulsions added ethanol and water, respectively. Measurement data for emulsions with soy lecithin as emulsifier are given in section D.4. The measurement data for the emulsions with antioxidants are presented in the same order as in the report, in section D.5 to D.13. In the tables, the experiments are presented in the same order for the tables with the oxidation rates and the tables with the initial drops in oxygen concentration.

D.1 Without Additives

OURS, calculated oxidation rates and pH measured before and after the oxidation experiments for different concentrations of Fe^{2+}, and 25 µM Fe^{3+} as prooxidants are given in Table D.1.1 for emulsions without any additives. The oxygen concentration before and after the initial drop and the calculated initial drops in oxygen concentration for different concentration of Fe^{2+} are given in Table D.1.2.

Table D.1.1: Oxygen uptake rates, calculated oxidation rates and pH measured before and after the oxidation experiments in emulsions with different concentration of Fe^{2+} and 25 µM Fe^{3+}.

Prooxidant (µM)		pH_1	Background OUR (µM/min)	OUR after addition of prooxidant (µM/min)	Oxidation rate (µM/min)	pH_2
Fe^{2+}	5	5.22	1.32645	3.05303	1.72658	4.23
			1.50383	2.98558	1.48175	
			1.99818	3.43411	1.43593	
	10	5.81	1.78616	4.06053	2.27437	3.92
			2.42391	5.16118	2.73727	
			0.90878	3.81081	2.90203	
	15	5.22	0.97454	4.73944	3.76490	3.80
			0.08039	5.06074	4.98036	
			0.27714	4.96754	4.69040	
	20	5.22	1.42326	6.21937	4.79611	3.70
			1.07536	6.30618	5.23082	
			1.19923	6.24236	5.04313	
	25	5.22	1.25101	6.88784	5.63683	3.39
			1.36707	7.84920	6.48213	
			0.95207	7.63778	6.68571	
		5.10	1.71420	8.83327	7.11907	3.37
			1.53426	8.33151	6.79725	
			1.63204	8.22606	6.59402	
		5.58	1.19687	7.66075	6.46388	3.53
			0.83110	7.30737	6.47627	
			1.54854	7.85656	6.30802	
		5.78	1.26705	8.80702	7.53997	3.65
			3.66331	11.7487	8.08539	
			1.56882	9.27401	7.70519	
		5.78	1.76970	8.91271	7.14301	3.49
			2.23080	10.6601	8.42930	
			1.89985	8.54711	6.64726	
	30	5.22	1.15623	8.74456	7.58833	3.29
			1.01621	9.44119	8.42498	
			1.32521	9.25070	7.92549	
Fe^{3+}	25	5.29	1.72685	6.94309	5.21624	3.60
			2.35971	8.66177	6.30206	
			1.61822	6.85301	5.23479	
		5.81	2.06208	6.86432	4.80224	3.57
			3.24802	9.02765	5.77963	
			1.66236	6.65102	4.98866	
		5.42	1.42308	6.22563	4.80255	3.49
			0.39064	5.83535	5.44471	
			0.12696	5.65701	5.53005	

Table D.1.2: Oxygen concentration in emulsions at the top and bottom of the initial drop, and calculated initial drop in oxygen concentration for different concentrations of Fe^{2+}.

Fe^{2+} (µM)	Initial oxygen concentration (µM)	Final oxygen concentration (µM)	Drop in oxygen concentration (µM)
5	211	198	13
	257	244	13
	257	246	11
10	207	172	35
	293	241	52
	227	188	39
15	207	152	55
	243	192	51
	245	187	58
20	211	115	96
	230	132	98
	256	156	100
25	212	86	126
	245	108	137
	255	117	138
	270	128	142
	219	84	135
	261	125	136
	262	129	133
	244	123	121
	271	136	135
	209	60	149
	305	116	189
	259	108	151
	213	63	150
	257	102	155
	238	105	133
30	222	80	142
	274	111	163
	250	99	151

D.2 Ethanol

The OURs, calculated oxidation rates and pH before and after the oxidation experiments for emulsions with ethanol (5%, 50 µL) when Fe^{2+} (25 µM) and Fe^{3+} (25 µM) were used as prooxidants are given in Table D.2.1. The oxygen concentration before and after the initial drop induced by Fe^{2+} and the calculated initial drops in oxygen concentration are given in Table D.2.2.

Table D.2.1: Oxygen uptake rates, calculated oxidation rates and pH measured before and after the oxidation experiments in emulsions with ethanol when Fe^{2+} (25 µM) and Fe^{3+} (25 µM) were used as prooxidant.

	pH_1	Background OUR (µM/min)	OUR after addition of ethanol (µM/min)	OUR after addition of Fe^{2+} (µM/min)	Oxidation rate (µM/min)	pH_2
Fe^{2+}	5.10	0.42725	0.58763	9.62046	9.19321	3.40
		0.048892	0.73409	8.66275	8.61386	
		0.13917	0.36987	8.58308	8.44391	
	5.29	1.46280	1.19193	10.7573	9.29450	3.53
		2.06330	1.82122	11.1906	9.12730	
		1.93965	2.15174	8.67423	6.73458	
	5.81	2.47517	2.26930	7.31484	4.83967	3.51
		2.27364	1.79754	9.95375	7.68011	
		1.50146	0.5917	8.24165	6.74019	
	5.42	0.10727	1.21549	8.47349	8.36622	3.63
		0.87416	0.86879	7.74988	6.87572	
		1.28084	1.32010	7.97147	6.69063	
Fe^{3+}	5.45	1.73549	1.02274	7.74160	6.00611	3.57
		1.22691	1.07067	6.32876	5.10185	
		1.65537	1.29042	6.61833	4.96296	
	5.29	2.60510	1.68124	6.94406	4.33896	3.42
		1.87226	1.14757	7.38230	5.51003	
		2.12290	1.33543	7.93692	5.81402	

Table D.2.2: Oxygen concentration in emulsions at the top and bottom of the initial drop, and calculated initial drop in oxygen concentration for emulsions with added ethanol (5%, 50 µL) when Fe^{2+} (25 µM) was used as prooxidant.

Initial oxygen concentration (µM)	Final oxygen concentration (µM)	Drop in oxygen concentration (µM)
262	115	147
224	104	120
264	142	122
204	36	168
302	116	186
253	95	158
206	62	144
304	107	197
238	78	160
248	101	147
241	98	143
223	82	141

D.3 Water

The OURs, calculated oxidation rates and pH before and after the oxidation experiments for emulsions with water (50 µL) when Fe^{2+} (25 µM) and Fe^{3+} (25 µM) were used as prooxidants are given in Table D.3.1. The oxygen concentration before and after the initial drop induced by Fe^{2+} and the calculated initial drops in oxygen concentration are given in Table D.3.2.

Table D.3.1: Oxygen uptake rates in emulsions added water (50 µL) when Fe^{2+} (25 µM) and Fe^{3+} (25 µM) were used as prooxidants.

	pH_1	Background OUR (µM/min)	OUR after addition of water (µM/min)	OUR after addition of Fe^{2+} (µM/min)	Oxidation rate (µM/min)	pH_2
Fe^{2+}	5.10	1.64533	1.41182	9.80914	8.16381	3.40
		1.20242	1.42731	8.76172	7.55930	
		1.69204	1.32891	8.89998	7.20794	
	5.78	2.20010	2.04790	9.03073	6.83063	3.42
		2.57888	2.14739	12.0743	9.49542	
		2.11999	1.16032	8.32206	6.20207	
Fe^{3+}	5.45	1.58559	0.64754	7.87592	6.29033	3.60
		0.62151	0.14655	6.07835	5.45684	
		1.90238	1.16471	6.52461	4.62223	
	5.45	2.25573	1.17585	7.14612	4.89039	3.52
		1.20843	1.03054	6.49849	5.29006	
		1.63380	1.26886	7.30144	5.66764	

Table D.3.2: Oxygen concentration in emulsions at the top and bottom of the initial drop, and calculated initial drop in oxygen concentration for emulsions with added water (50 µL) when Fe^{2+} (25 µM) was used as prooxidant.

Initial oxygen concentration (µM)	Final oxygen concentration (µM)	Drop in oxygen concentration (µM)
266	102	164
218	88	130
244	105	139
214	58	156
329	111	218*
265	111	154

D.4 Soy Lecithin

The OURs, calculated oxidation rates and pH before and after the oxidation experiments for emulsions with soy lecithin as emulsifier for different concentration of Fe^{2+}, and 25 µM Fe^{3+} as prooxidants are given in Table D.4.1. The oxygen concentration before and after the initial drop induced by Fe^{2+} and the calculated initial drops in oxygen concentration are given in Table D.4.2.

Table D.4.1: Oxygen uptake rates in emulsions with soy lecithin as emulsifier for different concentrations of Fe^{2+} and Fe^{3+}.

Prooxidant (µM)		pH_1	Background OUR (µM/min)	OUR after addition of prooxidant (µM/min)	Oxidation rate (µM/min)	pH_2
Fe^{2+}	10	6.05	1.07688	1.09274	0.01586	
			0.86205	0.59256	-0.26949	5.68
			1.00885	0.66575	-0.34310	
	20	6.25	1.56825	0.28947	-1.27878	
			1.39177	0.94948	-0.44229	5.27
			0.83273	0.94435	0.11162	
	25	6.25	1.53004	1.49310	-0.03694	
			1.62732	0.51868	-1.10864	5.12
			1.69038	1.06599	-0.62439	
	30	6.25	1.01474	0.55190	-0.46284	
			1.16137	0.22516	-0.93621	-
			1.18468	0.90242	-0.28226	
Fe^{3+}	25	6.05	-	2.02149	0.62302*	
			1.36000	0.59512	-0.76488	5.13
			1.43694	0.22765	-1.20929	

*The average background OUR from the parallel experiments were used for calculation of the oxidation rate.

Table D.4.2: Oxygen concentration in emulsions at the top and bottom of the initial drop, and calculated initial drop in oxygen concentration for emulsions with soy lecithin as emulsifier for different concentrations of Fe^{2+}.

Fe^{2+} (µM)	Initial oxygen concentration (µM)	Final oxygen concentration (µM)	Drop in oxygen concentration (µM)
10	259	254	5
	224	218	6
	282	276	6
20	256	247	9
	226	217	9
	275	263	12
25	284	263	21
	222	210	12
	272	255	17
30	272	254	18
	222	207	15
	259	241	18

D.5 EDTA

The OURs, calculated oxidation rates and pH before and after the oxidation experiments for emulsions with different concentrations of EDTA when Fe^{2+} (25 µM) and Fe^{3+} (25 µM) were used as prooxidants are given in Table D.5.1. The oxygen concentration before and after the initial drop induced by Fe^{2+} and the calculated initial drops in oxygen concentration are given in Table D.5.2.

Table D.5.1: Oxygen uptake rates in emulsions with different concentrations of EDTA. The concentration of prooxidant was 25 µM in all the experiments.

	EDTA (µM)	pH_1	Background OUR (µM/min)	OUR after addition of EDTA (µM/min)	OUR after addition of Fe^{2+} (µM/min)	Oxidation rate (µM/min)	pH_2
Fe^{2+}	7.5	5.25	0.90018	0.64274	6.45870	5.55852	3.35
			0.39597	-	7.59626	7.20029	
			0.93843	1.08782	7.93524	6.99681	
	15	5.22	0.73123	0.65000	4.47803	3.74680	3.38
			0.87426	0.63879	5.50650	4.63224	
			0.73565	0.72539	5.48340	4.74775	
	25	5.25	1.06241	0.48928	2.35789	1.29548	3.45
			1.37977	1.18382	3.19249	1.81272	
			1.00995	0.71012	2.85693	1.84698	
	50	5.25	1.31764	0.57468	0.44212	-0.87552	3.30
			1.23804	0.77851	0.54669	-0.69135	
			1.07818	0.67369	0.63531	-0.44287	
Fe^{3+}	25	5.87	1.58045	0.76247	1.55674	-0.02371	3.46
			1.80809	1.17607	1.75224	-0.05585	
			2.45137	0.69604	1.18027	-1.27110	

Table D.5.2: Oxygen concentration in emulsions at the top and bottom of the initial drop, and calculated initial drop in oxygen concentration for emulsions with different concentrations of EDTA when Fe^{2+} (25 µM) was used as prooxidant.

EDTA (µM)	Initial oxygen concentration (µM)	Final oxygen concentration (µM)	Drop in oxygen concentration (µM)
7.5	218	117	101
	254	131	123
	256	124	132
15	203	136	67
	214	121	93
	240	149	91
25	217	188	29
	239	203	36
	261	228	33
50	221	210	11
	231	220	11
	264	252	12

D.6 Citric Acid

The OURs, calculated oxidation rates and pH before and after the oxidation experiments for emulsions with different concentrations of citric acid when Fe^{2+} (25 µM) and Fe^{3+} (25 µM) were used as prooxidants are given in Table D.6.1.The oxygen concentration before and after the initial drop induced by Fe^{2+} and the calculated initial drops in oxygen concentration are given in D.6.2.

Table D.6.1: Oxygen uptake rates in emulsions with different concentrations of citric acid. The concentration of prooxidant was 25 µM in all the experiments.

	Citric acid (µM)	pH_1	Background OUR (µM/min)	OUR after addition of citric acid (µM/min)	OUR after addition of Fe^{2+} (µM/min)	Oxidation rate (µM/min)	pH_2
Fe^{2+}	7.5	5.29	1.09337	0.73890	6.45160	5.35823	3.44
			1.31996	1.33171	7.54577	6.22581	
			1.10999	0.80536	5.52591	4.41592	
	12.5	5.86	1.76464	2.24735	3.31398	1.54934	3.57
			1.93325	2.05510	3.69322	1.75997	
			1.81804	1.43329	2.62263	0.80459	
	25	5.86	1.79106	1.37928	2.08492	0.29386	3.42
			1.68520	1.24136	2.48102	0.79582	
			1.64720	1.43268	2.48567	0.83847	
	50	5.86	1.25650	0.86331	1.62118	0.36468	3.50
			2.45153	1.73104	2.31152	-0.14001	
			1.76523	1.29804	1.72614	-0.03909	
Fe^{3+}	25	5.87	1.79144	1.09221	1.57081	-0.22063	3.45
			2.14301	1.37523	2.24129	0.09828	
			1.94250	1.04795	1.68688	-0.25562	

Table D.6.2.: Oxygen concentration in emulsions at the top and bottom of the initial drop, and calculated initial drop in oxygen concentration for emulsions with different concentrations of citric acid when Fe^{2+} (25 µM) was used as prooxidant.

Citric acid (µM)	Initial oxygen concentration (µM)	Final oxygen concentration (µM)	Drop in oxygen concentration (µM)
7.5	205	59	146
	304	138	166
	257	126	131
12.5	202	56	146
	326	150	176
	255	123	132
25	209	66	143
	301	135	166
	265	127	138
50	215	74	141
	310	144	166
	256	129	127

D.7 Caffeic Acid

The OURs, calculated oxidation rates and pH before and after the oxidation experiments for emulsions with different concentrations of caffeic acid when Fe^{2+} (25 µM) and Fe^{3+} (25 µM) were used as prooxidants are given in Table D.7.1. The oxygen concentration before and after the initial drop induced by Fe^{2+} (25 µM) and the calculated initial drops in oxygen concentration are given in Table D.7.2.

Table D.7.1: Oxygen uptake rates in emulsions with different concentrations of caffeic acid. The concentration of prooxidant was 25 µM in all the experiments.

	Caffeic acid (µM)	pH_1	Background OUR (µM/min)	OUR after addition of caffeic acid (µM/min)	OUR after addition of Fe^{2+} (µM/min)	Oxidation rate (µM/min)	pH_2
Fe^{2+}	10	4.89	1.81444	1.17008	34.0033	32.18886	3.41
			2.16218	1.89868	39.2206	37.05842	
			2.19022	1.51119	31.6348	29.44458	
	25	4.89	0.85231	0.87363	47.5647	46.71239	3.48
			1.10866	1.05384	48.8838	47.77514	
			0.91821	0.48593	36.8851	35.96689	
	50	4.89	1.90699	1.15865	42.9474	41.04041	3.52
			1.20749	0.58195	49.0971	47.88961	
			0.23282	0.90185	41.1518	40.91898	
	100	5.87	1.34096	1.22492	30.6072	29.26624	3.71
			1.97297	1.60218	37.5398	35.56683	
			1.27389	0.67678	28.1207	26.84681	
	200	5.85	1.33913	0.95738	20.3240	18.9849	3.51
			1.78066	1.20734	25.1087	23.3280	
			1.01547	0.74824	21.7710	20.7555	
	500	5.85	1.43406	1.14631	13.2529	11.8188	3.52
			1.88681	1.47817	15.3388	13.4520	
			1.02962	0.95415	14.4157	13.3861	
Fe^{3+}	25	5.52	0.69177	0.69557	38.0109	37.3191	3.66
			0.05450	0.37829	33.0109	32.9564	
			0.18124	0.55513	32.9495	32.7683	

Table D.7.2: Oxygen concentration in emulsions at the top and bottom of the initial drop, and calculated initial drop in oxygen concentration for emulsions with different concentrations of caffeic acid when Fe^{2+} (25 µM) was used as prooxidant.

Caffeic acid (µM)	Initial oxygen concentration (µM)	Final oxygen concentration (µM)	Drop in oxygen concentration (µM)
10	197	58	139
	300	103	197
	252	89	163
25	205	124	81
	310	149	161
	278	145	133
50	194	108	86
	317	229	88
	259	166	93
100	191	126	65
	314	232	82
	246	176	70
200	183	138	45
	258	209	49
	253	209	44
500	168	138	30
	241	207	34
	238	203	35

D.8 Propyl Gallate

The OURs, calculated oxidation rates and pH before and after the oxidation experiments for emulsions with different concentrations of propyl gallate when Fe^{2+} (25 µM) and Fe^{3+} (25 µM) were used as prooxidants are given in Table D.8.1. The oxygen concentration before and after the initial drop induced by Fe^{2+} (25 µM) and the calculated initial drops in oxygen concentration are given in Table D.8.2.

Table D.8.1: Oxygen uptake rates in emulsions with different concentrations of propyl gallate. The concentration of prooxidant was 25 µM in all the experiments.

	PG (µM)	pH1	Background OUR (µM/min)	OUR after addition of PG (µM/min)	OUR after addition of Fe^{2+} (µM/min)	Oxidation rate (µM/min)	pH2
Fe^{2+}	25	5.40	1.40025	0.12782	7.74076	6.34051	3.42
			0.51033	0.34103	8.22451	7.71418	
			0.47765	0.63660	7.81782	7.34017	
	100	5.40	1.67148	0.92708	7.05429	5.48281	3.47
			-	1.17576	7.01555	5.34187*	
			1.67589	1.00473	6.85941	5.18352	
	200	5.40	1.59245	1.04753	6.04878	4.45633	3.41
			1.25747	0.88294	5.69618	4.43871	
			1.65498	1.05821	5.85505	4.20007	
	500	5.52	1.87654	0.72683	3.97147	2.09493	3.54
			1.82765	1.17709	4.73790	2.91025	
			1.20590	0.60543	3.81610	2.61020	
Fe^{3+}	100	5.52	0.66022	0.24206	1.88329	1.22307	3.57
			0.89951	0.43082	3.44671	2.54720	
			1.47186	0.73177	3.41266	1.94080	

*The average background OUR from the parallel experiments were used for calculation of the oxidation rate.

Table D.8.2: Oxygen concentration in emulsions at the top and bottom of the initial drop, and calculated initial drop in oxygen concentration for emulsions with different concentrations of propyl gallate when Fe^{2+} (25 µM) was used as prooxidant.

PG (µM)	Initial oxygen concentration (µM)	Final oxygen concentration (µM)	Drop in oxygen concentration (µM)
25	254	180	74
	226	137	89
	249	163	86
100	265	204	61
	242	184	58
	242	182	60
200	262	215	47
	217	173	44
	238	194	44
500	185	154	31
	313	277	36
	217	188	29

D.9 α-Tocoperhol

The OURs, calculated oxidation rates and pH before and after the oxidation experiments for emulsions with different concentrations of α-tocopherol when Fe^{2+} (25 µM) and was used as prooxidants are given in Table D.9.1. The oxygen concentration before and after the initial drop induced by Fe^{2+} (25 µM) and the calculated initial drops in oxygen concentration are given in D.9.2.

Table D.9.1: Oxygen uptake rates in emulsions with different concentrations of α-tocopherol. Fe^{2+} (25 µM) was used as prooxidant in all the experiments.

α-Tocopherol (µM)	pH_1	Background OUR (µM/min)	OUR after addition of Fe^{2+} (µM/min)	Oxidation rate (µM/min)	pH_2
100	5.92	0.68792	9.66300	8.97508	3.69
		0.32463	11.5133	11.18867	
		0.26181	10.3213	10.05949	
200	5.09	0.32154	12.0914	11.76986	3.57
		0.25067	11.4835	11.23283	
		0.44138	11.8172	11.37582	
	5.09	1.06804	13.4103	12.34226	3.48
		1.54291	12.7385	11.19559	
		1.77995	10.9532	9.17325	
300	5.94	0.33509	14.8806	14.54551	3.53
		0.37204	4.12680	3.75476*	
		0.50451	14.5564	14.05189	
	5.94	1.41454	15.3571	13.94256	3.69
		1.54405	13.0293	11.48525	
		1.41891	16.3208	14.90189	

* The value was left out when calculating the average.

Table D.9.2: Oxygen concentration in emulsions at the top and bottom of the initial drop, and calculated initial drop in oxygen concentration for emulsions with different concentrations of α-tocopherol when Fe^{2+} (25 µM) was used as prooxidant.

α-Tocopherol (µM)	Initial oxygen concentration (µM)	Final oxygen concentration (µM)	Drop in oxygen concentration (µM)
100	150	111	39
	255	205	50
	222	180	42
200	219	179	40
	228	195	33
	216	194	22
	237	189	48
	230	185	45
	223	186	37
300	198	176	22
	225	207	18
	268	238	30
	202	175	27
	215	188	27
	-	-	-

D.10 Ascorbic acid

The OURs, calculated oxidation rates and pH before and after the oxidation experiments for emulsions with different concentrations of ascorbic acid when Fe^{2+} (25 µM) and Fe^{3+} (25 µM) were used as prooxidants are given in Table D.10.1, and in Table D.10.2 for emulsions added EDTA prior to addition of ascorbic acid.

Table D.10.1: Oxygen uptake rates in emulsions with different concentrations of ascorbic acid. The concentration of prooxidant was 25 µM in all the experiments.

	AsA (µM)	pH_1	Background OUR (µM/min)	OUR after addition of AsA (µM/min)	OUR after addition of Fe^{2+} (µM/min)	Oxidation rates (µM/min)	pH_2
Fe^{2+}	25	5.58	1.52914	2.05796	7.96732	6.43818	3.50
			1.20514	1.84653	8.44647	7.24133	
			1.03654	2.10330	7.88231	6.84577	
		5.85	1.48945	2.01967	8.81383	7.32438	3.55
			2.12063	3.06552	10.1504	8.02977	
			0.81352	1.71279	9.95539	9.14187	
	50	5.86	0.84979	2.68168	8.77588	7.92609	3.50
			0.60300	2.71539	7.93878	7.33578	
			0.59640	2.93497	7.97844	7.38204	
	100	5.86	1.14826	5.78890	9.03467	7.88641	3.68
			0.67215	4.20291	7.32576	6.65361	
			0.56095	4.99821	8.61375	8.05280	
	200	5.87	1.33162	8.44629	11.64920	10.31758	3.48
			1.41237	9.82089	10.91770	9.50533	
			0.72654	6.91634	10.1788	9.45226	
Fe^{3+}	50	5.85	1.61705	3.04493	7.34297	5.72592	3.56
			1.71674	3.32263	7.95892	6.24218	
			0.82234	1.83309	8.03628	7.21394	

Table D.10.2: Oxygen uptake rates in emulsion added EDTA (50 µM), ascorbic acid (50 µM) and Fe^{2+} (25 µM).

pH_1	Background OUR (µM/min)	OUR after addition of EDTA (µM/min)	OUR after addition of AsA (µM/min)	OUR after addition of Fe^{2+} (µM/min)	Oxidation rate (µM/min	pH_2
5.85	1.16649	0.69397	0.89562	0.20165	0.13544	3.53
	1.73070	1.14406	1.30806	0.16400	0.37091	
	1.05913	0.69000	0.57196	-0.11804	0.38501	

D.11 Ascorbic Acid and α-Tocopherol

The OURs, calculated oxidation rates and pH before and after the oxidation experiments for emulsions with α-tocopherol and ascorbic acids (AsA) when Fe^{2+} (25 µM) was used as prooxidant are given in Table D.11.1.

Table D.11.1: Oxygen uptake rates in emulsions with different amount of α-tocopherol and ascorbic acid. Fe^{2+} (25 µM) was used as prooxidant in all the experiments.

Tocopherol (µM)	AsA (µM)	pH_1	Background OUR (µM/min)	OUR after addition of AsA (µM/min)	OUR after addition of Fe^{2+} (µM/min)	Oxidation rate (µM/min)	pH_2
100	50	-	0.89251	2.45462	8.80801	6.35339	3.46
			0.25241	-	-	-	
			1.76938	2.14684	9.40012	7.25328	
	100	5.92	0.31734	1.63739	9.09075	8.77341	3.68
			1.56589	1.96584	9.93637	8.37048	
			0.45656	1.93592	9.97702	9.52046	
	200	5.92	1.23492	5.15475	10.5392	9.30428	3.68
			1.18824	4.34075	10.4762	9.28796	
			1.63579	5.56120	10.7662	9.13041	
200	50	5.33	1.25858	1.93882	10.9130	9.65442	3.55
			1.48122	2.37197	10.3290	8.84778	
				2.25418	10.9067	9.53680	
300	50	5.94	1.84478	0.84103	14.60320	12.75842	-
			1.71504	1.64423	12.20900	10.49396	
			-	-	14.27790	12.49799*	

*The average background OUR from the parallel experiments were used for calculation of the oxidation rate.

D.12 β-Carotene

The OURs, calculated oxidation rates and pH before and after the oxidation experiments for emulsions with different concentrations of β-carotene when Fe^{2+} (25 µM) and Fe^{3+} (25 µM) were used as prooxidants are given in Table D.12.1. The oxygen concentration before and after the initial drop induced by Fe^{2+} (25 µM) and the calculated initial drops in oxygen concentration are given in Table D.12.2.

Table D.12.1: Oxygen uptake rates in emulsions with different concentrations of β-carotene. Fe^{2+} (25 µM) was used as prooxidant in all the experiments.

β-carotene (µM)	pH_1	Background OUR (µM/min)	OUR after addition of Fe^{2+} (µM/min)	Oxidation rate (µM/min)	pH_2
100	5.75	0.80114	8.36760	7.56646	3.44
		1.11234	7.83095	6.71861	
		-	-	-	
	5.75	0.03442	8.52557	8.49116	3.55
		0.14851	8.20696	8.05845	
		0.09146	8.69689	8.60543	
200	5.10	0.35057	10.0152	9.66463	3.42
		0.03150	7.90311	7.87161	
		0.11058	8.19733	8.08675	
	5.10	0.18148	8.70123	8.51975	3.67
		0.63361	8.11103	7.47742	
		0.78089	8.35894	7.57805	
300	5.66	0.88451	1.30696	0.42245*	3.57
		1.36260	7.54547	6.18287	
		1.74867	8.13836	6.38969	
	5.66	1.81038	9.16240	7.35202	3.53
		1.26761	9.95044	8.68283	
		-0.06200	0.53408	0.59608*	

* The values were left out when calculating the averages.

Table D.12.2: Oxygen concentration in emulsions at the top and bottom of the initial drop, and calculated initial drop in oxygen concentration for emulsions with different concentrations of β-carotene when Fe^{2+} (25 μM) was used as prooxidant.

β-Carotene (μM)	Initial oxygen concentration (μM)	Final oxygen concentration (μM)	Drop in oxygen concentration (μM)
100	202	72	130
	228	98	130
	243	111	132
	218	89	129
	244	112	132
	-	-	-
200	247	103	144
	249	122	127
	239	114	125
	263	129	134
	259	128	131
	252	124	128
300	233	122	111
	252	129	123
	230	119	111
	204	91	113
	292	153	139
	-	-	-

D.13 Astaxanthin

The OURs, calculated oxidation rates and pH before and after the oxidation experiments for emulsions with different concentrations of astaxanthin when Fe^{2+} (25 µM) and Fe^{3+} (25 µM) were used as prooxidants are given in Table D.13.1. The oxygen concentration before and after the initial drop induced by Fe^{2+} (25 µM) and the calculated initial drops in oxygen concentration are given in Table D.13.2.

Table D.13.1: Oxygen uptake rates in emulsions with different concentrations of astaxanthin. The concentration of prooxidant was 25 µM in all the experiments.

	Astaxanthin (µM)	pH_1	Background OUR (µM/min)	OUR after addition of Fe^{2+} (µM/min)	Oxidation rate (µM/min)	pH_2
Fe^{2+}	100	6.07	1.06340	7.33867	6.27527	3.62
			1.45762	8.08022	6.62260	
			0.25795	7.15699	6.89904	
		6.07	2.14301	8.00584	5.86283	3.49
			1.65597	7.95904	6.30307	
			1.28377	6.97760	5.69383	
	200	5.89	0.70439	6.64143	5.93704	3.46
			0.18877	7.28672	7.09795	
			0.04134	6.05540	6.01406	
		5.89	1.27863	7.57654	6.29791	3.44
			1.05506	7.78690	6.73184	
			0.67652	7.49339	6.81687	
	300	5.26	1.27544	6.53792	5.26248	3.53
			0.46397	7.39102	6.92705	
			0.59270	6.11646	5.52376	
		5.26	1.00587	6.91865	5.91278	3.44
			0.81329	7.75744	6.94415	
			0.79590	7.02294	6.22704	
Fe^{3+}	100	6.07	1.97854	6.61060	4.63206	3.41
			3.76747	8.30288	4.53541	
			4.32912	7.41730	3.08818	
	200	5.89	0.08310	5.58957	5.50647	3.46
			0.19676	6.37779	6.18103	
			0.14121	5.40388	5.26267	
	300	5.26	1.02186	5.91876	4.89690	3.46
			0.53784	7.25057	6.71273	
			1.23000	6.13463	4.90463	

Table D.13.2: Oxygen concentration in emulsions at the top and bottom of the initial drop, and calculated initial drop in oxygen concentration for emulsions with different concentrations of astaxanthin when Fe^{2+} (25 µM) was used as prooxidant.

Astaxanthin (µM)	Initial oxygen concentration (µM)	Final oxygen concentration (µM)	Drop in oxygen concentration (µM)
100	190	84	106
	231	104	127
	231	121	110
	210	88	122
	251	124	127
	230	116	114
200	193	101	92
	268	157	111
	248	154	94
	212	105	107
	277	164	113
	279	172	107
300	186	100	86
	270	165	105
	253	165	88
	193	101	92
	269	164	105
	294	194	100